

Supporting Information

Glycoside Hydrolase Stabilization of Transition State Charge: New Directions for Inhibitor Design

Weiwu Ren, Marco Farren-Dai, Natalia Sannikova, Katarzyna Świderek, Yang Wang, Oluwafemi Akintola, Robert Britton, Vicent Moliner, and Andrew J. Bennet

Table of Contents

Synthetic methods	SI 2–10
KIE measurement protocols	SI10–13
Computational methods	SI13–17
Equations S1–S4	SI 17
Tabulated KIEs values (Tables S1–2)	SI 18
Missing atom types, charges and parameters for inhibitor (Table S3)	SI 19
Average distances (in Å) computed between key atoms (Table S4)	SI 20
KIEs computed for covalent inhibition of <i>TmGalA</i> by 10 (Tables S5–6)	SI 21
Average values of computed atomic charges (Table S7)	SI 22–22
Electrostatic potential, by residue, on C5 atom of the carbasugar ring (Table S8)	SI 24–32
Cartesian coordinates of the GSs in water, TS _{alk} , and TS _{hyd} (Table S9)	SI 33–42
Structures for S-1 to S-7 (Figure S1)	SI 43
Typical plots of R versus fraction of reaction (F) for KIE measurements (Fig. S2)	SI 44
Atom labeling for the substrate structure (Figure S3)	SI 45
Graphs for 10 ns MM MD simulations that equilibrate starting structure (Fig. S4)	SI 45
Active site of <i>TmGalA</i> and PES for leaving group departure (Figure S5)	SI 46
PES at AM1/MM level showing two step leaving group departure (Figure S6)	SI 46
Key distances for free energy surfaces (Figure S7)	SI 47
PES and FES for formation of CI-1 for hydrolysis of CI-2 (Figure S8 and S9)	SI 47–48
Free energy surfaces for deprotonation of Asp387 (Figure S10)	SI 48
NMR spectra for all new compounds (Figures S11–S30)	SI 49–68
Enantiomeric excess determinations (Figures S31–S33)	SI 69–71
References	SI 72–73

Synthetic Methods

Nuclear magnetic resonance (NMR) spectra were recorded using CDCl₃ or CD₃OD. Signal positions (δ) are given in parts per million from tetramethylsilane and were measured relative to the signal of the solvent (¹H NMR: CDCl₃: δ 7.26, CD₃OD: δ 3.31; ¹³C NMR: CDCl₃: δ 77.16, CD₃OD: δ 49.00). Coupling constants (*J* values) are given in Hertz (Hz) and are reported to the nearest 0.1 Hz. ¹H NMR spectral data are tabulated in the order: multiplicity (s, singlet; d, doublet; t, triplet; q, quartet; m, multiplet; br., broad), coupling constants, number of protons. NMR spectra were recorded on a Bruker Avance 600 equipped with a QNP or TCI cryoprobe (600 MHz), Bruker 500 (500 MHz), or Bruker 400 (400 MHz). Infrared (IR) spectra were recorded on a Perkin Elmer Spectrum Two™ Fourier transform spectrometer with neat samples. Only selected, characteristic absorption data are provided for each compound.

High resolution mass spectra were performed on an Agilent 6210 TOF LC/MS using ESI-MS or were carried out by the Notre Dame University Mass Spectrometry Department using EI technique. Optical rotation was measured on a Perkin Elmer 341 Polarimeter at 589 nm. Isotopic enrichments were calculated using the method of Brauman.¹ All supporting information structures are shown in Figure S1.

(3*R,S*)-3-((triisopropylsilyl)oxy)-(3-²H)hexa-1,5-diene (S-1): Pyridinium chlorochromate (1.617 g, 7.5 mmol) and silica gel (1.617 g) were ground together until homogeneous. To the above powder in CH₂Cl₂ (12 mL) was added a solution of hexa-1,5-dien-3-ol (491 mg, 5.0 mmol) in CH₂Cl₂ (3 mL). The solution was stirred at ambient temperature for 2 h and was directly purified by flash column chromatography (pentane:diethyl ether, 10:1) to yield hexa-1,5-dien-3-one as a colorless oil. This ketone was dissolved in Et₂O (10 mL) and the resulting solution was added dropwise to a suspension of LiAlD₄ (174 g, 4.15 mmol) at 0 °C. The mixture was stirred at ambient temperature for 10 min and then heated to 40 °C for 2 h. The reaction was cooled down to 0 °C and was quenched by H₂O (0.12 mL), 15% NaOH (0.36 mL) and H₂O (0.12 mL), filtered through celite and then dried over Na₂SO₄. The solvents were removed *in vacuo* and the residue was dissolved in CH₂Cl₂ (25 mL). Following addition of imidazole (449 mg, 6.6 mmol) and TIPSCl (694 mg, 3.6 mmol) the resulting solution was stirred at ambient temperature for 12 h. The reaction was then treated with H₂O and extracted with Et₂O. The combined organic layers were washed with brine and then dried over Na₂SO₄. The solvents were removed *in vacuo*

and the residue was purified by flash column chromatography (hexane) to yield **S-1** as a colorless oil (332 mg, 26% for 3 steps).

IR (neat): 2943, 2866, 1463, 1110, 998, 918, 882 cm^{-1} ; ^1H NMR (600 MHz, CDCl_3): δ 5.84–5.77 (m, 2H), 5.15 (dd, $J = 17.2, 1.7$ Hz, 1H), 5.07–5.03 (m, 3H), 2.35 (dd, $J = 13.7, 7.4$ Hz, 1H), 2.29 (dd, $J = 13.7, 6.9$ Hz, 1H), 1.07–1.05 (m, 21H); ^{13}C [^1H]NMR (151 MHz, CDCl_3) δ 141.3, 134.7, 117.0, 114.1, 73.4 (t, $J = 21.6$ Hz), 43.1, 18.22, 18.21, 12.5; HRMS (ESI): m/z $[\text{M} + \text{H}]^+$ calcd for $\text{C}_{15}\text{H}_{30}\text{DOSi}$: 256.2201; found: 256.2198.

(1*S*,2*R*,3*S*)-1-((*S*)-2,2-dimethyl-5-methylene-1,3-dioxan-4-yl)-2-fluoro-3-

((triisopropylsilyloxy)-(3- ^2H)pent-4-en-1-ol (10): To a solution of **S-1** (672 mg, 2.63 mmol) in $t\text{BuOH}/\text{H}_2\text{O} = 13 \text{ mL}/13 \text{ mL}$ was added AD-mix- β (3.68 g, 2.63 mmol) at ambient temperature. The resulting solution was stirred at ambient temperature for 12 h and was quenched with $\text{Na}_2\text{S}_2\text{O}_3$ (aq.), then extracted with ethyl acetate. The solvents were removed *in vacuo* and the residue was dissolved in $\text{THF}/\text{H}_2\text{O} = 20 \text{ mL}/5 \text{ mL}$. To the above solution NaIO_4 (1.69 g, 7.89 mmol) was added and the reaction was stirred at ambient temperature for 1 h. The reaction was then treated with H_2O and extracted with Et_2O . The combined organic layers were washed with brine and then dried over Na_2SO_4 . The solvents were removed *in vacuo* and the residue was purified by flash column chromatography (pentane: CH_2Cl_2 , 4:1) to yield (3- ^2H)-**8** as a colorless oil (257 mg, 38% for 2 steps). To a solution of (3- ^2H)-**8** (257 mg, 1.0 mmol) in DMF (10 mL) at 5 $^\circ\text{C}$ were added Selectfluor $^\circledR$ (350 mg, 1.0 mmol) and (*R*)-proline (115 mg, 1.0 mmol). The mixture was stirred at 5 $^\circ\text{C}$ for 1 h, treated with H_2O , then extracted with Et_2O . The combined organic layers were washed with brine and then dried over Na_2SO_4 . The solvents were removed *in vacuo* and the residue was dissolved in CH_2Cl_2 (5 mL). (*R*)-proline (92 mg, 0.8 mmol) and 2,2-dimethyl-1,3-dioxan-5-one (**9**; 156 mg, 1.2 mmol) were then added at 0 $^\circ\text{C}$. The mixture was warmed to ambient temperature and stirred for 48 h. The resulting mixture was then treated with H_2O and extracted with Et_2O . The combined organic layers were washed with brine and then dried over Na_2SO_4 . The solvents were removed *in vacuo* to give crude ketone (**S-3**, Supporting Information) that was dissolved in THF (3 mL). In another flask LiHMDS (2.0 mL, 1.0 M in THF, 2.0 mmol) was added dropwise to a cooled (-78 $^\circ\text{C}$) solution of 5-(methanesulfonyl)-1-phenyl-1H-tetrazole (444 mg, 2.0 mmol) in THF (7 mL) and stirred at -78 $^\circ\text{C}$ for 30 min. Then the above solution of crude ketone (**S-3**) in THF (3 mL) was added dropwise at -78 $^\circ\text{C}$ and the mixture was stirred for another 1 h before quenching with H_2O . The mixture

was extracted with Et₂O and the combined organic layers were washed with brine and then dried over Na₂SO₄. The solvents were removed *in vacuo* and the residue was purified by flash column chromatography (pentane:diethyl ether, 15:1) to yield **10** and **11** as a colorless oils (161 mg, 40%). **10**: IR (neat): 3480, 2942, 2867, 1462, 1373, 1156, 1070, 1026, 996 cm⁻¹; ¹H NMR (400 MHz, CDCl₃): δ 5.88 (dd, *J* = 17.2, 10.5 Hz, 1H), 5.40 (dd, *J* = 17.2, 1.0 Hz, 1H), 5.33–5.30 (m, 2H), 5.02 (brs, 1H), 4.66 (d, *J* = 44.4 Hz, 1H), 4.43 (d, *J* = 8.5 Hz, 1H), 4.35 (d, *J* = 13.4 Hz, 1H), 4.26 (d, *J* = 13.4 Hz, 1H), 4.13 (ddd, *J* = 28.8, 8.5, 2.3 Hz, 1H), 3.97 (d, *J* = 2.5 Hz, 1H), 1.48 (s, 3H), 1.34 (s, 3H), 1.10–1.05 (m, 21H); ¹³C[¹H]NMR (101 MHz, CDCl₃) δ 142.1, 136.4 (d, *J* = 8.0 Hz), 118.2 (d, *J* = 1.4 Hz), 109.9, 99.6, 90.1 (d, *J* = 184.7 Hz), 76.2 (q, *J* = 22.1 Hz), 70.8 (d, *J* = 18.3 Hz), 70.5 (d, *J* = 3.8 Hz), 65.1, 28.3, 22.0, 18.04, 18.01, 17.8, 12.4; HRMS (ESI): *m/z* [M + Na]⁺ calcd for C₂₁H₃₈DFNaO₄Si: 426.2557; found: 426.2564; [α]_D²⁰ (CHCl₃, *c* = 0.5): +17.5. The enantiomeric ratio of the product was determined by chiral HPLC analysis of the 4-nitrobenzoyl ester derivative (Column Lux[®]3 μm Amylose-1; 98% hexane and 2% ⁱPrOH; flow rate = 0.45 mL/min; tR¹ = 2.515 min, 95.9%; tR² = 2.931 min, 4.1%).

(3*R,S*)-3-((triisopropylsilyloxy)-(3-¹³C)hexa-1,5-diene (S-2): To a solution of allyl bromide (1.21 g, 10.0 mmol) in CH₂Cl₂/H₂O = 10 mL/10 mL was added bis(triphenylphosphine)iminium chloride (287 mg, 0.5 mmol) and K¹³CN (782 mg, 12.0 mmol) at 0 °C. The resulting solution was stirred at 0 °C for 72 h and extracted with CH₂Cl₂. The combined organic layers were washed with brine and then dried over Na₂SO₄. The solvents were carefully removed *in vacuo* and the residue was dissolved in concentrated HCl (1 mL). The reaction was heated to reflux for 15 min and cooled down to ambient temperature. The mixture was then treated with H₂O and extracted with CH₂Cl₂. The solvents were removed *in vacuo* and the residue was dissolved in Et₂O (10 mL). The resulting solution was added dropwise to a suspension of LiAlH₄ (500 mg, 12 mmol) in Et₂O (10 mL) at 0 °C for 15 min, and then was refluxed for 2 h. The reaction was cooled down to ambient temperature and was stirred for 40 h before being quenched with H₂O (0.24 mL), 15% NaOH (0.72 mL) and H₂O (0.24 mL). The solution was then filtered through celite and dried over Na₂SO₄. The solvents were removed *in vacuo* and the crude (1-¹³C)but-3-en-1-ol was dissolved in CH₂Cl₂ (50 mL). Dess-Martin periodinane (5.09 g, 12 mmol) and NaHCO₃ (2.52 g, 30 mmol) was then added at 0 °C then stirred for 0.5 h. The reaction was quenched with Na₂S₂O₃ (aq.) and extracted with Et₂O and dried over Na₂SO₄. After filtration, the solution was cooled down to -78 °C and vinylmagnesium bromide (15.0 mL, 1.0 M in THF, 15.0

mmol) was added dropwise. After 1 h, NH₄Cl (aq.) was added and the mixture was extracted with Et₂O, and the organic layers was then dried over Na₂SO₄. The solvents were removed *in vacuo* and the residue was dissolved in CH₂Cl₂ (100 mL). Imidazole (1.50 g, 22.0 mmol) and TIPSCl (2.31 g, 12.0 mmol) were added and the resulting solution was stirred at ambient temperature for 12 h. The reaction was then treated with H₂O and extracted with Et₂O. The combined organic layers were washed with brine and then dried over Na₂SO₄. The solvents were removed *in vacuo* and the residue was purified by flash column chromatography (hexane) to yield **S-2** as a colorless oil (461 mg, 18% for 6 steps).

IR (neat): 2947, 2867, 1463, 1061, 992, 914, 884 cm⁻¹; ¹H NMR (600 MHz, CDCl₃): δ 5.85–5.78 (m, 2H), 5.15 (ddt, *J* = 17.2, 6.9, 1.4 Hz, 1H), 5.07–5.03 (m, 3H), 4.26 (ddd, *J* = 141.1, 12.1, 6.2 Hz, 1H), 2.37–2.27 (m, 2H), 1.08–1.06 (m, 21H); ¹³C[¹H]NMR (151 MHz, CDCl₃) δ 141.3 (d, *J* = 47.7 Hz), 134.7 (d, *J* = 1.5 Hz), 117.0 (d, *J* = 3.8 Hz), 114.1, 73.8 (t, *J* = 21.6 Hz), 43.2 (d, *J* = 38.0 Hz), 18.23, 18.22, 12.5; HRMS (ESI): *m/z* [M + H]⁺ calcd for C₁₄H₃₁OSi¹³C: 256.2172; found: 256.2176.

(1*S*,2*R*,3*S*)-1-((*S*)-2,2-dimethyl-5-methylene-1,3-dioxan-4-yl)-2-fluoro-3-

((triisopropylsilyloxy)-(3-¹³C)pent-4-en-1-ol (12): To a solution of **S-2** (Supporting Information; 672 mg, 2.63 mmol) in *t*BuOH/H₂O = 13 mL/13 mL was added AD-mix-β (3.68 g, 2.63 mmol) at ambient temperature. The resulting solution was stirred at ambient temperature for 12 h and was quenched with Na₂S₂O₃ (aq.), then extracted with ethyl acetate. The solvents were removed *in vacuo* and the residue was dissolved in THF/H₂O = 20 mL/5 mL. To the above solution NaIO₄ (1.69 g, 7.89 mmol) was added and the reaction was stirred at ambient temperature for 1 h. The reaction was then treated with H₂O and extracted with Et₂O. The combined organic layers were washed with brine and then dried over Na₂SO₄. The solvents were removed *in vacuo* and the residue was purified by flash column chromatography (pentane:CH₂Cl₂, 4:1) to yield (3-¹³C)-**8** as a colorless oil (257 mg, 38% for 2 steps). To a solution of (3-¹³C)-**8** (257 mg, 1.0 mmol) in DMF (10 mL) at 5 °C were added Selectfluor® (350 mg, 1.0 mmol) and (*R*)-proline (115 mg, 1.0 mmol). The mixture was stirred at 5 °C for 1 h, treated with H₂O, then extracted with Et₂O. The combined organic layers were washed with brine and then dried over Na₂SO₄. The solvents were removed *in vacuo* and the residue was dissolved in CH₂Cl₂ (5 mL). (*R*)-proline (92 mg, 0.8 mmol) and 2,2-dimethyl-1,3-dioxan-5-one (**9**; 156 mg, 1.2 mmol) were then added at 0 °C. The mixture was warmed to ambient

temperature and stirred for 48 h. The resulting mixture was then was treated with H₂O and extracted with Et₂O. The combined organic layers were washed with brine and then dried over Na₂SO₄. The solvents were removed *in vacuo* to give crude ketone (**S-4**, Supporting Information) that was dissolved in THF (3 mL). In another flask LiHMDS (2.0 mL, 1.0 M in THF, 2.0 mmol) was added dropwise to a cooled (−78 °C) solution of 5-(methanesulfonyl)-1-phenyl-1H-tetrazole (444 mg, 2.0 mmol) in THF (7 mL) and stirred at −78 °C for 30 min. Then the above solution of crude ketone (**S-4**) in THF (3 mL) was added dropwise at −78 °C and the mixture was stirred for another 1 h before quenching with H₂O. The mixture was extracted with Et₂O and the combined organic layers were washed with brine and then dried over Na₂SO₄. The solvents were removed *in vacuo* and the residue was purified by flash column chromatography (pentane:diethyl ether, 15:1) to yield **12** and **13** as colorless oils (161 mg, 40%).

12: IR (neat): 3487, 2947, 2928, 2870, 1463, 1378, 1223, 1072, 1030, 921 cm^{−1}; ¹H NMR (400 MHz, CDCl₃): δ 5.94–5.84 (m, 1H), 5.44–5.29 (m, 2H), 5.32 (brs, 1H), 5.03 (brs, 1H), 5.03–4.99 (m, 0.5H), 4.68–4.63 (m, 0.5H), 4.67 (dd, *J* = 45.3, 2.0 Hz, 1H), 4.44 (d, *J* = 8.5 Hz, 1H), 4.35 (d, *J* = 13.3 Hz, 1H), 4.27 (dd, *J* = 13.3, 0.9 Hz, 1H), 4.14 (ddd, *J* = 28.8, 8.5, 2.7 Hz, 1H), 3.96 (d, *J* = 2.5 Hz, 1H), 1.49 (s, 3H), 1.35 (s, 3H), 1.12–1.05 (m, 21H); ¹³C[¹H]NMR (101 MHz, CDCl₃) δ 142.3, 136.6 (dd, *J* = 46.5, 7.9 Hz), 118.1, 109.9, 99.6, 90.3 (dd, *J* = 184.6, 43.5 Hz), 76.5 (d, *J* = 22.9 Hz, 1H), 70.9 (d, *J* = 18.3 Hz, 1H), 70.7 (dd, *J* = 3.7, 2.1 Hz), 65.1, 28.2, 22.1, 18.1, 18.04, 18.03, 12.5; HRMS (ESI): *m/z* [M + Na]⁺ calcd for C₂₀H₃₉FNaO₄Si¹³C: 426.2527; found: 426.2532; [α]_D²⁰ (CHCl₃, *c* = 0.7): +12.3. The enantiomeric ratio of the product was determined by chiral HPLC analysis of the 4-nitrobenzoyl ester derivative (Column Lux[®]3 μm Amylose-1; 98% hexane and 2% ⁱPrOH; flow rate = 0.45 mL/min; tR¹ = 2.39 min, 96.2%; tR² = 2.791 min, 3.8%).

(1*S*,2*R*,3*R*)-1-((*S*)-2,2-dimethyl-5-methylene-1,3-dioxan-4-yl)-2-fluoro-3-

((triisopropylsilyloxy)-(3-¹³C)pent-4-en-1-ol (13**): IR (neat): 3460, 2939, 2867, 1463, 1381, 1223, 1081, 1031, 922 cm^{−1}; ¹H NMR (400 MHz, CDCl₃): δ 6.02–5.92 (m, 1H), 5.40 (dd, *J* = 17.3, 6.9 Hz, 1H), 5.29–5.23 (m, 1H), 5.21 (brs, 1H), 5.03 (brs, 1H), 4.82–4.79 (m, 0.5H), 4.46–4.42 (m, 0.5H), 4.70 (ddd, *J* = 46.0, 6.4, 2.9 Hz, 1H), 4.39 (d, *J* = 8.2 Hz, 1H), 4.29 (brs, 2H), 3.93 (ddd, *J* = 26.0, 8.0, 7.5 Hz, 1H), 2.44 (dd, *J* = 7.4, 1.9 Hz, 1H), 1.47, 1.36, 1.10–1.07 (m, 21H); ¹³C[¹H]NMR (101 MHz, CDCl₃) δ 142.6, 137.3 (dd, *J* = 46.8, 6.0 Hz), 117.8, 109.9, 99.8, 92.6 (dd, *J* = 182.3, 44.2 Hz), 74.8 (d, *J* = 22.2 Hz, 1H), 71.3 (dd, *J* = 2.8, 2.6 Hz), 70.8 (d, *J* =**

17.9 Hz, 1H), 64.7, 28.0, 22.7, 18.1, 18.01, 17.98, 12.6; HRMS (ESI): m/z $[M + Na]^+$ calcd for $C_{20}H_{39}FNaO_4Si^{13}C$: 426.2527; found: 426.2529; $[\alpha]_D^{20}$ ($CHCl_3$, $c = 0.57$): +16.2. The enantiomeric ratio of the product was determined by chiral HPLC analysis of the 4-nitrobenzoyl ester derivative (Column Lux[®]3 μ m Amylose-1; 98% hexane and 2% *i*PrOH; flow rate = 0.5 mL/min; $tR^1 = 2.201$ min, 96.9%; $tR^2 = 2.563$ min, 3.1%).

2,4-Dinitrophenyl 5,5a-didehydro-5a-carba-2-fluoro- α -L-arabino-(1-²H)hexopyranoside [(1-²H)-4]: This compound was synthesized from **10** according to our reported procedure.²

IR (neat): 3373, 2947, 2872, 1606, 1533, 1351, 1288, 1068 cm^{-1} ; ¹H NMR (600 MHz, CD_3OD): δ 8.70 (d, $J = 2.8$ Hz, 1H), 8.47 (dd, $J = 9.4, 2.8$ Hz, 1H), 7.70 (d, $J = 9.4$ Hz, 1H), 5.99–5.97 (m, 1H), 5.01 (dd, $J = 49.0, 10.1$ Hz, 1H), 4.30 (apparent t, $J = 4.3$ Hz, 1H), 4.26–4.23 (m, 2H), 4.15 (dd, $J = 15.3, 1.6$ Hz, 1H); ¹³C[¹H]NMR (151 MHz, CD_3OD) δ 157.4, 148.3 (d, $J = 1.6$ Hz), 141.6, 141.0, 129.7, 122.3, 117.7 (d, $J = 2.0$ Hz), 117.4 (d, $J = 4.5$ Hz), 90.3 (d, $J = 185.2$ Hz), 75.1 (td, $J = 36.2, 16.5$ Hz), 68.5 (d, $J_{C-F} = 7.9$ Hz), 68.4, 63.3; HRMS (ESI): m/z $[M + Na]^+$ calcd for $C_{13}H_{12}DFN_2NaO_8$: 368.0611; found: 368.0611; $[\alpha]_D^{20}$ (CH_3OH , $c = 0.25$): +128.4.

2,4-Dinitrophenyl 5,5a-didehydro-5a-carba-2-fluoro- α -L-arabino-(1-¹³C)hexopyranoside [(1-¹³C)-4]: This compound was synthesized from **12** according to our reported procedure.²

IR (neat): 3367, 2927, 2868, 1621, 1503, 1331, 1272 cm^{-1} ; ¹H NMR (600 MHz, CD_3OD): δ 8.70 (d, $J = 2.8$ Hz, 1H), 8.47 (dd, $J = 9.4, 2.8$ Hz, 1H), 7.70 (d, $J = 9.4$ Hz, 1H), 5.99–5.97 (m, 1H), 5.65 (ddd, $J = 152.4, 9.3, 4.8$ Hz, 1H), 5.01 (dddd, $J = 49.0, 10.1, 3.7, 3.7$ Hz, 1H), 4.30 (apparent t, $J = 4.3$ Hz, 1H), 4.28–4.24 (m, 1H), 4.24 (d, $J = 15.2$ Hz, 1H), 4.16 (d, $J = 15.2$ Hz, 1H); ¹³C[¹H]NMR (151 MHz, CD_3OD) δ 157.4 (d, $J = 1.8$ Hz), 148.2, 141.7, 141.0, 129.7, 122.3, 117.7 (dd, $J = 3.6, 2.2$ Hz), 117.5 (dd, $J = 46, 4.5$ Hz), 89.8 (dd, $J = 185.3, 40.2$ Hz), 75.3 (d, $J = 16.6$ Hz), 68.5 (d, $J = 17.8$ Hz), 68.4 (dd, $J = 6.4, 1.6$ Hz), 63.3 (d, $J = 5.0$ Hz); HRMS (ESI): m/z $[M + Na]^+$ calcd for $C_{12}H_{13}FN_2NaO_8^{13}C$: 368.0582; found: 368.0582; $[\alpha]_D^{20}$ (CH_3OH , $c = 0.33$): +98.0.

1-O-Acetyl-5,5a-didehydro-5a-carba-2-fluoro-4,6-isopropylidene- α -L-arabino-(1-

¹³C)hexopyranoside (16): To a solution of **13** (202 mg, 0.5 mmol) in CH_2Cl_2 (5 mL) at ambient temperature was added triethylamine (139 μ L, 1.0 mmol), acetic anhydride (71 μ L, 0.75 mmol), and 4-dimethylaminopyridine (6.1 mg, 0.05 mmol). The reaction mixture was stirred at ambient temperature for 48 h and then treated with NH_4Cl (aq.). The resulting mixture was extracted with Et_2O and the combined organic layers were washed with brine and then dried over Na_2SO_4 . The

solvents were removed *in vacuo* and the residue was dissolved in THF (5 mL). A solution of tetrabutylammonium fluoride (1.0 mL, 1.0 M in THF, 1.0 mmol) and acetic acid (60 μ L, 1.0 mmol) was added at 0 °C. The reaction mixture was stirred at ambient temperature for 48 h and then was treated with H₂O. The mixture was extracted with Et₂O and the combined organic layers were washed with brine and then were dried over Na₂SO₄. The solvents were removed *in vacuo* and the residue was purified by flash column chromatography (pentane:ethyl acetate, 3:1) and the desired deprotection product was dissolved in CH₂Cl₂ (18 mL) and Grubbs' II catalyst (31 mg, 0.036 mmol) was added. The mixture was heated to 40 °C under argon and maintained at that temperature for 1 h. The reaction was cooled to room temperature and concentrated *in vacuo*. The residue was then purified by flash column chromatography (pentane:ethyl acetate, 1:1) to yield **16** as a yellow oil (88 mg, 67% for 3 steps).

IR (neat): 3446, 2978, 2908, 1756, 1327, 1107, 1035 cm⁻¹; ¹H NMR (600 MHz, CDCl₃): δ 5.49 (brs, 1H), 5.35 (dd, $J_{C-H} = 150.4, 17.5$ Hz, 1H), 4.78 (dddd, $J = 45.3, 4.8, 3.1, 3.0$ Hz, 1H), 4.60 (d, $J = 3.0$ Hz, 1H), 4.46 (d, $J = 13.5$ Hz, 1H), 4.18 (d, $J = 13.5$ Hz, 1H), 4.17–4.14 (m, 1H), 2.67 (t, $J = 3.1$ Hz, 1H), 2.12 (s, 3H), 1.54 (s, 3H), 1.42 (s, 3H); ¹³C[¹H]NMR (151 MHz, CDCl₃) δ 170.4 (d, $J = 2.4$ Hz), 134.0, 117.1 (dd, $J = 47.6, 2.2$ Hz), 100.1, 89.3 (dd, $J = 173.9, 43.8$ Hz), 70.6 (d, $J = 20.8$ Hz), 67.9 (d, $J = 31.0$ Hz), 65.7 (d, $J = 6.8$ Hz), 63.0 (d, $J = 5.6$ Hz), 28.1, 21.1, 20.6; HRMS (ESI): m/z [M + Na]⁺ calcd for C₁₁H₁₇FN₂O₅¹³C: 284.0987; found: 284.0989; [α]_D²⁰ (CH₂Cl₂, c = 1.8): +8.1.

2,4-Dinitrophenyl 5,5a-didehydro-5a-carba-2-fluoro- α -L-arabino-(1-¹³C)- and (1-¹³C,1-¹⁸O)-hexopyranoside (1-¹³C)-4 and (1-¹³C,1-¹⁸O)-4: To a solution of **16** (26.1 mg, 0.1 mmol) in MeOH (1 mL) at 0 °C was added K₂CO₃ (13.8 mg, 0.1 mmol). The resulting mixture was stirred at 0 °C for 1 h and then filtered through a pad of silica gel. The solvents were removed *in vacuo* and the residue was dissolved in THF (2 mL). PPh₃ (31.5 mg, 0.12 mmol) and 4-nitro[¹⁸O₁]benzoic acid³ (17.0 mg, 0.1 mmol, 86% ¹⁸O incorporation) were added at ambient temperature. The reaction was cooled down to 0 °C and diisopropyl azodicarboxylate (23.6 μ L, 0.12 mmol) was added dropwise. The mixture was then warmed up to ambient temperature and stirred for 4 h, then was treated with H₂O. The reaction was extracted with Et₂O and the combined organic layers were washed with brine and then were dried over Na₂SO₄. The solvents were removed *in vacuo* and the residue was dissolved in MeOH (1 mL) and K₂CO₃ (13.8 mg, 0.1 mmol) was then added at 0 °C for 1 h. The solvents were removed *in vacuo* and the residue was

purified by flash column chromatography (pentane:ethyl acetate, 1:1.2) to yield diol **S-5** (Supporting Information) as a colorless oil. This compound was dissolved in DMF (0.4 mL). Quinuclidine (22 mg, 0.2 mmol) and 4Å molecular sieves (4 beads) were added and the resulting solution was stirred at ambient temperature for 30 min. Then a solution of 2,4-dinitrofluorobenzene (18.6 mg, 0.1 mmol) in DMF (0.1 mL) was added dropwise. The reaction mixture was then stirred at ambient temperature for 12 h then was treated with H₂O. The reaction was extracted with Et₂O and the combined organic layers were washed with brine and then were dried over Na₂SO₄. The solvents were removed *in vacuo* and the residue was dissolved in DCM (2 mL). TFA (30 μL) and H₂O (6 μL) were added and the reaction was stirred at ambient temperature for 5 h. The solvents were removed *in vacuo* and the residue was purified by flash column chromatography (CH₂Cl₂: methanol, 12:1) to yield an approximate 60:40 mixture of **(1-¹³C)-4** and **(1-¹³C,1-¹⁸O)-4** as a white foam (4.1 mg, 12% for 5 steps).

IR (neat): 3371, 2909, 2833, 1641, 1513, 1298, 1173 cm⁻¹; ¹H NMR (600 MHz, CD₃OD): δ 8.70 (d, *J* = 2.8 Hz, 1H), 8.47 (dd, *J* = 9.4, 2.8 Hz, 1H), 7.70 (d, *J* = 9.4 Hz, 1H), 5.99–5.97 (m, 1H), 5.65 (ddd, *J* = 152.4, 9.3, 4.8 Hz, 1H), 5.01 (dddd, *J* = 49.0, 10.1, 3.7, 3.7 Hz, 1H), 4.30 (apparent t, *J* = 4.3 Hz, 1H), 4.28–4.24 (m, 1H), 4.24 (d, *J* = 15.2 Hz, 1H), 4.16 (d, *J* = 15.2 Hz, 1H); ¹³C[¹H]NMR (151 MHz, CD₃OD) δ 157.4 (d, *J* = 1.8 Hz), 148.2, 141.7, 141.0, 129.7, 122.3, 117.7 (dd, *J* = 3.6, 2.2 Hz), 117.5 (dd, *J* = 46, 4.5 Hz), 89.8 (dd, *J* = 185.3, 40.2 Hz), 75.3 (d, *J* = 16.6 Hz), 75.2 (d, *J* = 16.6 Hz), 68.5 (d, *J* = 17.8 Hz), 68.4 (dd, *J* = 6.4, 1.6 Hz), 63.3 (d, *J* = 5.0 Hz); HRMS (ESI): *m/z* [M + Na]⁺ calcd for C₁₂H₁₃FN₂NaO₈¹³C: 368.0582; found: 368.0579; *m/z* [M + Na]⁺ calcd for C₁₂H₁₃FN₂NaO₇¹³C¹⁸O: 370.0624; found: 370.0617.

4-Nitrophenyl 5,5a-didehydro-5a-carba-2-fluoro-α-L-arabino-(1-¹³C)- and (1-¹³C,1-¹⁸O)-hexopyranoside (S-6) To a solution of **16** (26.1 mg, 0.1 mmol) in MeOH (1 mL) at 0 °C was added K₂CO₃ (13.8 mg, 0.1 mmol). The resulting mixture was stirred at 0 °C for 1 h and then filtered through a pad of silica gel. The solvents were removed *in vacuo* and the residue was dissolved in THF (2 mL). PPh₃ (31.5 mg, 0.12 mmol) and 4-nitrophenol⁴ (13.9 mg, 0.1 mmol, pNP¹⁶OH: pNP¹⁸OH = 1:1) were added at ambient temperature. The reaction was cooled down to 0 °C and diisopropyl azodicarboxylate (23.6 μL, 0.12 mmol) was added dropwise. The mixture was then warmed up to ambient temperature and stirred for 2 h, then was treated with H₂O. The reaction was extracted with Et₂O and the combined organic layers were washed with brine and then were dried over Na₂SO₄. The solvents were removed *in vacuo* and the residue was

purified by flash column chromatography (pentane:ethyl acetate, 5:1) to yield **S-7** as a yellow oil. This compound was then dissolved in MeOH (1 mL), and TFA (80 μ L) and H₂O (20 μ L) were added. The resulting solution was stirred at ambient temperature for 4 h. The solvents were removed *in vacuo* and the residue was purified by flash column chromatography (CH₂Cl₂:MeOH, 12:1) to yield **S-6** as a white foam (14.4 mg, 48% for 3 steps).

IR (neat): 3376, 3355, 2931, 2855, 1631, 1608, 1533, 1303, 1251, 1055 cm^{-1} ; ¹H NMR (600 MHz, CD₃OD): δ 8.21 (d, $J = 9.3$ Hz, 2H), 7.17 (d, $J = 9.3$ Hz, 2H), 5.96-5.94 (m, 1H), 5.40 (ddt, $J = 149.7, 7.0, 4.4$ Hz, 1H), 5.00 (ddd, $J = 49.4, 9.6, 3.7$ Hz, 1H), 4.30 (d, $J = 4.1$ Hz, 1H), 4.26-4.23 (m, 1H), 4.22 (d, $J = 15.0$ Hz, 1H), 4.15 (d, $J = 15.0$ Hz, 1H); ¹³C NMR (151 MHz, CD₃OD) δ 165.14, 165.12, 146.2, 142.9, 132.5, 132.4, 130.8, 130.6, 126.8, 118.9 (d, $J_{\text{C-F}} = 4.3$ Hz), 118.6 (d, $J_{\text{C-F}} = 4.3$ Hz), 116.80, 116.78, 90.5 (d, $J_{\text{C-F}} = 184.0$ Hz), 90.2 (d, $J_{\text{C-F}} = 184.3$ Hz), 73.22 (d, $J_{\text{C-F}} = 16.6$ Hz), 73.20 (d, $J_{\text{C-F}} = 16.6$ Hz), 68.8, 68.7, 68.31, 68.27, 63.4, 63.3; HRMS (ESI): m/z [M + Na]⁺ calcd for C₁₂H₁₄FNNaO₆¹³C: 323.0731; found: 323.0720; m/z [M + Na]⁺ calcd for C₁₂H₁₄FNNaO₅¹³C¹⁸O: 325.0773; found: 325.0758; $[\alpha]_{\text{D}}^{20}$ (CH₃OH, $c = 0.17$): +155.4.

KIE Measurements on $k_{\text{cat}}/K_{\text{m}}$; $k_{\text{H}}/k_{\text{D}}$. Competitive V/K KIEs were measured using ¹⁹F[¹H]NMR spectroscopy on a Bruker AVANCE III QCI cryoprobe 600 MHz spectrometer.⁵ Fluorine-19 T₁ values were measured for 2-fluorocyclohexanol (internal standard) and unlabelled compound at 25 °C and pH 7.4 using standard inversion recovery pulse sequence and determined to be 4.429 s and 1.226 s, respectively. In a typical experiment, a mixture of two labelled isotopologues (approx. 0.2 mg of each) and 2-fluorocyclohexanol (0.25 mg) was dissolved in 650 μ L buffer (25 mM HEPES, pH 7.4, 10% v/v D₂O) and transferred into a low pressure gas-tight "Young" 5 mm glass NMR tube. Reactions were initiated by the addition of enzyme (10 μ L of 7.3 mg mL⁻¹). The magnetic field was shimmed to obtain symmetrical (as close to a Lorentzian shape as possible) peaks. ¹H-NMR and ¹⁹F-NMR spectra were then acquired before sequentially acquiring 10–15 proton-decoupled ¹⁹F-NMR spectra using an inverse-gated pulse sequence.^{6, 7} Spectra were acquired every 12 hours at 25 °C, reactions were kept at 37 °C between acquisitions. FIDs were acquired for 32 scans (acquisition time per scan of 4.61 s) with a relaxation delay of 40.0 s (24 min per spectrum). The resultant quantitative ¹⁹F spectra were deconvoluted by performing the following operations: i) Fourier transformation of the FIDs was performed with two-fold zero-filling and application of an exponential line broadening of 6.0 Hz; ii) spectra were manually phased and baseline corrected using MestReNova version 10.0.2; iii)

spectra were fit using standard MestReNova line fitting algorithm for a generalized Lorentzian line shape; iv) to optimize the calculated fit peak positions, peak widths at half-height, peak heights and optimal combination of Lorentzian and Gaussian (L/G) shapes for each individual peak were allowed to vary; and v) the peak areas were normalized relative to that of the internal standard. Then, for each spectrum the apparent fraction of reaction (F_1) for the lighter isotopologue and the associated R values were calculated from the respective integrals. Next, we corrected these values for the presence of 4% of the L-enantiomer (ee = 92%) by subtraction of 4% of the initial integral for each isotopologue from all integrals in each experiment. The resulting data were then fit using GraphPad Prism 8.2 and a non-linear least squares regression to equation 1.⁸ Of note, this correction did not result in significant changes to the evaluated KIEs. Table S1 shows the calculated KIE values for enantiomeric excesses of 90–94%.

Determinations of k_{12}/k_{13} KIEs. We followed identical data acquisition, spectral deconvolution, and peak fitting procedures to those reported above for the ^2H KIE, using an isotopologue mixture of (1- ^2H)-**4** and (1- ^{13}C)-**4**. In this case, we first corrected for these values for the presence of 4% of the L-enantiomer (see above) and we then accounted for incomplete deuteration (95.6 atom % ^2H) by subtracting 4.4% of the ^2H -integral from the t_0 integral for ^{13}C -isotopologue (due to the overlap of the ^1H and ^{13}C isotopologue signals in the ^{19}F -NMR spectrum. The value of the integral to be subtracted due to incomplete deuteration was calculated using our measured ^2H -KIE of 1.17 and the measured fraction of reaction (F). That is, the relative amount of ^1H -**4** decreases faster than the corresponding amount ^2H -**4** due to the secondary deuterium KIE. Regardless, this calculated correction did not result in significant changes to the evaluated KIEs.

Determinations of k_{16}/k_{18} KIEs. Competitive V/K KIEs were measured using ^{13}C NMR spectroscopy on a Bruker AVANCE III QCI cryoprobe 600 MHz spectrometer.⁵ Carbon-13 T_1 values were measured for phenyl 1-thio- β -D-(1- ^{13}C)glucopyranoside (internal standard), and (1- ^{13}C)-**4** and (1- ^{13}C ,1- ^{18}O)-**4** (60:40) at 50 °C and pH 7.4 using standard inversion recovery pulse sequence and determined to be 1.6 s (standard), 0.774 s (^{13}C , ^{16}O) and 0.854 s (^{13}C , ^{18}O). In a typical experiment, (1- ^{13}C)-**4** and (1- ^{13}C ,1- ^{18}O)-**4** (approx. 0.6 mg total) and internal standard (0.25 mg) was dissolved in 650 μL buffer (25 mM HEPES, pH 7.4, 10% v/v ethanol- d_6) and transferred into a low pressure gas-tight (J.Young) 5 mm glass NMR tube. Reactions were initiated by the addition of enzyme (100 μL of 7.3 mg mL^{-1} stock). The magnetic field was

shimmed to obtain symmetrical (as close to a Lorentzian shape as possible) peaks. ^1H -NMR and ^{13}C -NMR spectra were then acquired before sequentially acquiring 25–30 proton-decoupled ^{13}C NMR spectra using an inverse-gated pulse sequence.^{6, 7} FIDs were acquired at 50 °C for 512 scans (acquisition time per scan of 0.87 s) with a relaxation delay of 16.0 s (2.4 h per spectrum).

The resultant quantitative ^{13}C spectra were deconvoluted by performing the following operations: i) Fourier transformation of the FIDs was performed with 4-fold zero-filling and application of an exponential line broadening of 0.8 Hz; ii) spectra were manually phased and baseline corrected using MestReNova version 10.0.2; iii) spectra were fit using standard MestReNova line fitting algorithm for a generalized Lorentzian line shape; iv) to optimize the calculated fit peak positions, peak widths at half-height, peak heights and optimal combination of Lorentzian and Gaussian (L/G) shapes for each individual peak were allowed to vary; and v) the peak areas were normalized relative to that of the internal standard. Next, we corrected these values for the presence of 3% of the L-enantiomer (ee = 94%) by subtraction of 3% of the initial integral for each isotopologue from all integrals in each experiment. Then, for each spectrum the fraction of reaction (F_1) for the lighter isotopologue and the associated R values were calculated from the respective integrals. These data were then fit using GraphPad Prism 8.2 and a non-linear least squares regression to equation 1 (Figure S2).

KIE Measurements on k_{react} ; $k_{\text{H}}/k_{\text{D}}$. Secondary ^2H kinetic isotope effects on V_{max} for the turnover of 2,4-dinitrophenyl 2-deoxy-2-fluoro-5,5a-didehydro-5a-carba- α -L-arabino-hexopyranoside (**4**) were measured by monitoring the change in absorbance at 400 nm, using a Cary 300 UV-Vis spectrophotometer equipped with a temperature controller, following the addition of concentrated substrate to HEPES buffer (50 mM, pH 7.4, 1 mg/mL BSA) T = 37 °C. Specifically, ten initial rate measurements for hydrolysis of 40 μM ($10 \times K_m$) **4** and ($1\text{-}^2\text{H}$)-**4** by *TmGala* were measured, which were performed in the order $^1\text{H } ^2\text{H}$, $^2\text{H } ^1\text{H}$, $^1\text{H } ^2\text{H}$, etc. The KIE was determined by calculating the ratio $k_{\text{H}}/k_{\text{D}}$, where k_{H} and k_{D} are the individual runs and the KIE was calculated as the mean of these ten rates.

Additional kinetic measurements

In order to determine whether we could measure competitive ^{18}O -leaving group V/K KIEs on the mixture of isotopologues, ($1\text{-}^{13}\text{C}$)-**S-6** and ($1\text{-}^{13}\text{C}, 1\text{-}^{18}\text{O}$)-**S-6**, we determined that the reaction occurred too slowly at 50 °C, pH 7.4, for the acquisition of data. Therefore, we raised the temperature to 70 °C and noted that over the course of 600 hrs, approximately 10% of **S-6** had

reacted, whereas, for a sample of (1-¹³C)-**4** and (1-¹³C,1-¹⁸O)-**4** containing the same concentration of enzyme at 50 °C, the fraction of reaction was 60% in 60 hrs. Taking these two points the 4-nitrophenyl inhibitor is around 100-fold less reactive at 70 °C than is the 2,4-dinitrophenyl at 50 °C. Importantly, given that the half-life of the covalent intermediate (at 37 °C) formed in these reactions is 20 minutes,² the rate-limiting step for turnover of these covalent inhibitors has changed from intermediate hydrolysis (DNP-inhibitor; **4**) to formation of the intermediate (PNP-inhibitor, **S-6**). As a result, the change in rate constant for formation of the covalent intermediate is greater than that measured for simple turnover of the inhibitors as the leaving group is changed from 4-nitrophenolate to 2,4-dinitrophenolate.

Computational details.

Molecular model set up. The starting structure for the computer simulations of the binding and hydrolysis of **4** (Figure S3) by *Thermotoga maritima* α -galactosidase (*TmGalA*) was adapted from the X-Ray structure in Protein Data Bank under code 5M12.⁹ This structure of *TmGalA* in complex with an intact cyclopropyl carbasugar was modified to correspond to intact covalent inhibitor **4** at the active site. The missing atoms of Lys77 and Glu80 residues in X-Ray structure were incorporated with Accelrys Discovery Studio Visualizer v 4.5.¹⁰ Charges and parameters for inhibitor **4** were calculated using Antechamber software package¹¹ with a general AMBER force field (GAFF),¹² listed in Table S3. Hydrogen atoms were added to the protein structure using the tLEAP¹² module of Amber Tools program. The protonation state of titratable amino acids at pH 7.4 was previously determined using pK_a results calculated with PROPKA ver. 3.1¹³ available on PDB2PQR server.¹⁴ The obtained results indicate that residues Asp387 and Glu459 are present in their protonated form. Furthermore, residue Glu224 was protonated to allow more favorable hydrogen bonding between neighboring Asp221 and inhibitor **4**. Additionally, His30 and His273 were protonated at the δ -position, all other histidine residues were protonated at the ϵ -position. The total charge of the system was neutralized by incorporation of 17 sodium cations (Na⁺) in the most electrostatically favorable positions. Subsequently, the system was placed in orthorhombic box of TIP3P¹⁵ water molecules with size of 89 × 96 × 79 Å³ and geometries of the remaining water molecules were then optimized. The full system consists of the protein (8453 atoms), the substrate (37 atoms in E•**4** and 23 atoms in CI-2), and 17398 solvation water molecules (52194 atoms).

Molecular dynamics (MD). Using NAMD molecular dynamics program,¹⁶ the prepared computational model was heated from 0 to 310 K with 0.001 K temperature increment, the system was then equilibrated at the E•I state using the Langevin-Verlet algorithm,¹⁷ and finally 10 ns of classical MD simulation (at temperature 310 K) was carried out in the NVT ensemble. Periodic boundary conditions (PBC) using the particle mesh Ewald method were applied. To improve calculation time, a nonbonding interaction cut-off was applied using a smooth switching function between 14.5 to 16.0 Å. The time dependence of RMSD, temperature and total energy confirms that the system is equilibrated after 10 ns of the MD simulation. (Figure S4).

QM/MM simulations. In this work, an additive hybrid QM/MM scheme was employed for the construction of the total Hamiltonian where the total energy is obtained from the sum of each contribution to the energy (Equation S1).

Here, E_{QM} describes the atoms in the QM part, $E_{\text{QM/MM}}$ defines the interaction between the QM and MM region and E_{MM} describes the rest of the MM part. As shown in Figure S5, the two active site aspartate residues, Asp327 and Asp387, together with full inhibitor **4** and one water molecule were described at QM level in the QM/MM simulations, E. To saturate the valence of the QM/MM frontier atoms, two link atoms¹⁸ were inserted where the QM/MM boundary intersected covalent bonds in the positions indicated on Figure S5. The Austin Model 1 (AM1)¹⁹ semiempirical and the Minnesota Functional M06-2X²⁰ with the standard 6-31+G(d,p) basis set were used to treat the QM sub-set of atoms, as implemented in Gaussian09 program.²¹

The last structure from the 10 ns MM MD simulation was used in order to run QM/MM calculations using a modified fDynamo library.²² To reduce time of calculations, positions of atoms presented beyond 20 Å from the inhibitor **4** were fixed.

Potential Energy Surfaces (PESs). The PES shown in Figure S6 reveals that deprotonation of Asp387, by the leaving group, and leaving group departure occur subsequent to covalent bond formation. The x-axis corresponds to the difference of leaving group oxygen-anomeric carbon distance and nucleophile aspartate oxygen-anomeric carbon distance; and the y-axis corresponds to the difference of general acid oxygen-proton distance and general acid proton-leaving group oxygen distance (Figure S7):

$$x = d(\text{C1}-\text{O}^{\text{LG}}) - d(\text{C1}-\text{O}^{\text{Asp327}}) \quad y = d(\text{H}^{\text{Asp387}}-\text{O}^{\text{Asp387}}) - d(\text{H}^{\text{Asp387}}-\text{O}^{\text{Asp387}})$$

The PES for the alkylation step, E•4 to CI-1 is shown in Figure S8 where the x-axis corresponds to the anomeric carbon-leaving group oxygen distance, and the y-axis corresponds to nucleophilic aspartate oxygen-anomeric carbon distance (Figure S7).

$$x = d(C1-O^{LG}) \quad y = d(C1-O^{Asp327})$$

To generate the PESs for the hydrolysis step, CI-2 to E•5 (Figure S9A), the leaving group and general acid Asp387 proton was previously removed from the system and the cavity was filled with 5 water molecules. Next, 500 ps of AM1/MM MD was run where the position of all atoms beyond distance of 20 Å from the substrate was fixed, thus generating the CI-2 intermediate after equilibration. Finally, the AM1/MM PES for the hydrolysis of this covalent intermediate and generation of compound E•5 in the active site was obtained by controlling key interatomic distances. The x-axis corresponds to the difference of general acid oxygen-proton distance and general acid proton-leaving group oxygen distance; the y-axis corresponds to the difference of Asp327 oxygen-anomeric carbon distance and nucleophilic water oxygen-anomeric carbon distance (Figure S9):

$$x = d(O^{Wat} - H^{Wat}) - d(H^{Wat} - O^{Asp387}) \quad y = d(O^{Asp327} - C1) - d(C1 - O^{Wat})$$

Free Energy Surfaces. In order to generate the free energy surfaces (FESs), in terms of 1D- or 2D- potential of mean force (PMFs), potential energy surfaces (PESs) were computed first to generate the required grid of structures (see above). Then, FESs were generated using the Umbrella Sampling approach^{23, 24} combined with the Weighted Histogram Analysis Method (WHAM).²⁵ For each structure of the grid generated to construct the PES, MD simulations were performed with a total of 5 ps of equilibration (with 1 fs time step) and 20 ps of production at 310 K using the Langevin-Verlet algorithm¹⁷ with a time step of 0.5 fs and an umbrella force constant of 5000 kJ·mol⁻¹·Å⁻² to constrain the key interatomic distances defining the reaction coordinates. 441, 80 and 2501 windows were employed for the FES of the alkylation step, proton transfer (Figure S10), and the hydrolysis steps, respectively (Fig. 3A, 3B and 3C, respectively).

Because a large number of structures have to be sampled during the QM/MM MD simulations, the semiempirical the Austin Model 1 (AM1)¹⁹ Hamiltonian was selected to describe the QM sub-set of atoms.

Spline corrections. In order to improve the quality of the FESs due to possible limitations associated to the semiempirical method, the FESs were corrected at DFT/MM level. Thus, based

on the work of Truhlar and co-workers for reactions in solution²⁶⁻²⁸ a spline under tension^{29, 30} is used to interpolate this correction term at any value of the reaction coordinate, ξ_1 and ξ_2 in the case of two dimensional PMFs, selected to generate the free energy surfaces.^{31, 32}

A continuous energy function is used to obtain the corrected PMFs (Equation S2) where S is the two-dimensional spline function and ΔE_{LL}^{HL} is the difference between the energies obtained at low-level (LL) and high-level (HL) of theory of the QM part. The AM1 semiempirical Hamiltonian was used as LL method, while a density functional theory (DFT)-based method was selected for the HL energy calculation. In particular, HL energy calculations were performed by means of the hybrid M06-2X²⁰ functional using the standard 6-31+G(d,p) basis set. These calculations were carried out using the Gaussian09 program.²¹

From the DFT corrected FESs, structures were selected for GS/TS localization with Baker's algorithm³³ at M06-2X/OPLS-AA/TIP3P level, using the 6-31+G(d,p) basis set for the treatment of the QM subset of atoms. The fDYNAMO library, in combination with Gaussian 09²¹ were used for these calculations. From the localized TS structures, the minimum energy path was traced to reactants and products using the Intrinsic Reaction Coordinate (IRC) method.³⁴

Water-solvated substrate ground state optimizations. The structure of substrate **4** was solvated in an orthorhombic box of water which extended 15 Å from the substrate. 20 ps of AM1/MM MD was produced on this system using the fDYNAMO library, after which GS localization was performed with the same aforementioned DFT/MM method, with the substrate described at the QM level and water molecules described with TIP3P force field.

Map of electrostatic potential (MEP). The MEP shown in Fig. 5A was visualized with GaussView5.0³⁵ (isovalue = 0.0375) from the electron density and potential cubes generated from the checkpoint files for the optimized structures of TS_{alk} obtained using with Gaussian09²¹ in combination with fDYNAMO.

Kinetic Isotope Effects (KIEs). KIEs were computed for isotopic substitutions of key atoms for alkylation and hydrolysis step. Standard deviations on these KIEs were computed based on the averages over all possible combinations of 3 RC and 3 TS structures optimized at M06-2X/MM level of theory, using the 6-31+G(d,p) basis set for the treatment of the QM subset of atoms. Additionally, average KIEs were computed at lower AM1/MM level of theory from 100 couples of stationary structures. This strategy of computing average values of KIEs at two different levels of theory with obviously different number of structures we have previously used in other

studies.³⁶ Then, from the definition of the free energy of a state, G_i , as a function of the internal energy, U_i , the total partition function, Q_i , and the zero-point vibrational energy, ZPE_i (Equation S3), the ratio between the rate constants corresponding to the light atom "L" and the heavier isotope "H" can be computed using Transition State Theory (TST) (Equation S4). In Equation S4, the total partition function, Q , was obtained as the product of the translational, rotational, and vibrational partition functions computed for the isotopologues in the ground and transition state. The Born–Oppenheimer, rigid-rotor, and harmonic oscillator approximations were considered to independently compute the different contributions, without the scaling of vibrational frequencies, as explained and applied in previous papers.^{37, 38} The full $3N \times 3N$ Hessians have been subjected to a projection procedure to eliminate translational and rotational components, which give rise to small nonzero frequencies, as previously described.³⁹ Thus, it has been assumed that the $3N-6$ vibrational degrees of freedom are separable from the 6 translational and rotational degrees of freedom of the substrate. The subset of atoms used to define the Hessian for all the KIE calculations were those of the QM region, consistent with the “cut-off rule” and the local nature of isotope effects.³⁹ Analysis of the transition vector of the TS_{alk} confirms that it is dominated by leaving-group departure, whereas TS_{hyd} is dominated by proton transfer.

$$E_{QM/MM} = E_{QM} + E_{QM/MM}^{elect} + E_{QM/MM}^{vdW} + E_{MM} \quad (\text{equation S1})$$

$$E = E_{LL/MM} + S[\Delta E_{LL}^{HL}(\xi_1, \xi_2)] \quad (\text{equation S2})$$

$$G_i = U_i - RT \ln Q_i + ZPE_i \quad (\text{equation S3})$$

$$KIE = \frac{\left(\frac{Q_{TS}}{Q_R}\right)_L}{\left(\frac{Q_{TS}}{Q_R}\right)_H} e^{-1/RT(\Delta ZPE_L - \Delta ZPE_H)} \quad (\text{equation S4})$$

Table S1. Calculated KIE values versus the enantiomeric excess for both **4** and **(1-²H)-4**.

Enantiomeric Excess	90	92	94
α -SDKIE (run 1) – k_H/k_D	1.168 ± 0.015	1.167 ± 0.015	1.167 ± 0.015
α -SDKIE (run 2) – k_H/k_D	1.165 ± 0.014	1.164 ± 0.014	1.163 ± 0.014
α -SDKIE (run 3) – k_H/k_D	1.186 ± 0.018	1.185 ± 0.018	1.184 ± 0.018

Table S2. Calculated KIE values for enantiomeric excess of 92% for **4**, **(1-²H)-4** and **(1-¹³C)-4** and 94% for the 60:40 mixture of **(1-¹³C)-4** and **(1-¹³C,1-¹⁸O)-4**.

Isotope Effect	Value	Weighted Values ^a
α -SDKIE (run 1) – k_H/k_D	1.167 ± 0.015	1.1704 ± 0.0088
α -SDKIE (run 2) – k_H/k_D	1.164 ± 0.014	
α -SDKIE (run 3) – k_H/k_D	1.185 ± 0.018	
¹³ C-KIE (run 1) – k_{13}/k_D	1.155 ± 0.027	1.1375 ± 0.0115
¹³ C-KIE (run 2) – k_{13}/k_D	1.124 ± 0.035	
¹³ C-KIE (run 3) – k_{13}/k_D	1.135 ± 0.014	
k_{12}/k_{13} calculated		1.029 ± 0.013
¹⁸ O KIE (run 1) – k_{16}/k_{18}	1.038 ± 0.003	1.042 ± 0.001
¹⁸ O KIE (run 2) – k_{16}/k_{18}	1.042 ± 0.001	
¹⁸ O KIE (run 3) – k_{16}/k_{18}	1.049 ± 0.013	

^a Weighted values calculated according to Taylor.⁴⁰

Table S3: Missing atom types, charges and parameters for inhibitor 4

Atom name	Atom type	Charge (e ⁻)	Missing parameters:
C1	c3	0.1532	IMPROPER
C2	c3	0.1255	ca-ca-ca-ha 1.1 180.0 2.0
C3	c3	0.0950	ca-ca-ca-no 1.1 180.0 2.0
C4	c3	0.1382	ca-ca-ca-os 1.1 180.0 2.0
C5	c2	-0.1595	c2-c3-c2-ha 1.1 180.0 2.0
C5a	c2	-0.1563	c2-c3-c2-c3 1.1 180.0 2.0
C6	c3	0.1645	
O1	os	-0.3030	
F2	f	-0.2204	
O3	oh	-0.5689	
O4	oh	-0.5889	
O6	oh	-0.5909	
H1	h1	0.0776	
H2	h1	0.0567	
H3	h1	0.1127	
H4	h1	0.1067	
H5a	ha	0.1599	
H6a	h1	0.0676	
H6b	h1	0.0677	
OH3	ho	0.4150	
OH4	ho	0.4030	
OH6	ho	0.4110	
C1'	ca	0.2200	
C2'	ca	-0.2133	
C3'	ca	0.0079	
C4'	ca	-0.2133	
C5'	ca	-0.0061	
C6'	ca	-0.2021	
N2'	no	0.3281	
O2'a	o	-0.1926	
O2'b	o	-0.1926	
N4'	no	0.3211	
O4'a	o	-0.1961	
O4'b	o	-0.1961	
H3'	ha	0.2059	
H5'	ha	0.1849	
H6'	ha	0.1779	

Table S4. Average distances (in Å) between key atoms computed for the substrate in water (Sub_{aq}), Michaelis complex (E•4) and transition state (TS_{alk} and TS_{hyd}) based on the geometries of 3 stationary structures optimized at M06-2X/MM level.

Distance	Sub _{aq}	E•4	TS _{alk}	TS _{hyd}
C1-O1	1.468 ± 0.005	1.477 ± 0.007	2.212 ± 0.060	C1-OAsp = 2.193 ± 0.019
C1-H1	1.103 ± 0.003	1.093 ± 0.001	1.086 ± 0.002	1.080 ± 0.005
C1-O ^{Nu}	–	3.563 ± 0.314	2.925 ± 0.683	C1-Owat = 2.449 ± 0.298
C1-C2	1.530 ± 0.007	1.516 ± 0.002	1.483 ± 0.004	1.492 ± 0.002
C2-F	1.402 ± 0.000	1.403 ± 0.006	1.378 ± 0.000	1.388 ± 0.005
C2-H2	1.095 ± 0.001	1.096 ± 0.001	1.102 ± 0.002	1.094 ± 0.002
C2-C3	1.516 ± 0.003	1.519 ± 0.002	1.526 ± 0.003	1.527 ± 0.003
C3-H3	1.099 ± 0.001	1.099 ± 0.000	1.095 ± 0.001	1.096 ± 0.003
C3-O3H	1.413 ± 0.004	1.414 ± 0.002	1.409 ± 0.003	1.414 ± 0.004
C3-C4	1.538 ± 0.007	1.532 ± 0.002	1.529 ± 0.003	1.529 ± 0.004
C4-H4	1.098 ± 0.001	1.098 ± 0.000	1.097 ± 0.000	1.097 ± 0.000
C4-O4H	1.424 ± 0.004	1.411 ± 0.000	1.410 ± 0.001	1.412 ± 0.000
C4-C5	1.512 ± 0.002	1.513 ± 0.001	1.516 ± 0.002	1.507 ± 0.003
C5-C7	1.513 ± 0.009	1.506 ± 0.003	1.490 ± 0.004	1.501 ± 0.003
C5-C6	1.335 ± 0.002	1.335 ± 0.001	1.365 ± 0.003	1.356 ± 0.006
C6-H6	1.088 ± 0.000	1.088 ± 0.001	1.085 ± 0.001	1.083 ± 0.000
C6-C1	1.493 ± 0.003	1.497 ± 0.002	1.405 ± 0.009	1.417 ± 0.010
O1-C1'	1.330 ± 0.016	1.336 ± 0.003	1.276 ± 0.002	–
C1'-C2'	1.404 ± 0.008	1.404 ± 0.001	1.435 ± 0.001	–
C2'-H2'	1.092 ± 0.007	1.085 ± 0.002	1.086 ± 0.001	–
C2'-C3'	1.382 ± 0.004	1.382 ± 0.001	1.369 ± 0.003	–
C3'-H3'	1.085 ± 0.003	1.084 ± 0.000	1.084 ± 0.001	–
C3'-C4'	1.398 ± 0.005	1.394 ± 0.000	1.408 ± 0.002	–
C4'-N4'	1.450 ± 0.010	1.455 ± 0.002	1.439 ± 0.001	–
C4'-C5'	1.390 ± 0.005	1.389 ± 0.005	1.385 ± 0.007	–
C5'-H5'	1.088 ± 0.004	1.090 ± 0.009	1.086 ± 0.003	–
C5'-C6'	1.381 ± 0.001	1.383 ± 0.001	1.387 ± 0.004	–
C6'-N6'	1.464 ± 0.003	1.465 ± 0.005	1.454 ± 0.009	–
C6'-C1'	1.414 ± 0.005	1.408 ± 0.002	1.439 ± 0.002	–

Table S5. Average KIEs computed for departure of 2,4-dinitrophenolate from the covalent inhibitor **4** within the active site with an aqueous solvated ground state, optimized at AM1/MM and M06-2X/MM level at temperatures of 310 K and 323 K. Results are derived from 10×10 and 3×3 combinations of structures optimized at AM1/MM and M06-2X/MM level, respectively. Uncertainties correspond to the standard deviations.

1°-KIE	T = 310 K		T = 323 K	
	AM1	M06-2X	AM1	M06-2X
[1- ¹³ C]	1.056 ± 0.003	1.041 ± 0.004		
[1- ¹⁸ O]			1.042 ± 0.002	1.056 ± 0.005
[1- ² H]	1.179 ± 0.020	1.246 ± 0.022		

Table S6. Average secondary deuterium KIE computed for hydrolysis of the covalent enzyme intermediate within the active site with the Michaelis complex (E•**4**) as the ground state, optimized at AM1/MM and M06-2X/MM level at a temperatures of 310 K. Results are derived from 10×10 and 3×3 combinations of structures optimized at AM1/MM and M06-2X/MM level. Uncertainties correspond to the standard deviations.

T = 310 K	E• 4 ⇌ TS _{hyd}	
	AM1	M06-2X
[1- ² H]	1.074 ± 0.009	1.107 ± 0.078

Table S7. Average values of atomic charges (e^-) computed at key atoms using ChelpG method for the substrate in water (GS), and enzyme transition state (TS_{alk}) structures optimized at M06-2X/MM level.

atom	Ground state structures in water					Transition states for covalent labeling					$TS_{charge} - GS_{charge}$	
	GS1	GS2	GS3	average	dev.	TS1	TS2	TS3	average	dev.	charge	dev.
C1	0.427	0.420	0.290	0.379	0.077	0.337	0.475	0.444	0.419	0.072	0.040	0.011
C2	-0.274	-0.115	-0.102	-0.164	0.096	0.114	0.283	0.218	0.205	0.085	0.368	0.265
C3	0.574	0.478	0.424	0.492	0.076	0.362	0.318	0.347	0.342	0.022	-0.150	-0.025
C4	0.488	0.260	0.313	0.354	0.119	0.122	0.170	0.039	0.111	0.066	-0.243	-0.167
C5	0.139	0.260	0.220	0.206	0.062	0.389	0.358	0.485	0.411	0.066	0.205	0.070
C5a	-0.286	-0.345	-0.318	-0.316	0.030	-0.117	-0.224	-0.197	-0.179	0.056	0.137	0.045
C6	0.471	0.387	0.427	0.428	0.042	0.310	0.060	0.215	0.195	0.126	-0.233	-0.153
O1	-0.501	-0.519	-0.536	-0.518	0.018	-0.509	-0.508	-0.532	-0.516	0.014	0.002	0.000
F2	-0.415	-0.401	-0.402	-0.406	0.008	-0.326	-0.277	-0.325	-0.309	0.028	0.097	0.009
O3	-0.519	-0.431	-0.497	-0.482	0.046	-0.487	-0.457	-0.431	-0.458	0.028	0.024	0.003
O4	-0.449	-0.457	-0.502	-0.470	0.029	-0.440	-0.459	-0.419	-0.439	0.020	0.030	0.002
O6	-0.469	-0.417	-0.476	-0.454	0.032	-0.436	-0.612	-0.600	-0.549	0.098	-0.096	-0.018
H1	0.020	0.003	0.007	0.010	0.009	0.038	0.053	0.058	0.050	0.010	0.040	0.038
H2	-0.084	0.037	0.011	-0.012	0.064	0.045	0.047	0.058	0.050	0.007	0.062	0.329
H3	0.189	0.170	0.182	0.180	0.010	0.033	0.071	0.065	0.057	0.020	-0.124	-0.045
H4	0.139	0.196	0.129	0.155	0.036	0.125	0.157	0.123	0.135	0.019	-0.020	-0.005
H5a	0.258	0.224	0.256	0.246	0.019	0.191	0.171	0.213	0.192	0.021	-0.054	-0.007
H6a	0.470	0.452	0.452	0.458	0.011	0.424	0.457	0.427	0.436	0.018	-0.022	-0.001
H6b	0.009	0.066	0.055	0.043	0.030	0.092	0.093	0.103	0.096	0.006	0.053	0.037
OH3	0.080	0.076	0.112	0.090	0.020	0.125	0.057	0.074	0.085	0.035	-0.004	-0.002
OH4	0.229	0.206	0.188	0.208	0.020	0.148	0.193	0.222	0.188	0.037	-0.020	-0.005
OH6	0.512	0.487	0.497	0.499	0.013	0.626	0.640	0.640	0.635	0.008	0.137	0.004
C1'	0.551	0.433	0.540	0.508	0.065	0.680	0.662	0.651	0.664	0.015	0.156	0.020
C2'	-0.201	-0.157	-0.278	-0.212	0.061	-0.297	-0.195	-0.372	-0.288	0.089	-0.076	-0.032
C3'	-0.033	-0.046	0.004	-0.025	0.026	-0.119	-0.132	-0.032	-0.094	0.055	-0.069	-0.082

C4'	-0.054	-0.122	-0.091	-0.089	0.034	0.010	0.028	-0.003	0.012	0.016	0.101	0.141
C5'	-0.117	-0.116	-0.105	-0.113	0.007	-0.143	-0.144	-0.099	-0.129	0.025	-0.016	-0.003
C6'	-0.366	-0.197	-0.229	-0.264	0.090	-0.219	-0.251	-0.256	-0.242	0.020	0.022	0.008
N2'	0.742	0.800	0.789	0.777	0.031	0.700	0.658	0.669	0.676	0.022	-0.101	-0.005
O2'a	-0.604	-0.635	-0.458	-0.566	0.094	-0.881	-0.920	-0.838	-0.880	0.041	-0.314	-0.054
O2'b	-0.861	-0.830	-0.793	-0.828	0.034	-0.699	-0.761	-0.723	-0.728	0.031	0.100	0.006
N4'	0.887	0.771	0.845	0.835	0.059	0.785	0.903	0.788	0.825	0.067	-0.009	-0.001
O4'a	-0.774	-0.684	-0.717	-0.725	0.046	-0.823	-0.854	-0.841	-0.840	0.015	-0.115	-0.008
O4'b	-0.782	-0.860	-0.763	-0.802	0.052	-0.878	-0.848	-0.897	-0.874	0.024	-0.073	-0.005
H3'	0.016	0.011	0.010	0.012	0.004	0.117	0.163	0.154	0.145	0.024	0.133	0.045
H5'	0.046	0.031	0.007	0.028	0.020	0.035	0.052	0.003	0.030	0.025	0.002	0.003
H6'	0.539	0.564	0.508	0.537	0.028	0.558	0.569	0.561	0.563	0.005	0.026	0.001
CB						-0.642	-0.629	-0.619	-0.630	0.012		
HB3						0.142	0.147	0.143	0.144	0.003		
HB2						0.176	0.161	0.165	0.167	0.008		
CG						1.113	1.108	1.129	1.117	0.011		
OD1						-0.988	-1.001	-1.002	-0.997	0.008		
OD2						-0.942	-0.942	-0.969	-0.951	0.016		
CB						-0.380	-0.380	-0.352	-0.370	0.016		
HB3						0.146	0.111	0.105	0.120	0.022		
HB2						0.098	0.096	0.104	0.099	0.004		
CG						1.010	1.023	0.931	0.988	0.050		
OD1						-0.872	-0.868	-0.723	-0.821	0.085		
OD2						-0.828	-0.825	-0.855	-0.836	0.017		
HD2						0.670	0.693	0.649	0.671	0.022		
link-atom						0.154	0.153	0.157	0.155	0.002		
link-atom						0.149	0.156	0.145	0.150	0.006		

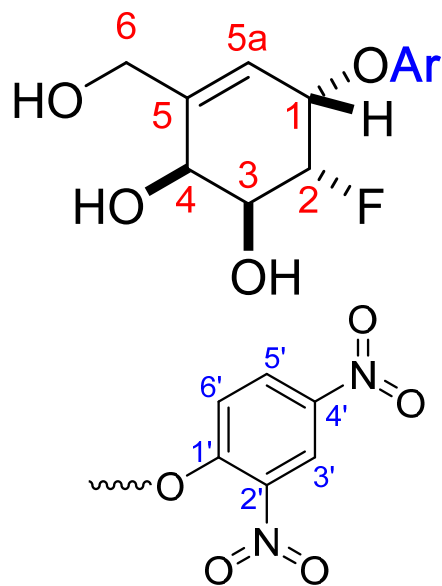


Table S8. Electrostatic potential (in $\text{kJ}\cdot\text{mol}^{-1}\cdot\text{e}^{-1}$) generated by each residue of the protein on the C5 atom of the carbasugar computed in the three TS_{alk} (TS1, TS2 and TS3) optimized at DFT/MM level.

	TS1	TS2	TS3	avg	dev		TS1	TS2	TS3	avg	dev
MET-1	32.257	32.597	32.371	32.409	0.173	HIS-30	-0.929	-0.938	-0.938	-0.935	0.005
GLU-2	-30.971	-31.296	-31.062	-31.109	0.168	LEU-31	-0.203	-0.208	-0.205	-0.206	0.003
ILE-3	0.374	0.381	0.376	0.377	0.004	GLY-32	0.281	0.289	0.283	0.284	0.004
PHE-4	0.455	0.465	0.458	0.460	0.005	TRP-33	-0.501	-0.508	-0.507	-0.505	0.004
GLY-5	0.266	0.271	0.268	0.268	0.002	LYS-34	37.697	38.008	37.873	37.860	0.156
LYS-6	28.020	28.267	28.089	28.125	0.128	ILE-35	-0.448	-0.453	-0.453	-0.452	0.003
THR-7	-0.217	-0.219	-0.218	-0.218	0.001	SER-36	0.591	0.601	0.595	0.596	0.005
PHE-8	0.015	0.017	0.015	0.016	0.001	GLY-37	-0.351	-0.354	-0.354	-0.353	0.002
ARG-9	25.484	25.672	25.558	25.571	0.095	ARG-38	32.024	32.260	32.112	32.132	0.120
GLU-10	-28.355	-28.561	-28.459	-28.458	0.103	VAL-39	-0.154	-0.152	-0.155	-0.154	0.002
GLY-11	-0.328	-0.333	-0.330	-0.331	0.003	LYS-40	31.196	31.419	31.251	31.289	0.116
ARG-12	30.871	31.103	30.968	30.980	0.117	GLY-41	-0.470	-0.478	-0.474	-0.474	0.004
PHE-13	0.011	0.015	0.011	0.012	0.002	SER-42	-0.050	-0.049	-0.050	-0.050	0.000
VAL-14	0.250	0.253	0.250	0.251	0.002	PRO-43	0.084	0.081	0.085	0.083	0.003
LEU-15	-0.155	-0.155	-0.156	-0.155	0.000	GLY-44	0.121	0.127	0.117	0.122	0.005
LYS-16	27.755	27.964	27.809	27.842	0.108	ARG-45	49.272	50.092	49.395	49.587	0.442
GLU-17	-30.094	-30.381	-30.149	-30.208	0.153	LEU-46	-0.634	-0.652	-0.639	-0.642	0.009
LYS-18	29.775	30.064	29.820	29.887	0.156	GLU-47	-35.847	-36.284	-35.953	-36.028	0.228
ASN-19	-0.259	-0.263	-0.262	-0.261	0.002	VAL-48	0.760	0.778	0.767	0.768	0.009
PHE-20	0.241	0.242	0.243	0.242	0.001	LEU-49	-0.455	-0.468	-0.456	-0.459	0.007
THR-21	-0.300	-0.306	-0.300	-0.302	0.004	ARG-50	36.031	36.486	36.142	36.220	0.237
VAL-22	0.411	0.417	0.414	0.414	0.003	THR-51	-0.159	-0.166	-0.158	-0.161	0.004
GLU-23	-30.592	-30.825	-30.676	-30.698	0.118	LYS-52	31.855	32.206	31.955	32.005	0.181
PHE-24	0.401	0.406	0.405	0.404	0.002	ALA-53	0.594	0.611	0.598	0.601	0.009
ALA-25	-0.431	-0.440	-0.433	-0.435	0.005	PRO-54	-0.105	-0.113	-0.103	-0.107	0.006
VAL-26	0.287	0.292	0.290	0.290	0.003	GLU-55	-36.366	-36.788	-36.510	-36.555	0.214
GLU-27	-33.632	-33.894	-33.773	-33.767	0.131	LYS-56	39.353	39.834	39.520	39.569	0.244
LYS-28	30.889	31.143	31.018	31.017	0.127	VAL-57	-0.120	-0.127	-0.119	-0.122	0.004
ILE-29	0.238	0.237	0.240	0.238	0.002	LEU-58	0.901	0.932	0.951	0.928	0.025

	TS1	TS2	TS3	avg	dev		TS1	TS2	TS3	avg	dev
VAL-59	-0.223	-0.229	-0.229	-0.227	0.004	SER-90	0.029	-0.101	0.105	0.011	0.104
ASN-60	-0.321	-0.335	-0.296	-0.317	0.020	VAL-91	0.367	0.368	0.400	0.378	0.019
ASN-61	-1.635	-1.787	-1.727	-1.716	0.077	VAL-92	0.419	0.516	0.450	0.462	0.050
TRP-62	-0.129	-0.185	-0.134	-0.149	0.031	PRO-93	0.586	0.648	0.578	0.604	0.038
GLN-63	-3.093	-3.450	-3.433	-3.325	0.202	ASP-94	-49.634	-50.470	-49.773	-49.959	0.448
SER-64	5.681	4.611	5.517	5.269	0.576	VAL-95	0.794	0.839	0.806	0.813	0.023
TRP-65	4.244	0.025	2.972	2.413	2.164	LEU-96	1.097	1.125	1.086	1.103	0.020
GLY-66	-2.880	-3.125	-3.310	-3.105	0.216	GLU-97	-56.394	-57.203	-56.565	-56.720	0.426
PRO-67	0.108	0.402	0.357	0.289	0.158	ARG-98	43.823	44.587	44.003	44.138	0.400
CYS-68	-0.855	-0.973	-0.844	-0.891	0.071	ASN-99	-0.666	-0.768	-0.701	-0.711	0.052
ARG-69	70.222	71.457	69.186	70.288	1.137	LEU-100	0.758	0.767	0.766	0.763	0.005
VAL-70	-0.916	-1.052	-0.944	-0.971	0.072	GLN-101	-1.853	-1.938	-1.594	-1.795	0.179
VAL-71	0.193	0.175	0.178	0.182	0.010	SER-102	0.344	0.359	0.328	0.344	0.016
ASP-72	-41.886	-42.457	-42.053	-42.132	0.294	ASP-103	-63.482	-64.747	-64.666	-64.298	0.708
ALA-73	-0.282	-0.294	-0.280	-0.285	0.007	TYR-104	1.212	1.241	1.255	1.236	0.022
PHE-74	-0.324	-0.337	-0.322	-0.328	0.008	PHE-105	-1.041	-1.104	-1.053	-1.066	0.034
SER-75	0.126	0.131	0.133	0.130	0.003	VAL-106	0.269	0.279	0.272	0.273	0.005
PHE-76	0.893	0.950	0.932	0.925	0.030	ALA-107	-0.404	-0.420	-0.406	-0.410	0.009
LYS-77	50.752	50.482	50.828	50.687	0.182	GLU-108	-38.186	-38.625	-38.372	-38.395	0.220
PRO-78	0.474	0.560	0.534	0.523	0.044	GLU-109	-38.743	-39.131	-38.943	-38.939	0.194
PRO-79	0.951	0.849	0.820	0.873	0.069	GLY-110	0.480	0.487	0.485	0.484	0.004
GLU-80	-50.470	-50.985	-50.461	-50.639	0.300	LYS-111	35.524	35.902	35.682	35.703	0.190
ILE-81	1.897	1.977	1.873	1.916	0.054	VAL-112	0.713	0.731	0.721	0.721	0.009
ASP-82	-85.115	-83.075	-85.660	-84.617	1.363	TYR-113	-0.158	-0.163	-0.162	-0.161	0.003
PRO-83	-0.416	-0.662	-0.355	-0.478	0.162	GLY-114	0.897	0.919	0.907	0.908	0.011
ASN-84	-1.569	2.357	-2.802	-0.671	2.694	PHE-115	-0.433	-0.441	-0.442	-0.438	0.005
TRP-85	1.055	-0.566	1.141	0.543	0.962	LEU-116	-0.418	-0.419	-0.424	-0.420	0.003
ARG-86	60.473	61.263	60.477	60.738	0.455	SER-117	0.691	0.687	0.694	0.691	0.003
TYR-87	0.896	1.229	1.067	1.064	0.166	SER-118	-1.367	-1.412	-1.381	-1.387	0.023
THR-88	0.524	0.615	1.356	0.831	0.456	LYS-119	43.130	43.472	43.331	43.311	0.172
ALA-89	-0.248	-0.214	-0.213	-0.225	0.020	ILE-120	-0.766	-0.783	-0.766	-0.772	0.010

	TS1	TS2	TS3	avg	dev		TS1	TS2	TS3	avg	dev
ALA-121	-0.527	-0.529	-0.536	-0.531	0.005	LEU-152	0.464	0.478	0.469	0.470	0.007
HIS-122	0.598	0.595	0.757	0.650	0.093	VAL-153	-0.442	-0.457	-0.445	-0.448	0.008
PRO-123	-1.239	-1.287	-1.278	-1.268	0.025	VAL-154	0.207	0.214	0.210	0.210	0.004
PHE-124	0.769	0.800	0.776	0.782	0.017	LEU-155	-0.278	-0.287	-0.280	-0.282	0.005
PHE-125	-0.877	-0.908	-0.883	-0.889	0.016	GLU-156	-33.702	-34.024	-33.852	-33.859	0.161
ALA-126	0.343	0.358	0.343	0.348	0.009	ASP-157	-35.371	-35.650	-35.556	-35.526	0.142
VAL-127	-0.477	-0.493	-0.478	-0.482	0.009	PRO-158	-0.423	-0.432	-0.427	-0.427	0.005
GLU-128	-39.437	-39.999	-39.554	-39.663	0.297	ASN-159	-0.909	-0.929	-0.919	-0.919	0.010
ASP-129	-34.532	-34.959	-34.627	-34.706	0.224	THR-160	0.265	0.276	0.266	0.269	0.006
GLY-130	0.148	0.154	0.147	0.150	0.004	PRO-161	-0.647	-0.656	-0.656	-0.653	0.005
GLU-131	-34.049	-34.456	-34.155	-34.220	0.211	LEU-162	-0.618	-0.625	-0.626	-0.623	0.004
LEU-132	0.673	0.691	0.679	0.681	0.009	LEU-163	-0.210	-0.209	-0.212	-0.210	0.002
VAL-133	-0.582	-0.600	-0.587	-0.590	0.009	LEU-164	-0.065	-0.065	-0.065	-0.065	0.000
ALA-134	0.574	0.587	0.581	0.581	0.006	GLU-165	-45.052	-45.346	-45.362	-45.253	0.175
TYR-135	-0.493	-0.509	-0.501	-0.501	0.008	LYS-166	36.424	36.676	36.624	36.574	0.133
LEU-136	0.618	0.633	0.624	0.625	0.007	TYR-167	-0.453	-0.460	-0.458	-0.457	0.004
GLU-137	-48.626	-49.362	-48.749	-48.913	0.394	ALA-168	0.045	0.049	0.048	0.048	0.002
TYR-138	0.026	0.027	0.025	0.026	0.001	GLU-169	-45.154	-45.414	-45.452	-45.340	0.162
PHE-139	0.102	0.109	0.091	0.101	0.009	LEU-170	0.165	0.178	0.169	0.170	0.007
ASP-140	-39.202	-39.650	-39.247	-39.366	0.247	VAL-171	0.489	0.503	0.499	0.497	0.007
VAL-141	0.465	0.469	0.463	0.466	0.003	GLY-172	0.267	0.275	0.273	0.272	0.004
GLU-142	-34.110	-34.395	-34.146	-34.217	0.155	MET-173	0.290	0.306	0.296	0.297	0.008
PHE-143	0.285	0.287	0.287	0.286	0.001	GLU-174	-41.402	-41.722	-41.597	-41.574	0.162
ASP-144	-32.026	-32.241	-32.071	-32.113	0.113	ASN-175	0.204	0.212	0.211	0.209	0.004
ASP-145	-34.585	-34.829	-34.665	-34.693	0.124	ASN-176	-0.429	-0.438	-0.438	-0.435	0.005
PHE-146	-0.024	-0.022	-0.025	-0.024	0.001	ALA-177	1.183	1.204	1.203	1.197	0.012
VAL-147	0.498	0.500	0.501	0.500	0.001	ARG-178	53.897	53.910	54.145	53.984	0.140
PRO-148	-0.474	-0.487	-0.474	-0.478	0.007	VAL-179	0.860	0.873	0.873	0.869	0.007
LEU-149	0.010	0.021	0.011	0.014	0.006	PRO-180	0.756	0.741	0.754	0.751	0.008
GLU-150	-47.117	-47.649	-47.328	-47.365	0.268	LYS-181	46.730	46.541	46.938	46.736	0.199
PRO-151	-0.902	-0.924	-0.911	-0.912	0.011	HIS-182	-0.184	-0.282	-0.220	-0.229	0.050

	TS1	TS2	TS3	avg	dev		TS1	TS2	TS3	avg	dev
THR-183	0.760	0.819	0.692	0.757	0.063	PHE-214	1.866	1.814	1.863	1.848	0.029
PRO-184	0.141	0.174	-0.086	0.076	0.141	GLU-215	-56.305	-55.856	-56.767	-56.309	0.455
THR-185	2.376	2.252	2.257	2.295	0.070	VAL-216	1.412	1.315	1.259	1.329	0.077
GLY-186	0.655	0.532	0.613	0.600	0.062	PHE-217	0.996	1.124	0.920	1.013	0.103
TRP-187	-1.112	-0.689	-1.040	-0.947	0.226	GLN-218	2.803	5.357	3.371	3.844	1.341
CYS-188	-3.176	-2.671	-3.127	-2.991	0.278	ILE-219	-1.579	-0.609	-1.137	-1.108	0.486
SER-189	2.668	2.605	2.450	2.574	0.112	ASP-220	-317.437	-302.073	-328.961	-316.157	13.490
TRP-190	-16.766	-15.473	-18.227	-16.822	1.378	ASP-221	-194.125	-201.983	-190.982	-195.697	5.667
TYR-191	-11.411	-8.414	-10.550	-10.125	1.543	ALA-222	-0.117	-0.489	0.126	-0.160	0.310
HIE-192	2.102	1.571	1.561	1.745	0.310	TYR-223	7.537	7.528	7.532	7.532	0.004
TYR-193	5.695	5.248	5.543	5.495	0.227	GLU-224	4.666	4.568	4.375	4.536	0.148
PHE-194	5.159	6.028	4.943	5.377	0.574	LYS-225	64.047	63.261	63.559	63.622	0.397
LEU-195	-0.202	0.129	0.807	0.245	0.514	ASP-226	-95.846	-95.410	-94.060	-95.105	0.931
ASP-196	-86.182	-88.108	-83.537	-85.942	2.295	ILE-227	4.808	4.537	4.602	4.649	0.141
LEU-197	0.637	0.103	0.257	0.332	0.275	GLY-228	1.491	1.305	1.458	1.418	0.099
THR-198	-3.975	-3.746	-4.228	-3.983	0.241	ASP-229	-72.838	-71.978	-72.322	-72.379	0.433
TRP-199	-1.488	-1.543	-1.493	-1.508	0.031	TRP-230	0.453	0.595	0.472	0.506	0.077
GLU-200	-58.428	-57.184	-58.165	-57.926	0.656	LEU-231	0.550	0.551	0.537	0.546	0.008
GLU-201	-71.159	-69.738	-70.622	-70.506	0.717	VAL-232	-2.391	-2.301	-2.345	-2.346	0.045
THR-202	-2.156	-2.058	-2.155	-2.123	0.056	THR-233	3.863	3.692	3.820	3.792	0.089
LEU-203	-0.216	-0.223	-0.235	-0.224	0.009	ARG-234	105.782	105.335	104.911	105.342	0.436
LYS-204	70.798	69.378	70.299	70.159	0.720	GLY-235	0.699	0.834	0.630	0.721	0.104
ASN-205	2.902	2.604	2.774	2.760	0.149	ASP-236	-72.726	-70.573	-72.737	-72.012	1.246
LEU-206	0.760	0.745	0.752	0.752	0.008	PHE-237	1.553	1.312	1.565	1.477	0.143
LYS-207	50.001	49.141	49.900	49.680	0.470	PRO-238	-2.517	-2.491	-2.474	-2.494	0.022
LEU-208	1.469	1.397	1.456	1.441	0.038	SER-239	-0.383	-0.357	-0.396	-0.379	0.020
ALA-209	1.146	1.076	1.129	1.117	0.036	VAL-240	0.282	0.285	0.260	0.276	0.014
LYS-210	51.620	50.728	51.609	51.319	0.512	GLU-241	-53.540	-52.720	-53.412	-53.224	0.441
ASN-211	-0.042	-0.070	-0.054	-0.055	0.014	GLU-242	-57.375	-56.362	-57.119	-56.952	0.527
PHE-212	0.680	0.580	0.689	0.650	0.060	MET-243	0.316	-0.409	0.249	0.052	0.400
PRO-213	-0.229	-0.240	-0.191	-0.220	0.026	ALA-244	0.168	0.121	0.157	0.149	0.025

	TS1	TS2	TS3	avg	dev		TS1	TS2	TS3	avg	dev
LYS-245	49.625	48.898	49.511	49.345	0.391	TRP-276	-1.003	-1.032	-1.008	-1.014	0.016
VAL-246	1.106	1.058	1.101	1.088	0.027	VAL-277	1.589	1.619	1.576	1.595	0.022
ILE-247	1.773	1.703	1.766	1.747	0.038	VAL-278	-0.484	-0.468	-0.465	-0.472	0.010
ALA-248	0.485	0.455	0.472	0.470	0.015	LYS-279	49.656	49.980	49.502	49.713	0.244
GLU-249	-48.311	-47.579	-48.300	-48.063	0.419	GLU-280	-57.931	-58.199	-56.829	-57.653	0.726
ASN-250	1.761	1.689	1.749	1.733	0.039	ASN-281	-1.638	-1.675	-1.631	-1.648	0.024
GLY-251	0.263	0.242	0.255	0.254	0.011	GLY-282	0.083	0.095	0.088	0.088	0.006
PHE-252	1.331	1.398	1.383	1.371	0.035	GLU-283	-50.166	-50.697	-50.006	-50.290	0.361
ILE-253	-1.388	-1.250	-1.367	-1.335	0.075	PRO-284	-0.248	-0.225	-0.107	-0.193	0.076
PRO-254	0.251	0.253	0.275	0.260	0.013	LYS-285	62.061	63.538	62.012	62.537	0.867
GLY-255	1.817	1.917	1.608	1.781	0.158	MET-286	2.386	1.499	2.125	2.003	0.456
ILE-256	2.622	1.957	2.548	2.376	0.364	ALA-287	1.385	1.392	1.380	1.386	0.006
TRP-257	5.293	9.819	6.476	7.196	2.347	TYR-288	-4.078	-4.815	-4.114	-4.336	0.415
THR-258	-0.591	-0.917	-0.454	-0.654	0.238	ARG-289	76.276	75.973	75.153	75.801	0.581
ALA-259	0.909	1.002	1.028	0.980	0.063	ASN-290	17.840	13.098	15.288	15.409	2.373
PRO-260	2.406	2.297	2.202	2.302	0.102	TRP-291	9.139	7.699	8.896	8.578	0.771
PHE-261	1.898	1.854	1.728	1.827	0.088	ASN-292	2.395	2.838	2.322	2.518	0.279
SER-262	-5.520	-5.251	-5.507	-5.426	0.152	LYS-293	79.364	82.450	79.350	80.388	1.786
VAL-263	-0.778	-0.738	-0.783	-0.766	0.024	LYS-294	67.916	68.333	67.252	67.834	0.545
SER-264	3.903	3.911	4.208	4.007	0.174	ILE-295	1.800	1.700	1.832	1.777	0.069
GLU-265	-72.517	-73.218	-72.081	-72.605	0.574	TYR-296	-3.782	-3.544	-3.805	-3.710	0.145
THR-266	0.452	0.277	0.550	0.426	0.138	ALA-297	0.491	1.633	0.489	0.871	0.660
SER-267	2.117	1.967	2.034	2.040	0.075	LEU-298	-0.884	-0.314	-0.961	-0.720	0.353
ASP-268	-57.150	-56.894	-56.923	-56.989	0.140	ASP-299	-54.115	-54.537	-54.086	-54.246	0.253
VAL-269	2.134	2.049	2.065	2.083	0.045	LEU-300	1.111	1.141	1.106	1.119	0.019
PHE-270	1.762	1.684	1.705	1.717	0.040	SER-301	1.456	1.485	1.454	1.465	0.017
ASN-271	2.734	2.690	2.679	2.701	0.029	LYS-302	46.202	46.359	46.118	46.226	0.122
GLU-272	-50.094	-49.971	-49.880	-49.982	0.108	ASP-303	-46.243	-46.299	-46.229	-46.257	0.037
HIS-273	-0.636	-0.614	-0.628	-0.626	0.011	GLU-304	-45.670	-45.751	-45.604	-45.675	0.074
PRO-274	-0.899	-0.924	-0.901	-0.908	0.014	VAL-305	-0.706	-0.662	-0.687	-0.685	0.022
ASP-275	-48.717	-48.872	-48.578	-48.722	0.147	LEU-306	-1.087	-1.059	-1.083	-1.076	0.015

	TS1	TS2	TS3	avg	dev		TS1	TS2	TS3	avg	dev
ASN-307	-1.420	-1.381	-1.411	-1.404	0.020	LYS-339	42.833	43.010	42.808	42.883	0.110
TRP-308	0.078	0.158	0.066	0.101	0.050	LYS-340	42.301	42.504	42.329	42.378	0.110
LEU-309	-0.760	-0.705	-0.755	-0.740	0.031	ASN-341	1.113	1.136	1.112	1.120	0.014
PHE-310	-1.142	-1.098	-1.145	-1.128	0.026	ILE-342	-0.033	-0.037	-0.026	-0.032	0.006
ASP-311	-57.112	-56.660	-56.989	-56.920	0.233	THR-343	-0.549	-0.525	-0.548	-0.541	0.014
LEU-312	0.939	1.008	0.945	0.964	0.038	PRO-344	-0.893	-0.980	-0.980	-0.951	0.050
PHE-313	-0.106	-0.045	-0.086	-0.079	0.031	ILE-345	-1.275	-1.317	-1.316	-1.303	0.024
SER-314	0.391	0.418	0.379	0.396	0.020	GLN-346	-0.415	-0.420	-0.428	-0.421	0.007
SER-315	1.899	1.899	1.889	1.896	0.006	ALA-347	-0.163	-0.125	-0.175	-0.154	0.026
LEU-316	1.216	1.240	1.207	1.221	0.017	PHE-348	-0.551	-0.517	-0.564	-0.544	0.024
ARG-317	57.522	57.048	57.572	57.381	0.289	ARG-349	53.543	54.077	53.799	53.806	0.267
LYS-318	48.964	48.462	48.872	48.766	0.267	LYS-350	48.683	48.877	48.766	48.776	0.097
MET-319	-0.537	-0.469	-0.510	-0.505	0.034	GLY-351	0.390	0.471	0.506	0.456	0.059
GLY-320	0.320	0.336	0.334	0.330	0.008	ILE-352	0.047	0.107	0.014	0.056	0.047
TYR-321	3.076	2.990	3.228	3.098	0.121	GLU-353	-52.219	-52.392	-52.367	-52.326	0.093
ARG-322	60.344	59.537	60.410	60.097	0.486	THR-354	0.713	0.736	0.737	0.729	0.014
TYR-323	-3.718	2.150	-4.055	-1.874	3.489	ILE-355	1.629	1.671	1.618	1.639	0.028
PHE-324	3.006	3.006	2.770	2.927	0.136	ARG-356	62.342	62.267	62.664	62.424	0.211
LYS-325	274.942	286.990	278.411	280.114	6.202	LYS-357	48.451	48.498	48.557	48.502	0.053
ILE-326	-0.149	-0.211	-0.081	-0.147	0.065	ALA-358	1.404	1.414	1.408	1.409	0.005
PHE-328	9.866	11.299	9.433	10.199	0.977	VAL-359	1.204	1.232	1.225	1.220	0.015
LEU-329	2.838	2.623	2.650	2.704	0.117	GLY-360	-1.909	-1.875	-1.925	-1.903	0.026
PHE-330	4.129	4.671	4.283	4.361	0.279	GLU-361	-51.986	-51.803	-52.214	-52.001	0.206
ALA-331	4.390	4.528	4.333	4.417	0.100	ASP-362	-56.774	-56.206	-56.905	-56.628	0.372
GLY-332	2.299	2.156	2.232	2.229	0.072	SER-363	1.275	1.267	1.291	1.277	0.012
ALA-333	1.759	1.858	1.717	1.778	0.073	PHE-364	-0.563	-0.658	-0.628	-0.617	0.049
VAL-334	1.243	1.191	1.199	1.211	0.028	ILE-365	2.742	2.598	2.586	2.642	0.087
PRO-335	-0.899	-0.919	-0.853	-0.890	0.034	LEU-366	-2.363	-1.991	-1.937	-2.097	0.232
GLY-336	-0.063	-0.072	-0.072	-0.069	0.005	GLY-367	-0.309	-0.821	-0.864	-0.665	0.309
GLU-337	-45.547	-45.964	-45.490	-45.667	0.259	CYS-368	5.465	5.826	5.123	5.471	0.352
ARG-338	61.790	62.482	61.738	62.004	0.415	GLY-369	4.174	4.811	4.575	4.520	0.322

	TS1	TS2	TS3	avg	dev		TS1	TS2	TS3	avg	dev
SER-370	-0.386	-0.614	1.211	0.070	0.994	PRO-402	3.879	3.644	3.858	3.794	0.130
PRO-371	-0.617	-0.638	-0.001	-0.419	0.362	ALA-403	-1.989	-1.844	-1.922	-1.918	0.073
LEU-372	0.360	0.372	0.577	0.436	0.122	ALA-404	-1.269	-0.985	-0.846	-1.033	0.215
LEU-373	0.108	0.152	0.091	0.117	0.032	ARG-405	60.215	60.567	60.175	60.319	0.215
PRO-374	0.760	0.777	0.778	0.772	0.010	TRP-406	0.886	0.778	0.662	0.775	0.112
ALA-375	0.918	1.049	1.038	1.002	0.072	ALA-407	1.451	1.378	1.254	1.361	0.100
VAL-376	0.349	0.356	0.388	0.364	0.021	LEU-408	-0.400	-0.493	-0.469	-0.454	0.048
GLY-377	0.831	0.830	0.828	0.830	0.001	ARG-409	71.198	72.264	71.947	71.803	0.548
CYS-378	0.041	0.113	0.072	0.075	0.036	ASN-410	6.246	7.016	6.690	6.651	0.386
VAL-379	2.747	2.780	2.755	2.761	0.018	ALA-411	0.995	1.234	0.920	1.050	0.164
ASP-380	-63.571	-63.308	-63.904	-63.594	0.299	ILE-412	0.546	0.567	0.529	0.547	0.019
GLY-381	0.649	0.729	0.580	0.652	0.075	THR-413	0.346	0.594	0.396	0.445	0.131
MET-382	-1.567	-1.864	-1.432	-1.621	0.221	ARG-414	87.545	90.265	89.245	89.019	1.374
ARG-383	165.053	158.471	165.413	162.979	3.908	TYR-415	0.087	0.051	0.023	0.054	0.032
ILE-384	0.119	-0.142	0.051	0.009	0.135	PHE-416	0.109	-0.051	-0.031	0.009	0.087
GLY-385	-4.801	-5.083	-5.071	-4.985	0.159	MET-417	-0.806	-0.758	-0.882	-0.815	0.063
PRO-386	-10.518	-10.896	-11.579	-10.998	0.538	HIE-418	0.344	-0.417	0.241	0.056	0.413
THR-388	-4.091	-3.997	-4.279	-4.122	0.144	ASP-419	-48.931	-49.064	-49.299	-49.098	0.186
ALA-389	-0.037	-0.085	-0.137	-0.086	0.050	ARG-420	52.165	52.524	52.585	52.425	0.227
PRO-390	2.090	2.064	2.024	2.059	0.034	PHE-421	1.066	1.097	1.121	1.095	0.028
PHE-391	-3.071	-3.159	-3.158	-3.129	0.051	TRP-422	1.487	1.485	1.544	1.505	0.034
TRP-392	-2.313	-2.468	-2.530	-2.437	0.112	LEU-423	-0.964	-1.158	-1.537	-1.220	0.292
GLY-393	-0.521	-0.716	-0.707	-0.648	0.110	ASN-424	2.058	2.296	2.086	2.147	0.130
GLU-394	-51.235	-51.358	-51.332	-51.308	0.065	ASP-425	-130.806	-126.864	-131.406	-129.692	2.467
HIE-395	0.113	-0.375	-0.374	-0.212	0.282	PRO-426	-4.912	-4.597	-4.952	-4.820	0.195
ILE-396	1.028	1.210	1.002	1.080	0.113	ASP-427	-143.908	-132.624	-133.651	-136.728	6.240
GLU-397	-56.108	-57.109	-56.229	-56.482	0.546	CYS-428	-0.406	-3.752	-3.996	-2.718	2.006
ASP-398	-67.874	-69.926	-68.659	-68.820	1.036	LEU-429	-4.267	-4.341	-4.563	-4.390	0.154
ASN-399	0.837	1.231	-1.714	0.118	1.598	ILE-430	0.400	0.303	0.225	0.309	0.087
GLY-400	-1.885	-2.301	-0.706	-1.630	0.827	LEU-431	1.344	1.266	1.332	1.314	0.042
ALA-401	1.028	1.898	1.713	1.546	0.458	ARG-432	90.504	89.473	90.874	90.284	0.726

	TS1	TS2	TS3	avg	dev		TS1	TS2	TS3	avg	dev
GLU-433	-52.701	-52.331	-52.844	-52.626	0.265	SER-464	2.156	2.094	2.167	2.139	0.039
GLU-434	-54.135	-53.579	-54.118	-53.944	0.316	LEU-465	1.093	1.092	1.136	1.107	0.025
LYS-435	64.792	63.873	64.691	64.452	0.504	VAL-466	0.529	0.542	0.542	0.538	0.007
THR-436	1.398	1.330	1.468	1.399	0.069	ARG-467	50.201	49.609	50.223	50.011	0.348
ASP-437	-57.923	-58.102	-57.933	-57.986	0.101	ASP-468	-45.295	-44.902	-45.430	-45.209	0.274
LEU-438	0.583	0.604	0.632	0.606	0.024	HIE-469	-1.207	-1.183	-1.221	-1.204	0.019
THR-439	-1.495	-1.494	-1.519	-1.503	0.014	GLY-470	-0.078	-0.084	-0.076	-0.079	0.004
GLN-440	-0.708	-0.720	-0.727	-0.718	0.010	LYS-471	54.379	53.638	54.482	54.166	0.460
LYS-441	42.976	43.011	43.145	43.044	0.089	LYS-472	42.201	41.980	42.362	42.181	0.192
GLU-442	-59.724	-59.765	-59.950	-59.813	0.120	VAL-473	0.350	0.340	0.345	0.345	0.005
LYS-443	58.227	58.303	58.423	58.318	0.099	LEU-474	0.174	0.136	0.167	0.159	0.020
GLU-444	-48.909	-48.801	-49.153	-48.955	0.181	LYS-475	46.351	45.897	46.506	46.252	0.317
LEU-445	-0.326	-0.334	-0.341	-0.333	0.008	GLU-476	-44.854	-44.656	-45.069	-44.860	0.206
TYR-446	-0.572	-0.629	-0.443	-0.548	0.096	THR-477	0.559	0.531	0.555	0.548	0.016
SER-447	-1.868	-1.895	-1.923	-1.896	0.028	LEU-478	0.277	0.259	0.273	0.270	0.009
TYR-448	-0.110	-0.100	-0.119	-0.110	0.009	GLU-479	-42.524	-42.344	-42.737	-42.535	0.197
THR-449	1.695	1.667	1.713	1.692	0.023	LEU-480	0.994	0.983	1.005	0.994	0.011
CYS-450	-0.911	-0.956	-0.954	-0.940	0.025	LEU-481	1.557	1.561	1.578	1.565	0.011
GLY-451	-0.302	-0.315	-0.288	-0.302	0.014	GLY-482	1.075	1.081	1.092	1.083	0.009
VAL-452	0.337	0.343	0.345	0.342	0.004	GLY-483	-0.375	-0.367	-0.378	-0.373	0.006
LEU-453	0.152	0.151	0.138	0.147	0.008	ARG-484	46.338	46.553	46.661	46.517	0.165
ASP-454	-55.031	-55.162	-55.490	-55.228	0.236	PRO-485	0.476	0.461	0.480	0.472	0.010
ASN-455	-1.411	-1.396	-1.451	-1.420	0.028	ARG-486	41.598	41.827	41.863	41.763	0.144
MET-456	0.167	0.321	0.104	0.197	0.112	VAL-487	0.179	0.185	0.180	0.181	0.004
ILE-457	-0.147	0.003	-0.129	-0.091	0.082	GLN-488	0.631	0.628	0.640	0.633	0.006
ILE-458	2.898	1.822	1.739	2.153	0.646	ASN-489	-0.426	-0.405	-0.435	-0.422	0.015
GLU-459	-0.394	-0.577	-0.723	-0.565	0.165	ILE-490	-0.599	-0.623	-0.604	-0.608	0.013
SER-460	-4.070	-4.399	-4.186	-4.218	0.167	MET-491	-0.444	-0.452	-0.451	-0.449	0.004
ASP-461	-83.732	-82.701	-84.211	-83.548	0.772	SER-492	-0.498	-0.496	-0.510	-0.501	0.007
ASP-462	-71.107	-69.934	-70.990	-70.677	0.646	GLU-493	-48.934	-49.623	-49.171	-49.243	0.350
LEU-463	1.424	1.327	1.386	1.379	0.049	ASP-494	-44.584	-44.998	-44.823	-44.802	0.208

	TS1	TS2	TS3	avg	dev		TS1	TS2	TS3	avg	dev
LEU-495	-0.388	-0.392	-0.391	-0.390	0.002	SUM	-900.83	-864.94	-908.33	-891.37	23.19
ARG-496	40.602	40.830	40.818	40.750	0.128						
TYR-497	-0.586	-0.623	-0.585	-0.598	0.022						
GLU-498	-39.551	-39.776	-39.774	-39.701	0.129						
ILE-499	0.828	0.841	0.839	0.836	0.007						
VAL-500	-1.052	-1.069	-1.067	-1.063	0.010						
SER-501	0.778	0.776	0.789	0.781	0.007						
SER-502	-0.668	-0.682	-0.678	-0.676	0.007						
GLY-503	-0.395	-0.393	-0.400	-0.396	0.003						
THR-504	1.921	1.919	1.945	1.928	0.014						
LEU-505	0.877	0.874	0.887	0.879	0.007						
SER-506	0.760	0.763	0.771	0.765	0.006						
GLY-507	-0.130	-0.135	-0.132	-0.132	0.003						
ASN-508	-0.567	-0.567	-0.573	-0.569	0.003						
VAL-509	0.175	0.167	0.175	0.172	0.005						
LYS-510	39.690	39.869	39.920	39.827	0.121						
ILE-511	0.165	0.157	0.165	0.162	0.004						
VAL-512	-0.150	-0.137	-0.151	-0.146	0.008						
VAL-513	0.293	0.284	0.307	0.294	0.011						
ASP-514	-45.982	-46.289	-46.216	-46.162	0.161						
LEU-515	0.106	0.137	0.127	0.123	0.015						
ASN-516	-1.428	-1.455	-1.432	-1.438	0.015						
SER-517	0.216	0.233	0.223	0.224	0.009						
ARG-518	56.049	56.296	56.289	56.212	0.141						
GLU-519	-43.806	-43.907	-43.992	-43.902	0.093						
TYR-520	0.410	0.426	0.416	0.418	0.008						
HIE-521	-0.519	-0.530	-0.523	-0.524	0.005						
LEU-522	0.601	0.595	0.608	0.601	0.006						
GLU-523	-37.544	-37.627	-37.741	-37.638	0.099						
LYS-524	42.813	42.689	43.038	42.847	0.177						
GLU-525	-70.618	-70.618	-70.965	-70.734	0.200						

Table S9. Cartesian coordinates (in Å) of the QM atoms for the structures of the ground state in water, TS_{alk} and TS_{hyd} optimized at DFT/MM level.

	GS1				GS2			
	atom	x	y	z	atom	x	y	z
1	C	-2.525	1.375	0.14	C	-2.472	1.616	-0.063
2	C	-3.658	1.813	-0.516	C	-3.719	1.981	-0.549
3	C	-4.563	0.902	-1.073	C	-4.62	0.987	-0.92
4	C	-4.408	-0.474	-0.91	C	-4.382	-0.363	-0.725
5	C	-3.249	-0.879	-0.278	C	-3.179	-0.679	-0.119
6	C	-2.247	-0.002	0.207	C	-2.177	0.271	0.157
7	O	-1.155	-0.569	0.699	O	-0.969	-0.22	0.5
8	C	-0.2	0.219	1.496	C	-0.147	0.483	1.494
9	C	0.451	-0.723	2.451	C	0.281	-0.512	2.526
10	C	1.767	-0.927	2.534	C	1.536	-0.946	2.679
11	C	2.311	-1.836	3.607	C	1.906	-1.802	3.883
12	C	2.783	-0.295	1.605	C	2.685	-0.513	1.797
13	O	3.247	-1.186	4.474	O	3.262	-2.225	3.869
14	C	2.147	0.342	0.35	C	2.232	0.259	0.545
15	O	3.542	0.631	2.384	O	3.509	0.271	2.651
16	C	0.805	0.997	0.632	C	1.057	1.165	0.856
17	F	0.198	1.28	-0.6	F	0.649	1.796	-0.327
18	O	3.002	1.348	-0.144	O	3.324	1.059	0.124
19	N	-5.692	1.397	-1.826	N	-5.92	1.387	-1.454
20	O	-6.385	0.609	-2.458	O	-6.302	0.882	-2.503
21	O	-5.924	2.601	-1.849	O	-6.557	2.205	-0.819
22	N	-3.062	-2.302	0.025	N	-2.935	-2.064	0.282
23	O	-3.766	-2.763	0.901	O	-2.611	-2.238	1.447
24	O	-2.196	-2.912	-0.573	O	-3.067	-2.942	-0.544
25	H	-1.876	2.092	0.659	H	-1.745	2.377	0.198
26	H	-3.833	2.879	-0.593	H	-3.952	3.039	-0.644

27	H	-5.157	-1.191	-1.257	H	-5.107	-1.134	-0.967
28	H	-0.798	0.945	2.067	H	-0.781	1.274	1.937
29	H	-0.209	-1.181	3.184	H	-0.482	-0.828	3.234
30	H	2.812	-2.691	3.131	H	1.287	-2.704	3.903
31	H	1.498	-2.21	4.232	H	1.686	-1.223	4.789
32	H	3.672	-0.467	3.974	H	3.803	-1.422	3.842
33	H	3.457	-1.087	1.252	H	3.238	-1.402	1.466
34	H	4.473	0.706	2.027	H	4.341	0.536	2.208
35	H	3.278	1.228	-1.078	H	3.455	1.086	-0.848
36	H	1.992	-0.464	-0.381	H	1.947	-0.463	-0.231

GS3				
	atom	x	y	z
1	C	-2.552	1.541	0.666
2	C	-3.69	1.993	0.03
3	C	-4.477	1.113	-0.725
4	C	-4.183	-0.245	-0.797
5	C	-3.069	-0.683	-0.111
6	C	-2.182	0.184	0.573
7	O	-1.079	-0.36	1.046
8	C	-0.064	0.447	1.723
9	C	0.579	-0.454	2.725
10	C	1.835	-0.893	2.65
11	C	2.37	-1.838	3.697
12	C	2.781	-0.418	1.573
13	O	3.774	-1.731	3.896
14	C	2.01	0	0.319
15	O	3.479	0.672	2.162
16	C	0.925	0.988	0.692
17	F	0.212	1.344	-0.462

18	O	2.904	0.599	-0.593
19	N	-5.614	1.623	-1.453
20	O	-6.161	0.908	-2.29
21	O	-6.001	2.762	-1.237
22	N	-2.807	-2.122	-0.082
23	O	-2.593	-2.638	1.003
24	O	-2.854	-2.735	-1.131
25	H	-1.952	2.23	1.269
26	H	-3.952	3.042	0.099
27	H	-4.805	-0.943	-1.348
28	H	-0.564	1.287	2.231
29	H	-0.048	-0.722	3.573
30	H	2.202	-2.866	3.358
31	H	1.825	-1.685	4.636
32	H	4.01	-0.795	3.96
33	H	3.482	-1.216	1.298
34	H	4.305	0.883	1.67
35	H	2.664	0.324	-1.498
36	H	1.56	-0.909	-0.106

	TS _{alk-1}				TS _{alk-2}			
	atom	x	y	z	atom	x	y	z
1	C	42.914	36.169	40.17	C	43.218	36.407	40.367
2	H	42.51	35.159	40.293	H	42.862	35.379	40.488
3	H	43.995	36.041	40.287	H	44.302	36.337	40.495
4	C	42.684	36.617	38.7	C	42.981	36.851	38.896
5	O	42.066	37.703	38.474	O	42.304	37.907	38.693
6	O	43.149	35.858	37.813	O	43.489	36.144	37.991
7	C	43.733	38.545	28.412	C	44.067	38.634	28.438
8	H	44.007	37.655	27.827	H	44.544	37.751	27.99
9	H	42.943	39.043	27.849	H	43.307	38.974	27.737
10	C	43.101	37.999	29.666	C	43.375	38.151	29.679
11	O	41.888	37.867	29.789	O	42.153	38.099	29.781
12	O	43.931	37.568	30.603	O	44.181	37.737	30.639
13	H	43.44	37.202	31.379	H	43.645	37.405	31.416
14	C	40.366	37.495	32.972	C	40.708	37.959	32.512
15	C	39.097	37.51	32.452	C	39.386	38.098	32.187
16	C	38.637	36.416	31.695	C	38.692	36.993	31.651
17	C	39.414	35.266	31.572	C	39.315	35.779	31.449
18	C	40.696	35.271	32.09	C	40.65	35.647	31.793
19	C	41.283	36.415	32.734	C	41.43	36.734	32.321
20	O	42.506	36.497	33.091	O	42.679	36.666	32.581
21	C	42.982	35.853	35.093	C	43.047	36.32	34.799
22	C	42.824	34.448	35.087	C	42.641	34.992	34.926
23	C	43.893	33.634	34.861	C	43.539	33.975	34.75
24	C	43.805	32.145	34.968	C	43.167	32.542	34.887
25	C	45.289	34.164	34.589	C	45.013	34.216	34.487
26	O	42.664	31.685	35.661	O	41.839	32.332	35.331
27	C	45.262	35.624	34.13	C	45.254	35.608	33.898
28	O	45.976	34.089	35.818	O	45.609	34.121	35.76

29	C	44.356	36.417	35.068	C	44.488	36.64	34.726
30	F	44.339	37.753	34.728	F	44.693	37.908	34.226
31	O	46.572	36.147	34.156	O	46.631	35.885	33.93
32	N	37.379	36.514	31.003	N	37.326	37.12	31.22
33	O	36.695	37.524	31.162	O	36.777	38.219	31.339
34	O	37.05	35.607	30.245	O	36.78	36.154	30.712
35	N	41.469	34.035	31.946	N	41.238	34.352	31.522
36	O	42.669	34.126	31.773	O	42.238	34.011	32.116
37	O	40.847	32.984	32.01	O	40.666	33.63	30.695
38	H	40.734	38.325	33.57	H	41.277	38.797	32.901
39	H	38.435	38.352	32.621	H	38.875	39.043	32.329
40	H	39.043	34.373	31.074	H	38.765	34.947	31.027
41	H	42.178	36.502	35.424	H	42.359	37.145	34.974
42	H	41.86	34.013	35.329	H	41.605	34.767	35.154
43	H	44.739	31.766	35.411	H	43.904	32.049	35.535
44	H	43.761	31.754	33.94	H	43.27	32.087	33.89
45	H	42.855	31.734	36.607	H	41.836	32.203	36.286
46	H	45.774	33.556	33.815	H	45.407	33.463	33.793
47	H	46.356	33.157	35.982	H	46.026	33.19	35.934
48	H	46.738	36.649	33.34	H	46.877	36.479	33.189
49	H	44.839	35.667	33.12	H	44.86	35.626	32.875
50	H	44.709	36.33	36.106	H	44.824	36.62	35.777
51	H	44.52	39.157	28.494	H	44.744	39.354	28.589
52	H	42.597	36.768	40.906	H	42.862	36.983	41.103

TS_{alk-3}				
	atom	x	y	z
1	C	43.093	36.254	40.399
2	H	42.736	35.228	40.534
3	H	44.182	36.177	40.484
4	C	42.799	36.704	38.942
5	O	42.2	37.81	38.765
6	O	43.188	35.949	38.019
7	C	43.646	38.494	28.473
8	H	43.93	37.564	27.966
9	H	42.895	38.989	27.859
10	C	43.003	38.105	29.783
11	O	41.871	38.394	30.115
12	O	43.798	37.333	30.551
13	H	43.366	37.12	31.414
14	C	40.481	37.524	33.093
15	C	39.267	37.7	32.49
16	C	38.873	36.825	31.459
17	C	39.627	35.718	31.12
18	C	40.837	35.516	31.777
19	C	41.389	36.488	32.687
20	O	42.596	36.491	33.093
21	C	42.963	35.98	35.204
22	C	42.869	34.578	35.159
23	C	43.972	33.83	34.862
24	C	43.966	32.342	34.815
25	C	45.339	34.45	34.66
26	O	42.786	31.753	35.322
27	C	45.258	35.922	34.265
28	O	45.963	34.357	35.921

29	C	44.297	36.631	35.21
30	F	44.198	37.967	34.885
31	O	46.538	36.511	34.35
32	N	37.644	37.072	30.753
33	O	36.987	38.071	31.059
34	O	37.298	36.292	29.885
35	N	41.528	34.272	31.498
36	O	42.629	34.067	31.96
37	O	40.919	33.44	30.808
38	H	40.83	38.208	33.861
39	H	38.612	38.512	32.781
40	H	39.305	35.035	30.336
41	H	42.112	36.593	35.484
42	H	41.918	34.091	35.342
43	H	44.876	31.975	35.32
44	H	44.066	32.057	33.756
45	H	42.901	31.63	36.272
46	H	45.895	33.9	33.891
47	H	46.384	33.435	36.029
48	H	46.75	36.947	33.505
49	H	44.858	35.997	33.25
50	H	44.642	36.551	36.252
51	H	44.443	39.092	28.559
52	H	42.773	36.84	41.144

	TS _{hyd-1}				TS _{hyd-2}			
	atom	x	y	z	atom	x	y	z
1	C	43.228	36.563	40.133	C	43.262	36.569	40.143
2	H	42.85	35.538	40.199	H	42.891	35.542	40.212
3	H	44.31	36.464	40.259	H	44.345	36.481	40.265
4	C	43.011	37.064	38.683	C	43.031	37.066	38.692
5	O	42.289	38.066	38.437	O	42.325	38.081	38.451
6	O	43.628	36.405	37.792	O	43.619	36.39	37.796
7	C	44.17	38.48	29.266	C	44.187	38.486	29.282
8	H	44.653	37.539	28.975	H	44.679	37.545	29.004
9	H	43.299	38.621	28.629	H	43.321	38.616	28.637
10	C	43.729	38.271	30.706	C	43.738	38.29	30.722
11	O	42.493	38.055	30.907	O	42.501	38.055	30.911
12	O	44.564	38.272	31.644	O	44.557	38.319	31.669
13	C	43.695	36.907	35.665	C	43.688	36.891	35.677
14	C	43.595	35.552	35.243	C	43.59	35.537	35.253
15	C	44.686	34.884	34.805	C	44.682	34.875	34.809
16	C	44.68	33.39	34.646	C	44.68	33.38	34.648
17	C	46.051	35.513	34.675	C	46.044	35.511	34.678
18	O	43.789	32.801	35.581	O	43.806	32.784	35.594
19	C	46.004	37.044	34.657	C	45.992	37.041	34.653
20	O	46.746	35.097	35.831	O	46.731	35.105	35.842
21	C	45.05	37.53	35.743	C	45.041	37.52	35.746
22	F	44.931	38.916	35.696	F	44.908	38.903	35.709
23	O	47.311	37.519	34.929	O	47.299	37.515	34.923
24	H	42.827	37.492	35.923	H	42.823	37.477	35.938
25	H	42.649	35.039	35.37	H	42.649	35.018	35.387
26	H	45.7	32.992	34.799	H	45.703	32.991	34.779
27	H	44.351	33.112	33.638	H	44.334	33.1	33.647
28	H	44.168	32.882	36.47	H	44.165	32.916	36.486

29	H	46.547	35.165	33.76	H	46.544	35.16	33.767
30	H	47.01	34.114	35.791	H	47.034	34.119	35.788
31	H	47.482	38.365	34.496	H	47.467	38.36	34.483
32	H	45.649	37.383	33.675	H	45.634	37.376	33.671
33	H	45.472	37.275	36.719	H	45.472	37.257	36.716
34	O	43.1	37.97	33.747	O	43.046	37.951	33.761
35	H	42.768	38.853	33.954	H	42.754	38.841	33.998
36	H	43.658	38.071	32.901	H	43.61	38.064	32.926
37	H	44.81	39.237	29.132	H	44.823	39.245	29.144
38	H	42.877	37.115	40.89	H	42.907	37.122	40.898

TS_{hyd}-3				
	atom	x	y	z
1	C	43.346	36.439	40.106
2	H	42.994	35.407	40.196
3	H	44.43	36.375	40.236
4	C	43.11	36.925	38.656
5	O	42.428	37.965	38.459
6	O	43.649	36.244	37.734
7	C	44.306	38.801	28.506
8	H	44.838	37.954	28.058
9	H	43.524	39.141	27.825
10	C	43.684	38.278	29.776
11	O	42.443	38.377	29.893
12	O	44.409	37.757	30.661
13	C	43.749	36.671	35.563
14	C	43.512	35.331	35.213
15	C	44.544	34.537	34.812
16	C	44.424	33.045	34.777
17	C	45.937	35.069	34.614

18	O	43.489	32.602	35.745
19	C	45.97	36.581	34.417
20	O	46.568	34.768	35.841
21	C	45.136	37.214	35.534
22	F	45.107	38.591	35.42
23	O	47.301	37.033	34.523
24	H	42.938	37.379	35.708
25	H	42.527	34.907	35.367
26	H	45.416	32.598	34.958
27	H	44.076	32.714	33.791
28	H	43.884	32.675	36.628
29	H	46.431	34.578	33.767
30	H	46.866	33.783	35.877
31	H	47.568	37.475	33.704
32	H	45.54	36.837	33.446
33	H	45.598	36.967	36.497
34	O	43.515	38.068	33.156
35	H	43.653	39.008	33.311
36	H	43.773	37.916	32.21
37	H	44.964	39.535	28.669
38	H	42.976	37.005	40.842

Figure S1. Compounds **S-1** to **S-7**.

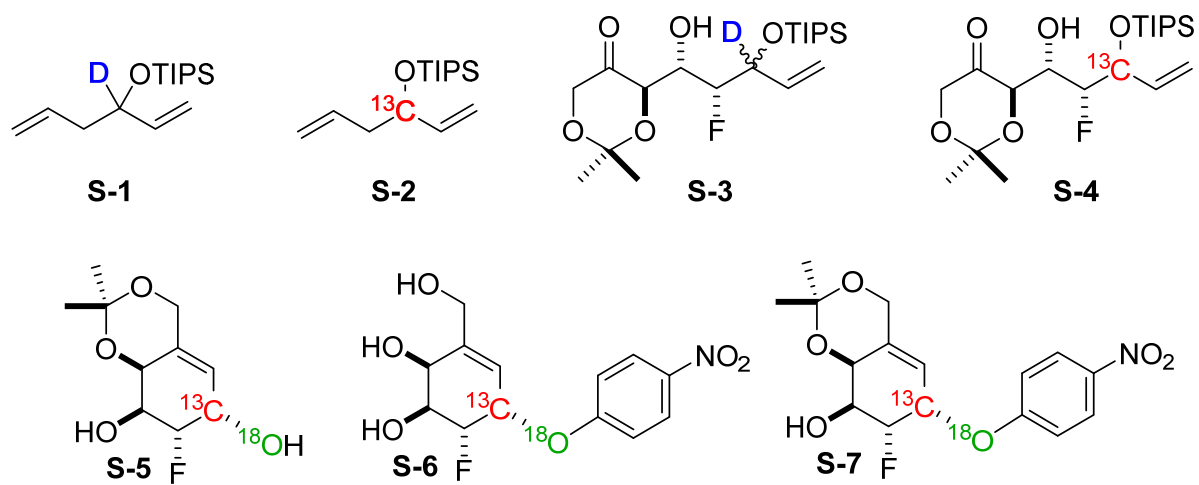


Figure S2: Change in integrated peak intensities R versus fraction of reaction (F) for the measurement of KIE values: A) data from a measurement of $k_{(^{16}\text{O})}/k_{(^{18}\text{O})}$ using the 60:40 mixture of $(1\text{-}^{13}\text{C})\text{-4}$ and $(1\text{-}^{13}\text{C},1\text{-}^{18}\text{O})\text{-4}$; B) data from an measurement of $k_{(^{13}\text{C})}/k_{(^2\text{H})}$ using $(1\text{-}^2\text{H})\text{-4}$ and $(1\text{-}^{13}\text{C})\text{-4}$; and C) data from an measurement of $k_{\text{H}}/k_{\text{D}}$ using $[1\text{-}^2\text{H}_{0,1}]\text{-4}$.

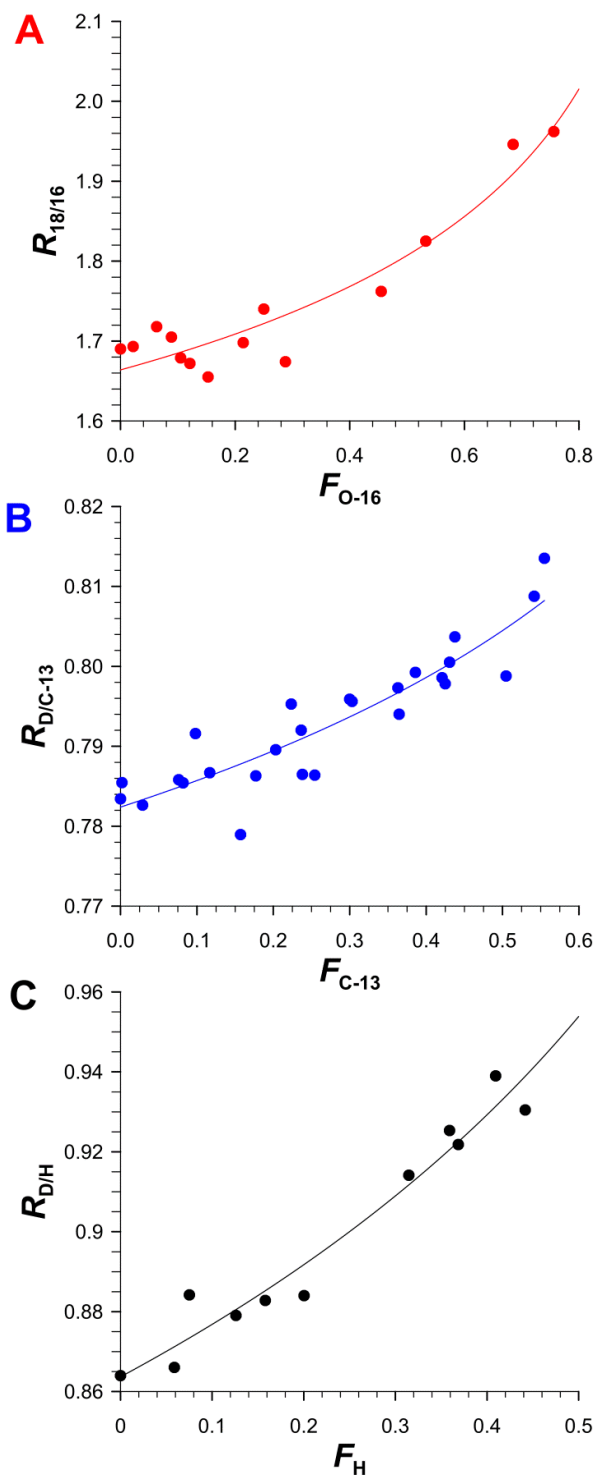


Figure S3. Structure of the substrate. Atoms in red are those where isotopic substitutions were made.

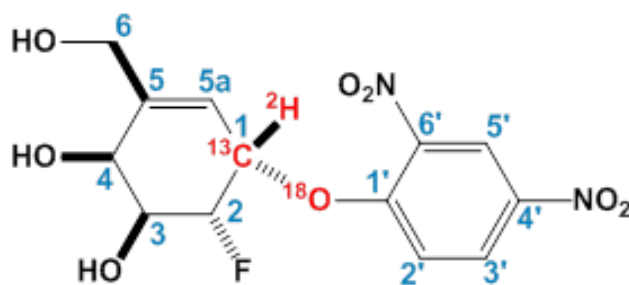


Figure S4. Time dependence of RMSD computed for the backbone atoms of the protein. Total Energy and Temperature during 10 ns MM MD simulations performed to equilibrate the starting structure generated from the X-ray structure.

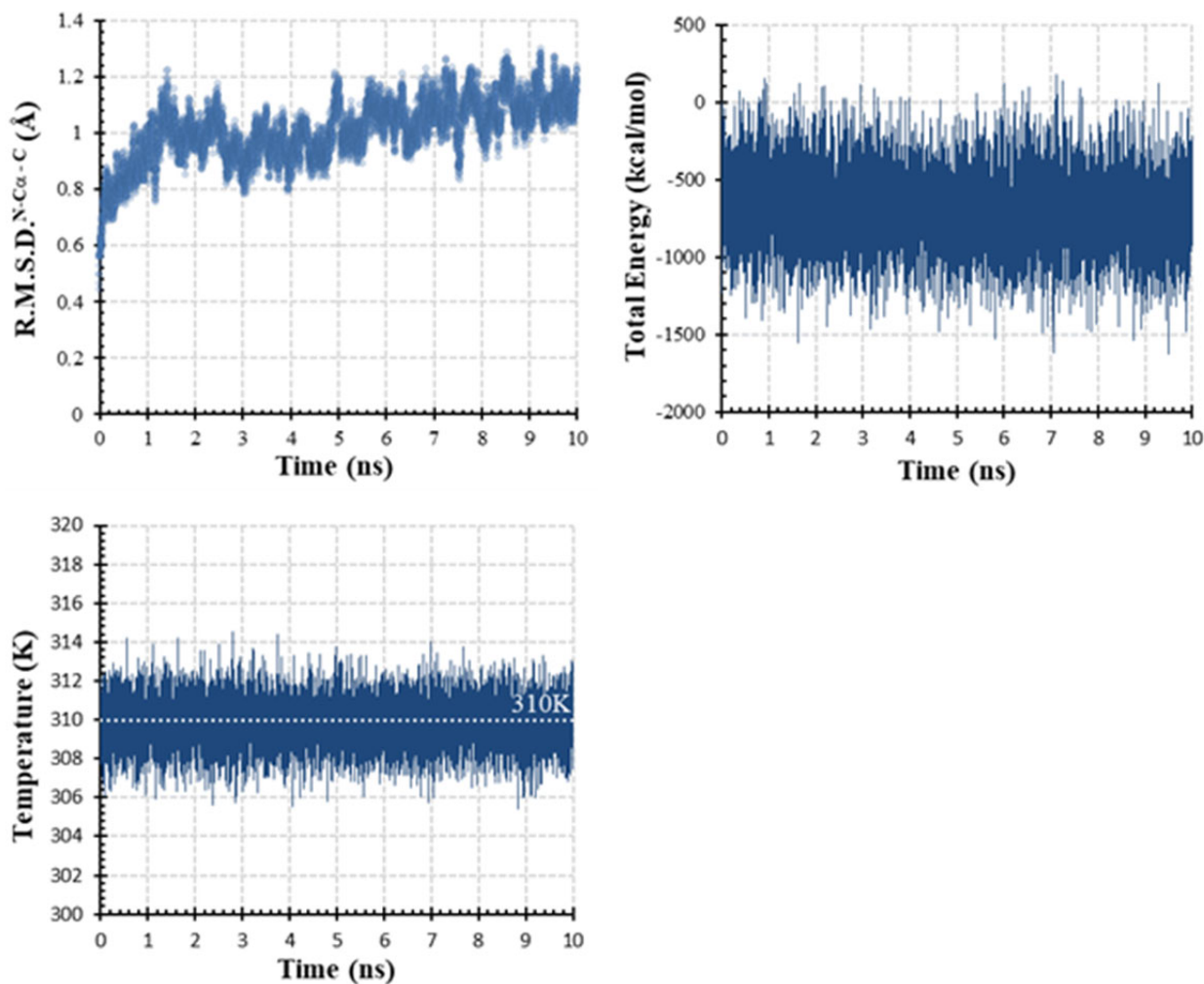


Figure S5. Schematic representation of the active site of *Tm*GalA. The grey region corresponds to the atoms included in the QM region in QM/MM calculations for the alkylation step (left) and for the hydrolysis step (right). Link atoms are indicated as black dots.

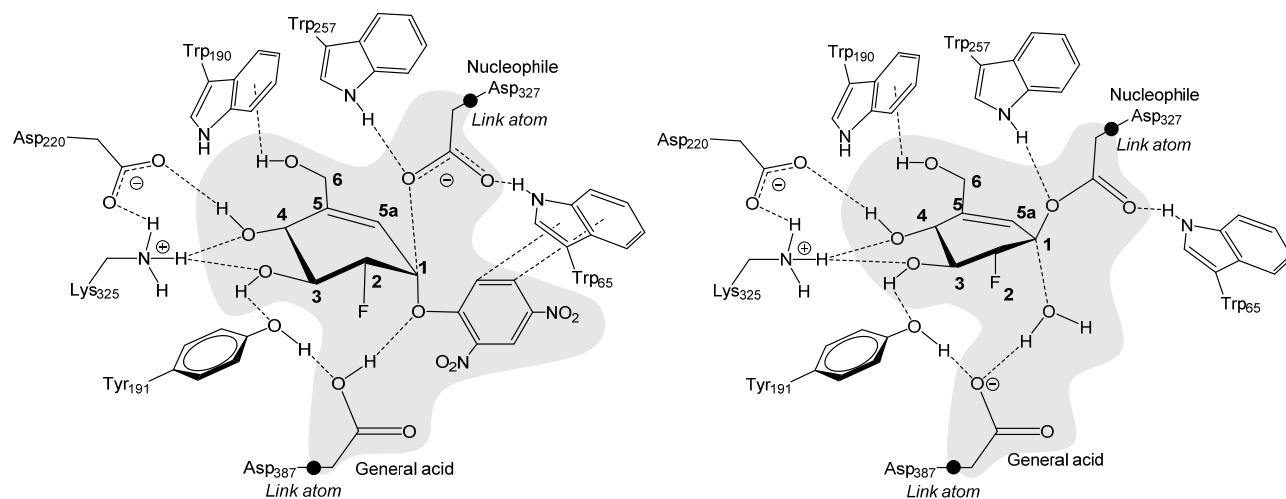


Figure S6. Potential energy surface at AM1/MM level of theory that justifies the existence of two steps process of leaving group departure. The white area represents the region with high potential energies. Distances of axis are in Å.

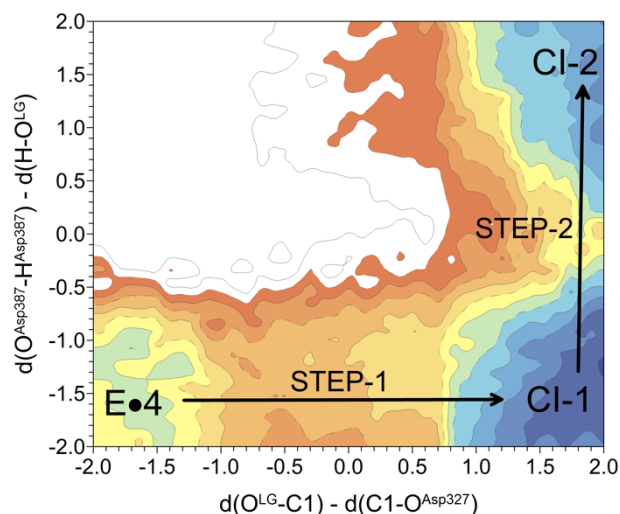


Figure S7. Definition of key distances used in exploration of potential and free energy surfaces for the alkylation step (left) and for the hydrolysis step (right).

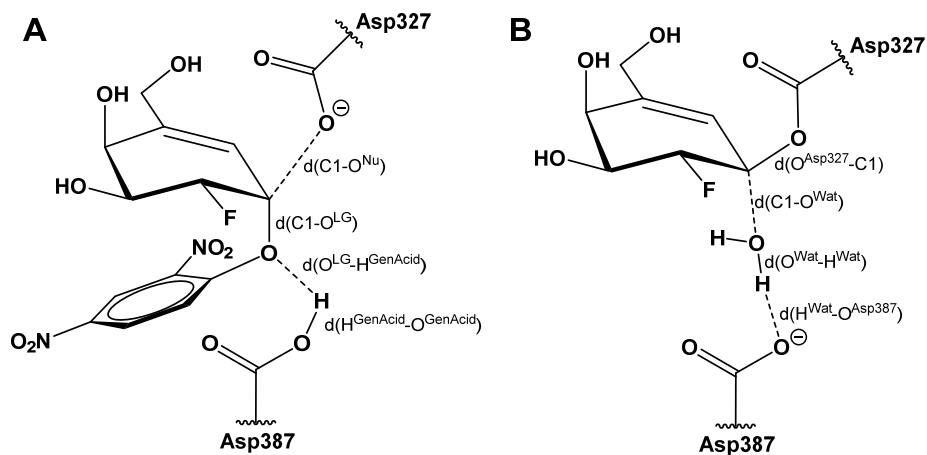


Figure S8. Potential energy surface (A) and free energy surface (B) computed at AM1/MM level for the covalent adduct formation (CI-1) and leaving group cleavage. White area represents the region with high potential (A) and free (B) energies. Distances of axis are in Å.

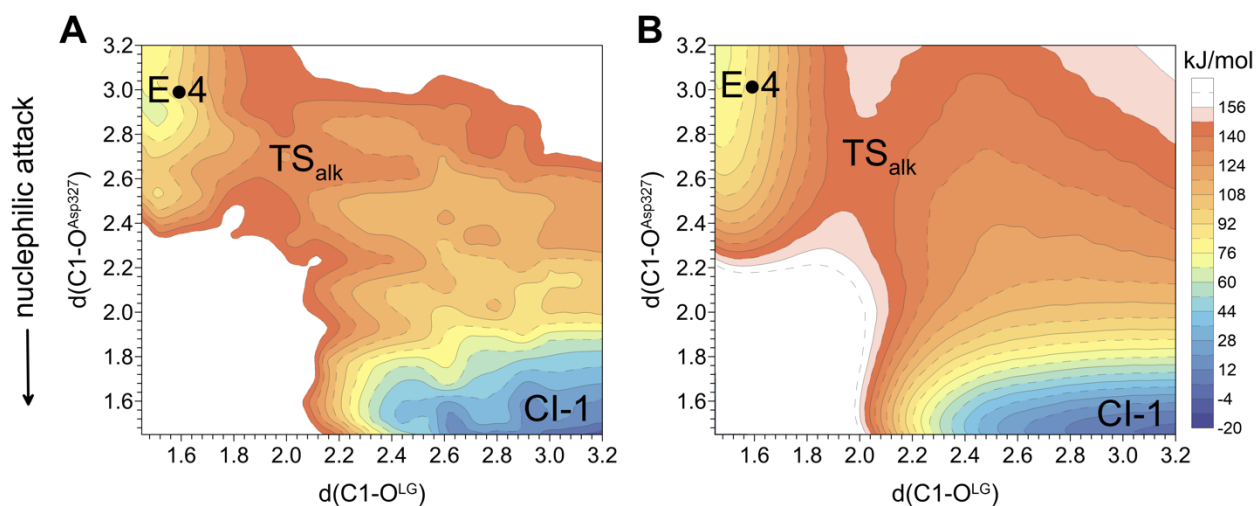


Figure S9. Potential energy surface (A) and free energy surface (B) computed at AM1/MM level for hydrolysis of the covalent adduct (CI-2) by an enzyme bound water molecule that is activated by Asp387. The white area represents the region with high potential (A) and free (B) energies. Distances of axis are in Å.

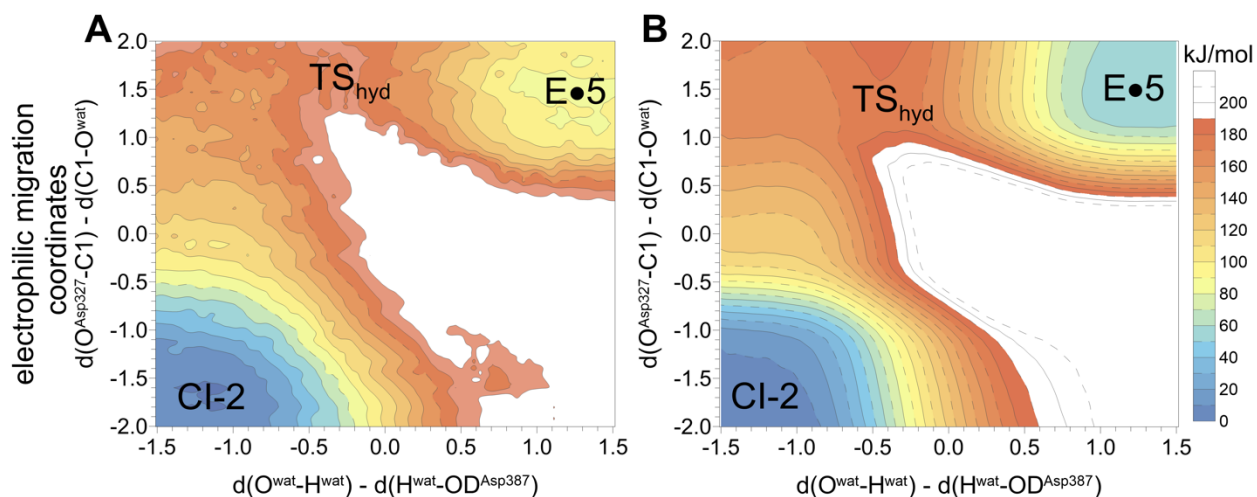


Figure S10. Free energy surfaces computed at AM1/MM (A) and corrected at M06-2X/MM (B) level of theory for the deprotonation of Asp387 by the leaving group.

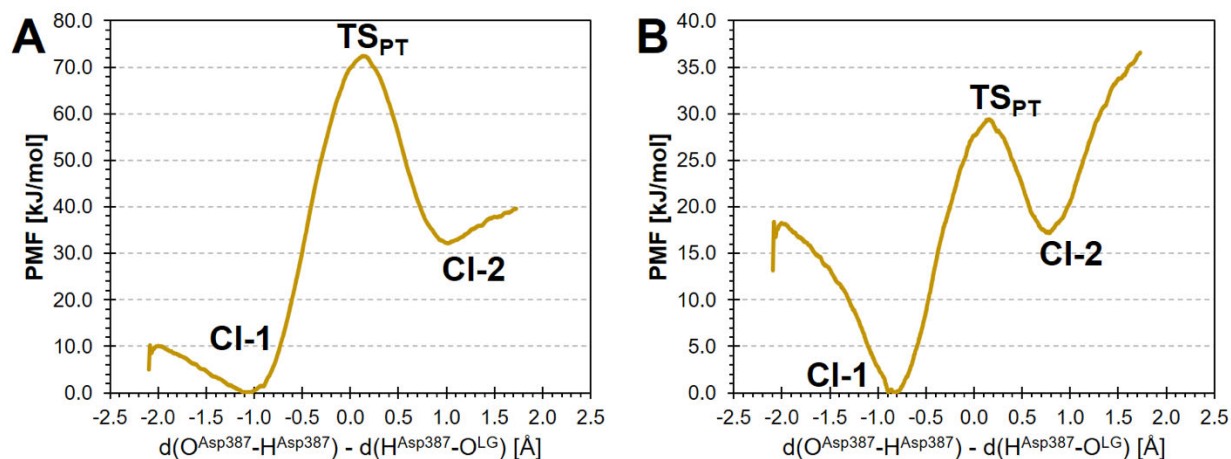


Figure S11. ^1H NMR spectrum for **S-1** in CDCl_3 .

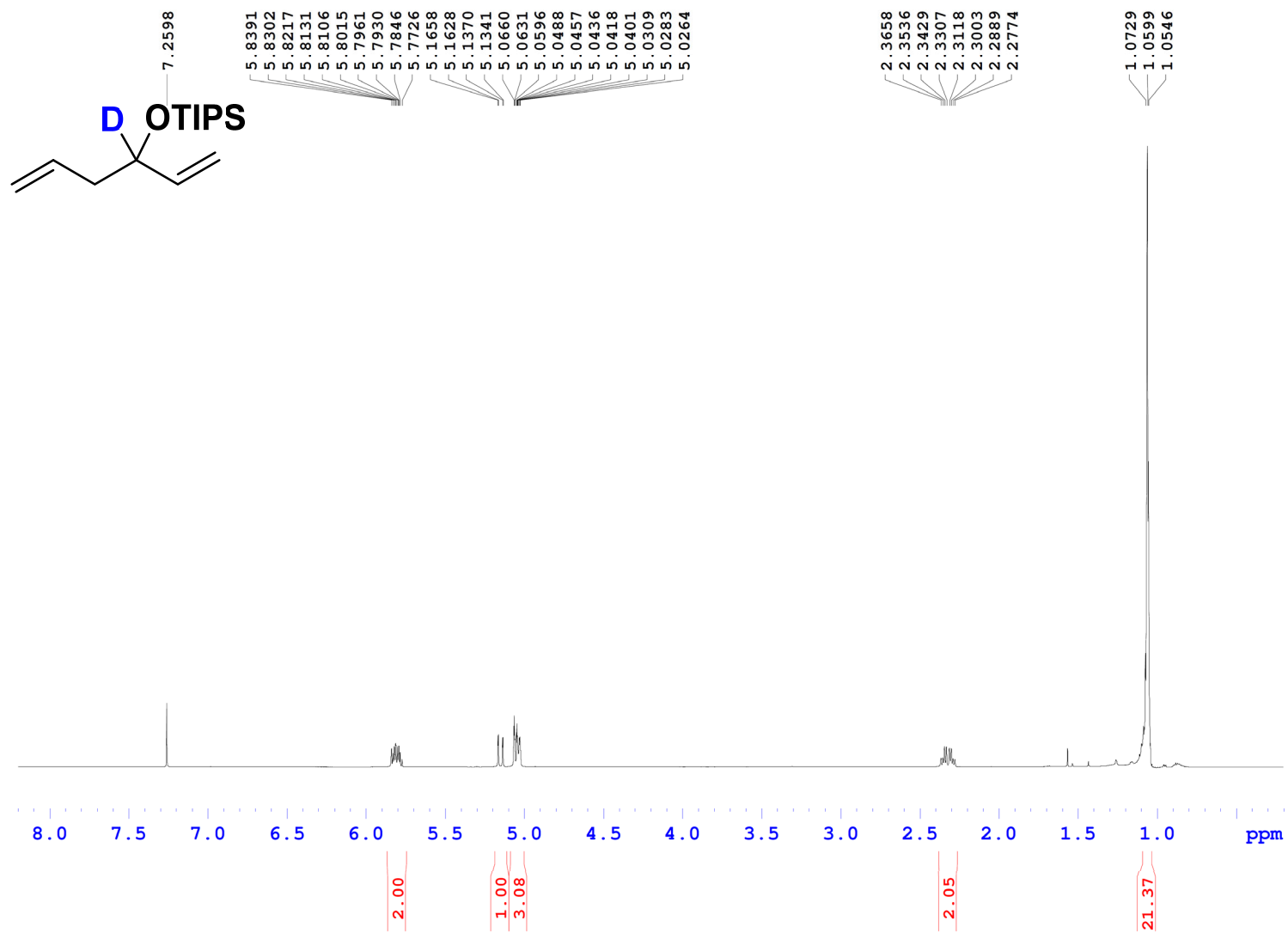


Figure S12. ^{13}C NMR spectrum for S-1 in CDCl_3 .

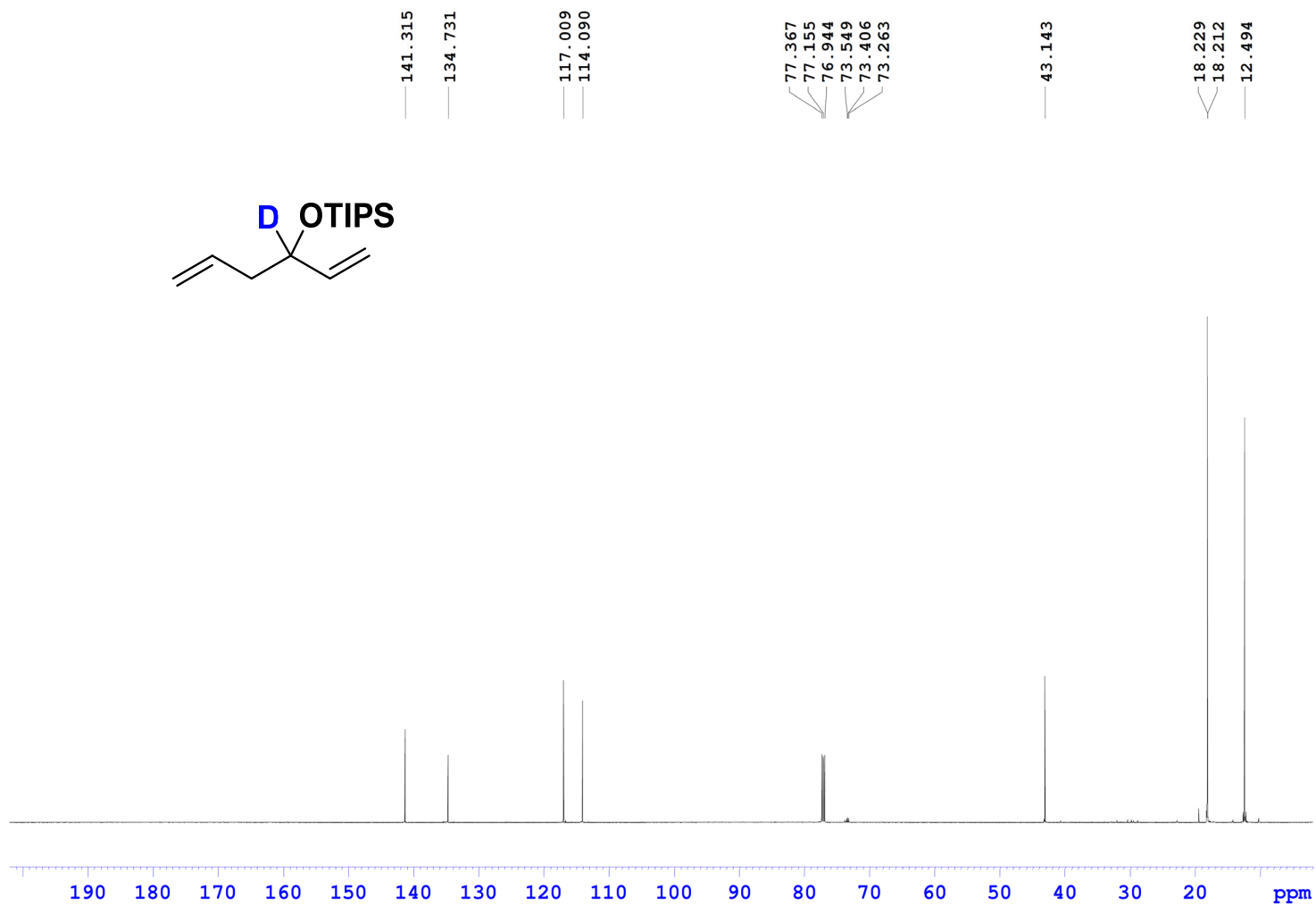


Figure S13. ¹H NMR spectrum for S-2 in CDCl₃.

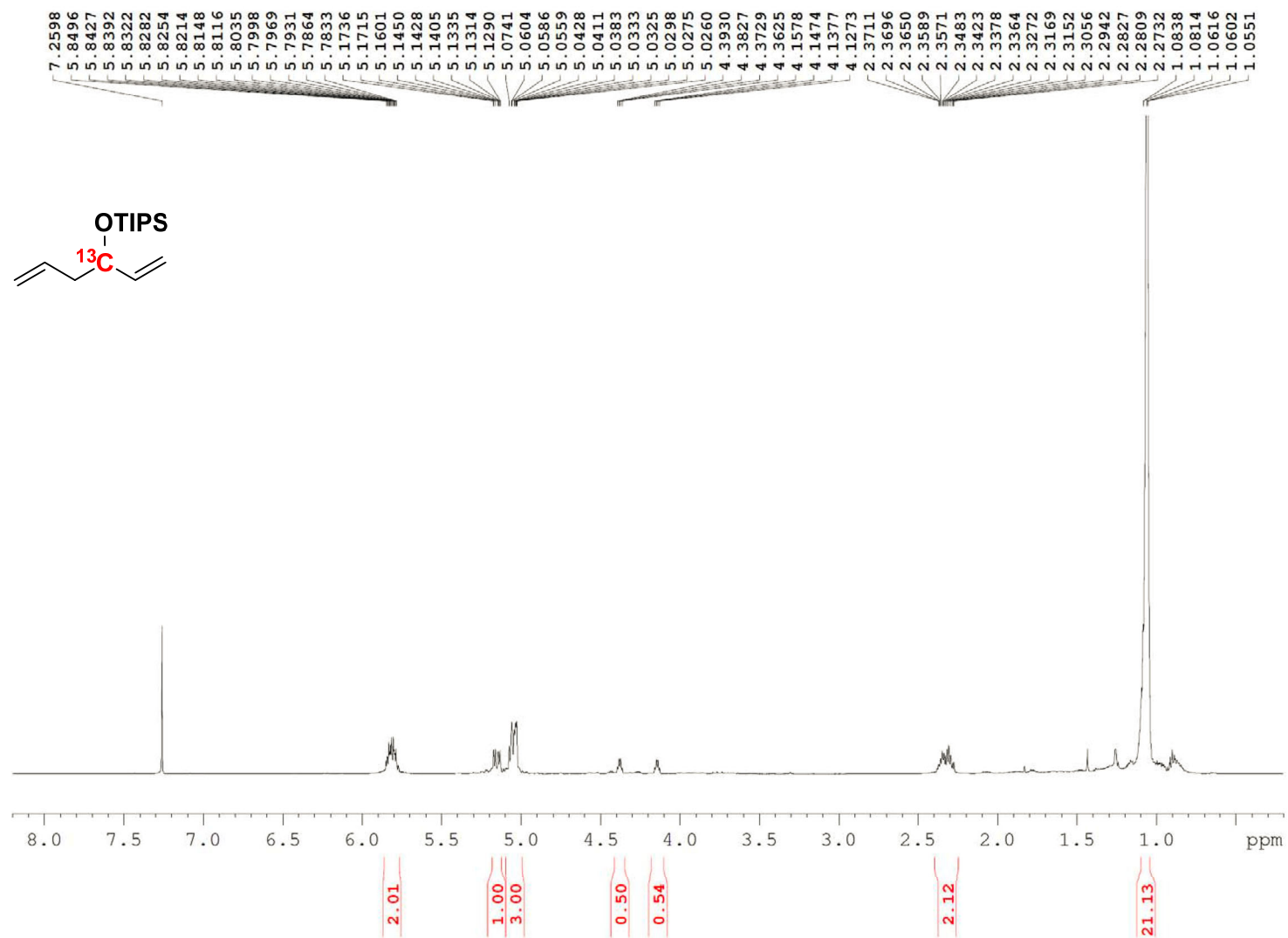


Figure S14. ^{13}C NMR spectrum for S-2 in CDCl_3 .

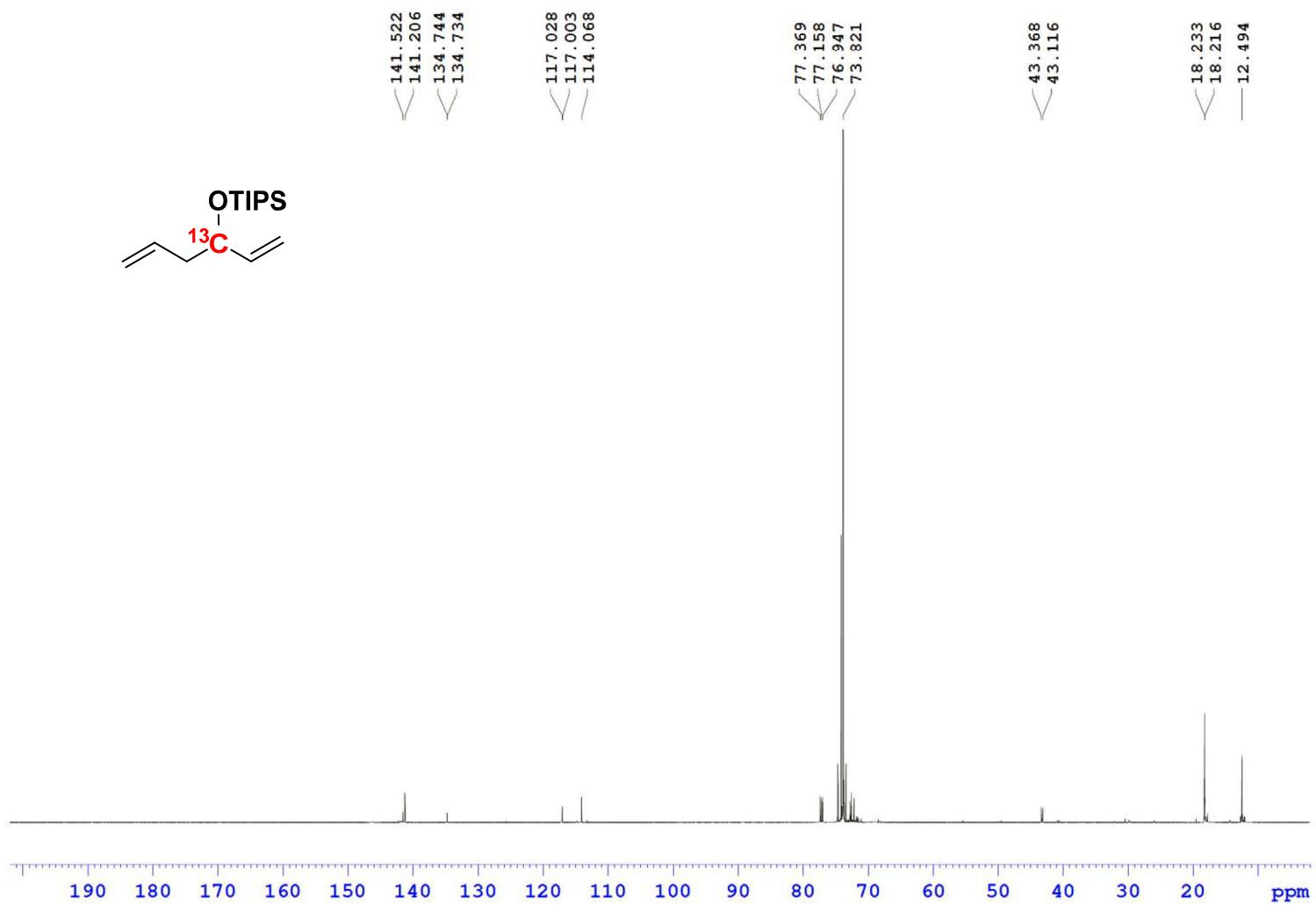


Figure S15. ^1H NMR spectrum for **10** in CDCl_3 .

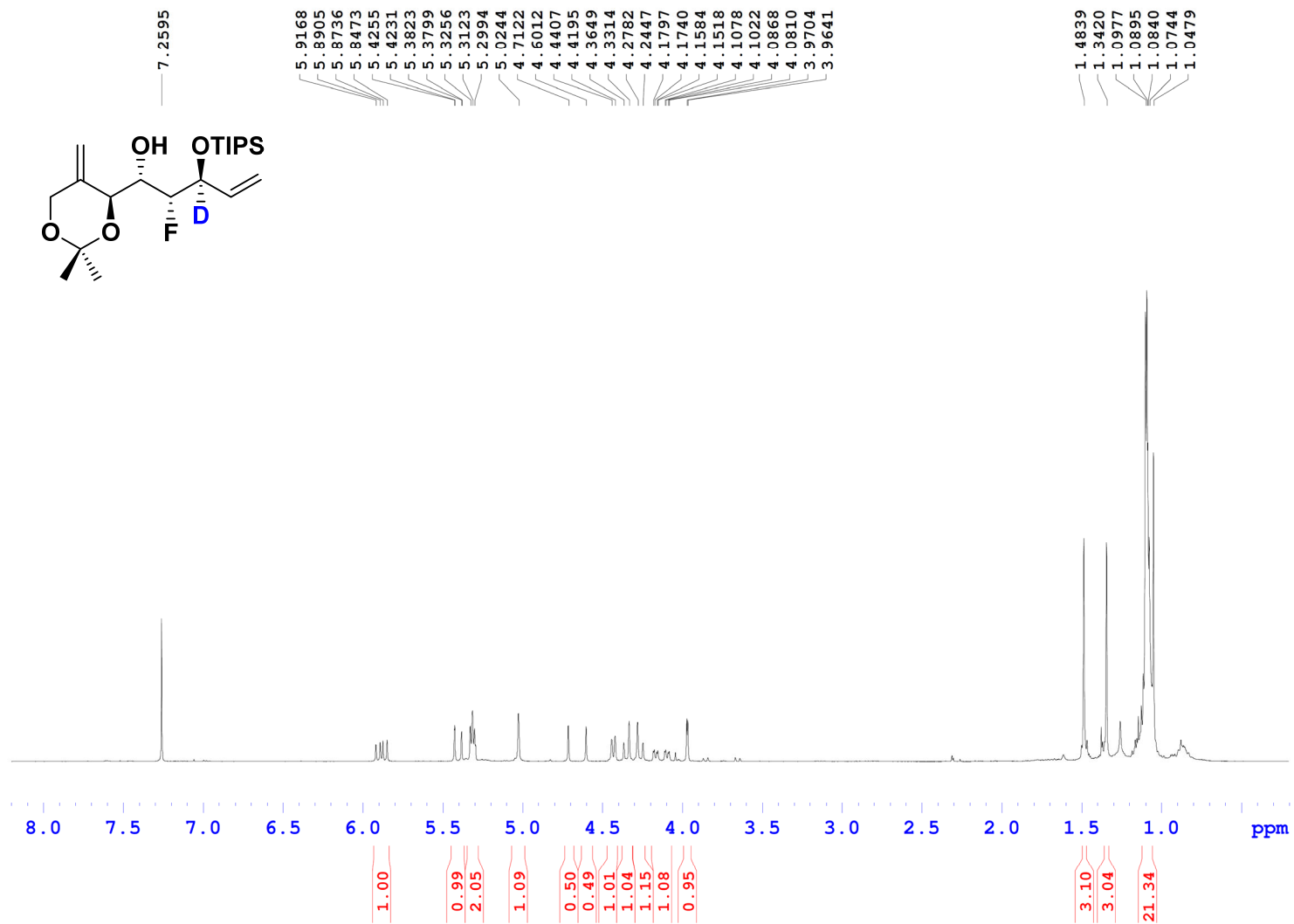


Figure S16. ^{13}C NMR spectrum for **10** in CDCl_3 .

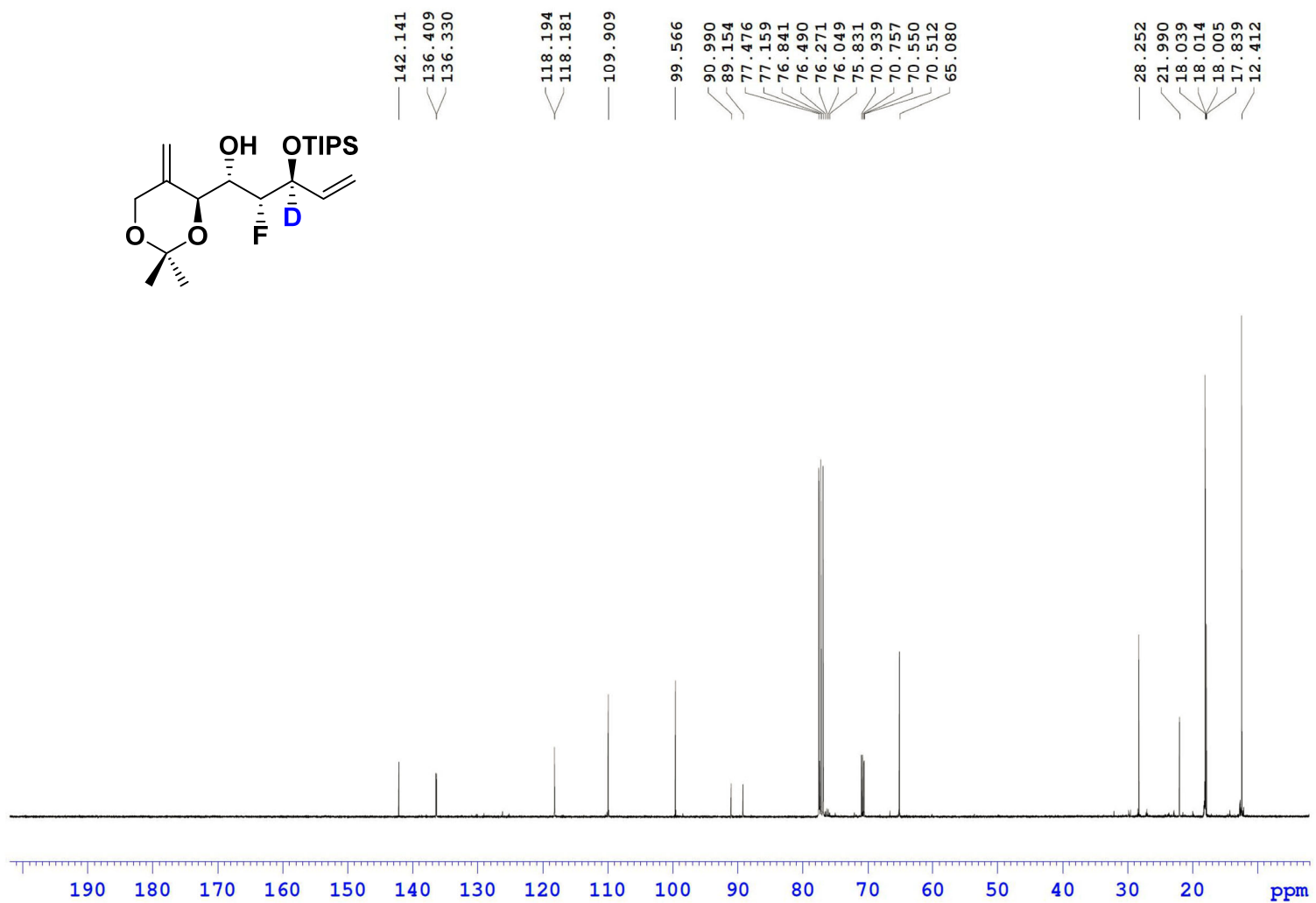


Figure S17. ^1H NMR spectrum for **12** in CDCl_3 .

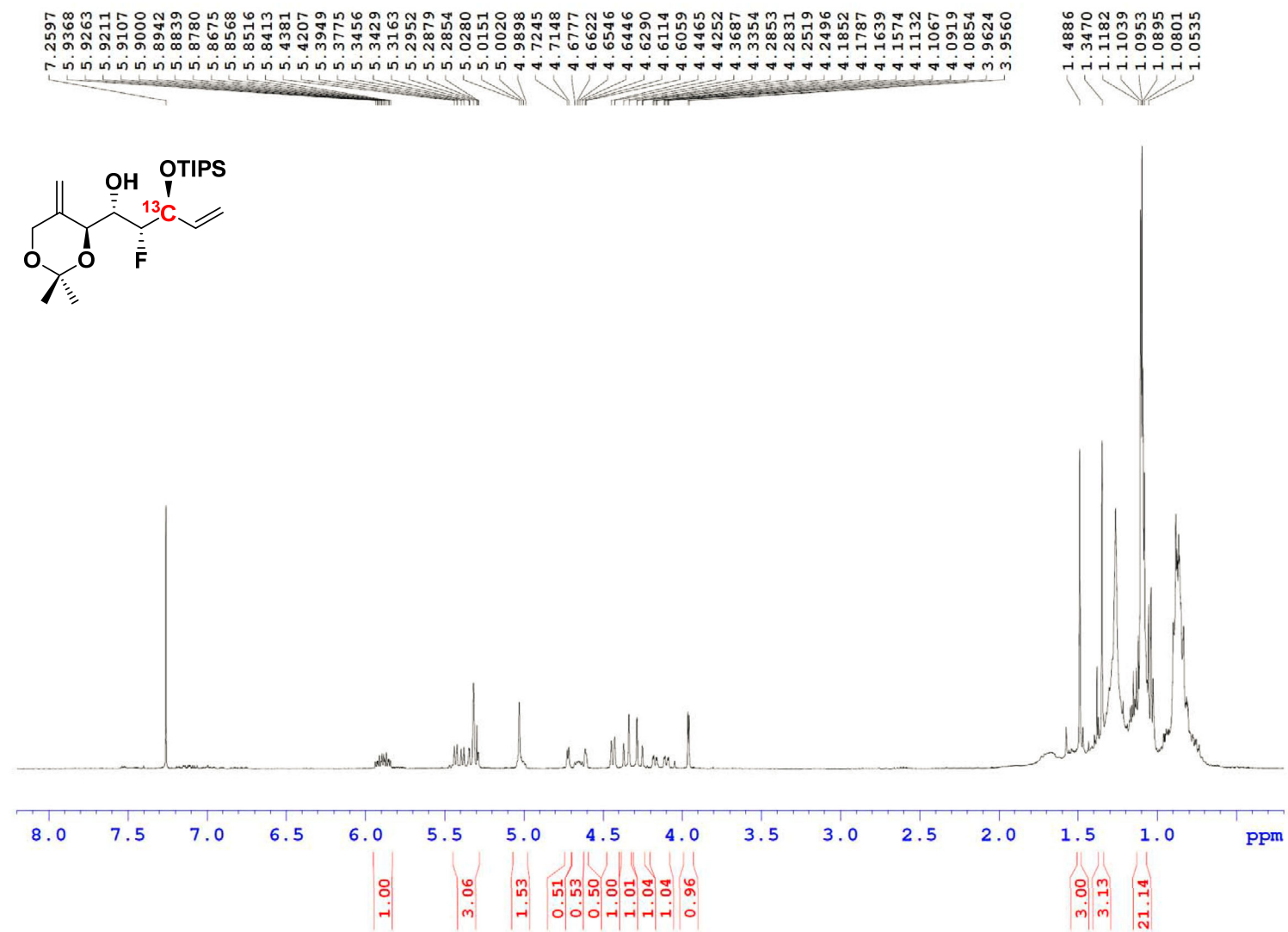


Figure S18. ^{13}C NMR spectrum for **12** in CDCl_3 .

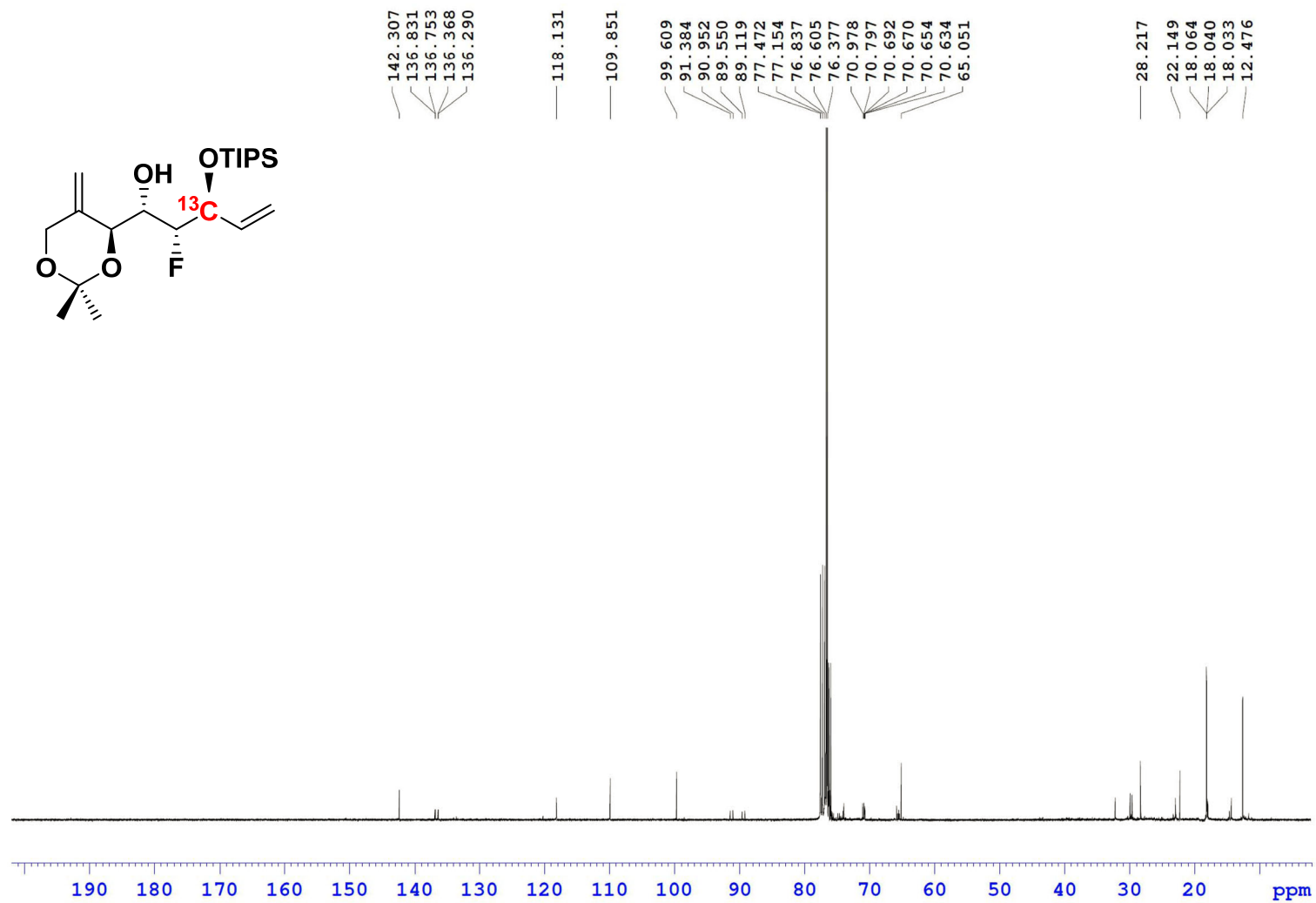


Figure S19. ¹H NMR spectrum for **13** in CDCl₃.

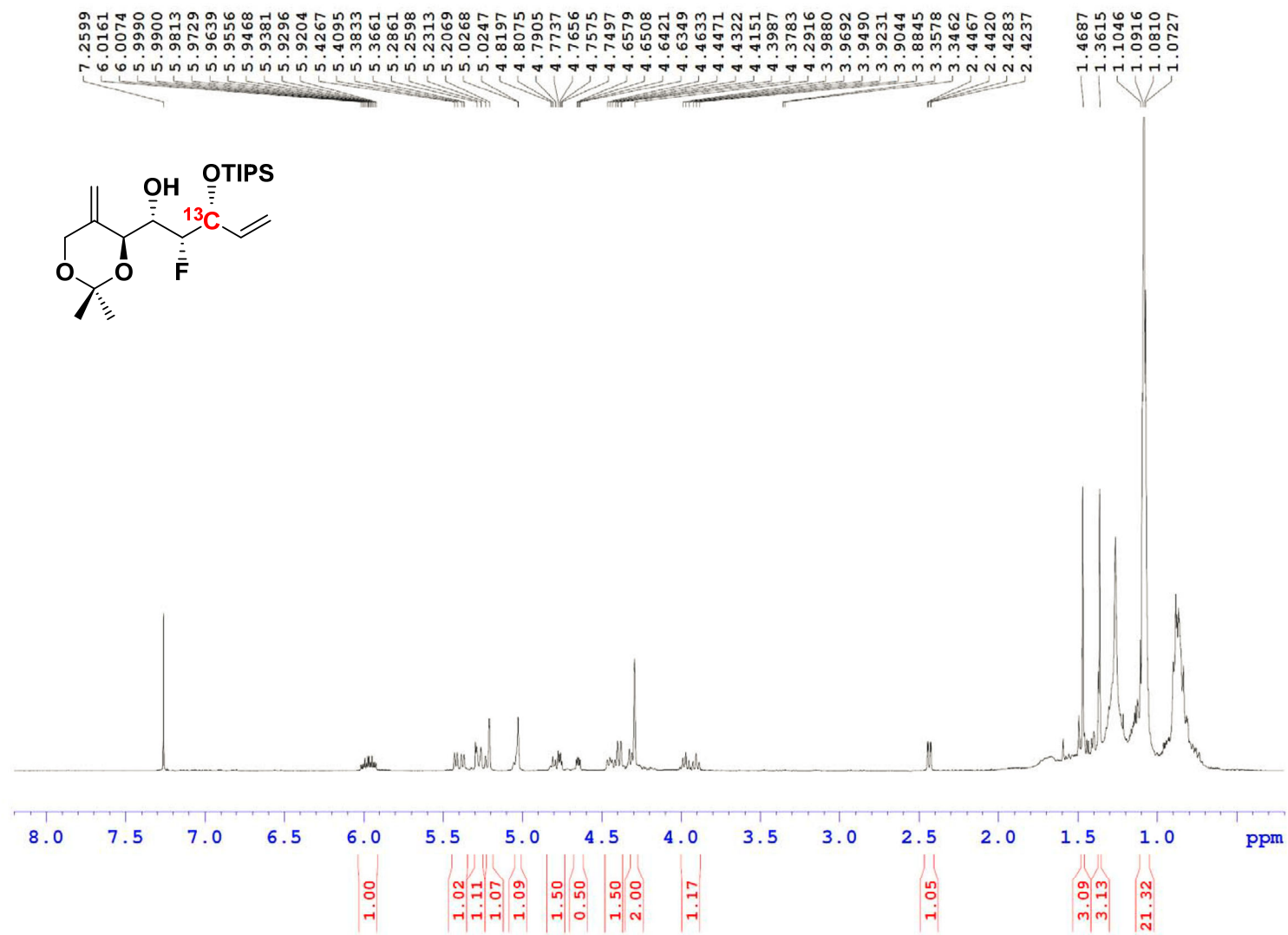


Figure S20. ^{13}C NMR spectrum for **13** in CDCl_3 .

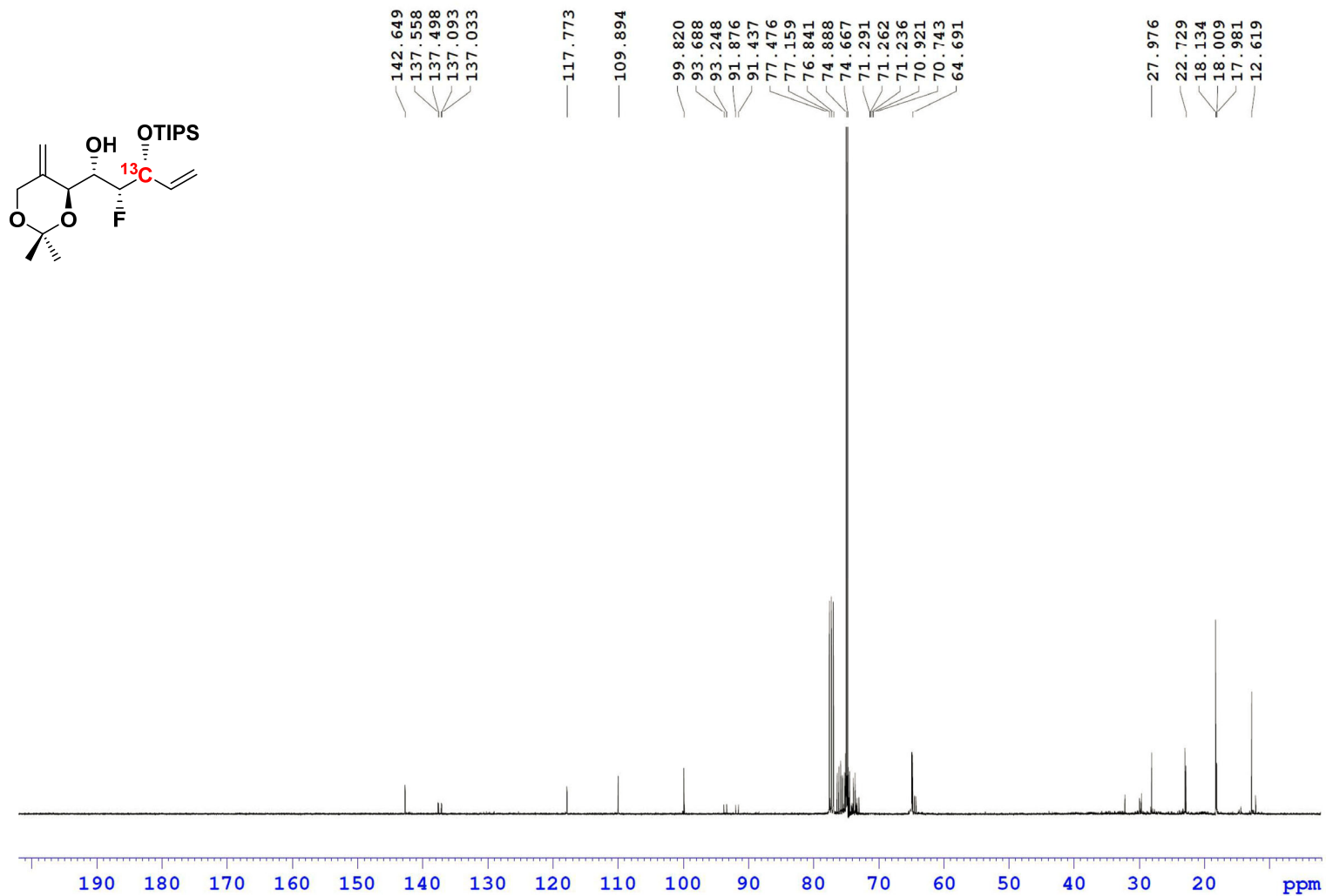


Figure S21. ^1H NMR spectrum for (1- ^2H)-4 in CDCl_3 .

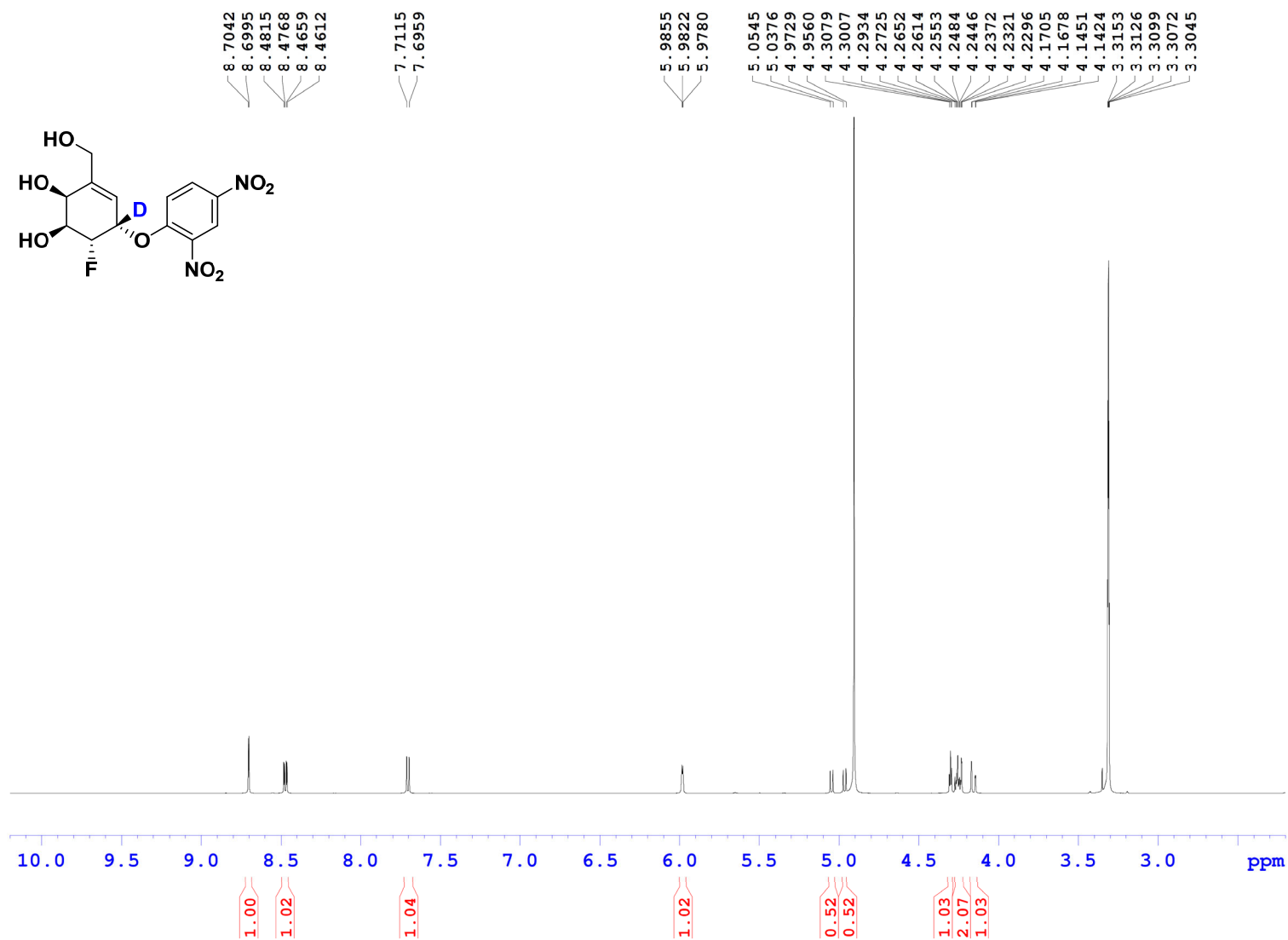


Figure S22. ^{13}C NMR spectrum for (1- ^2H)-4 in CDCl_3 .

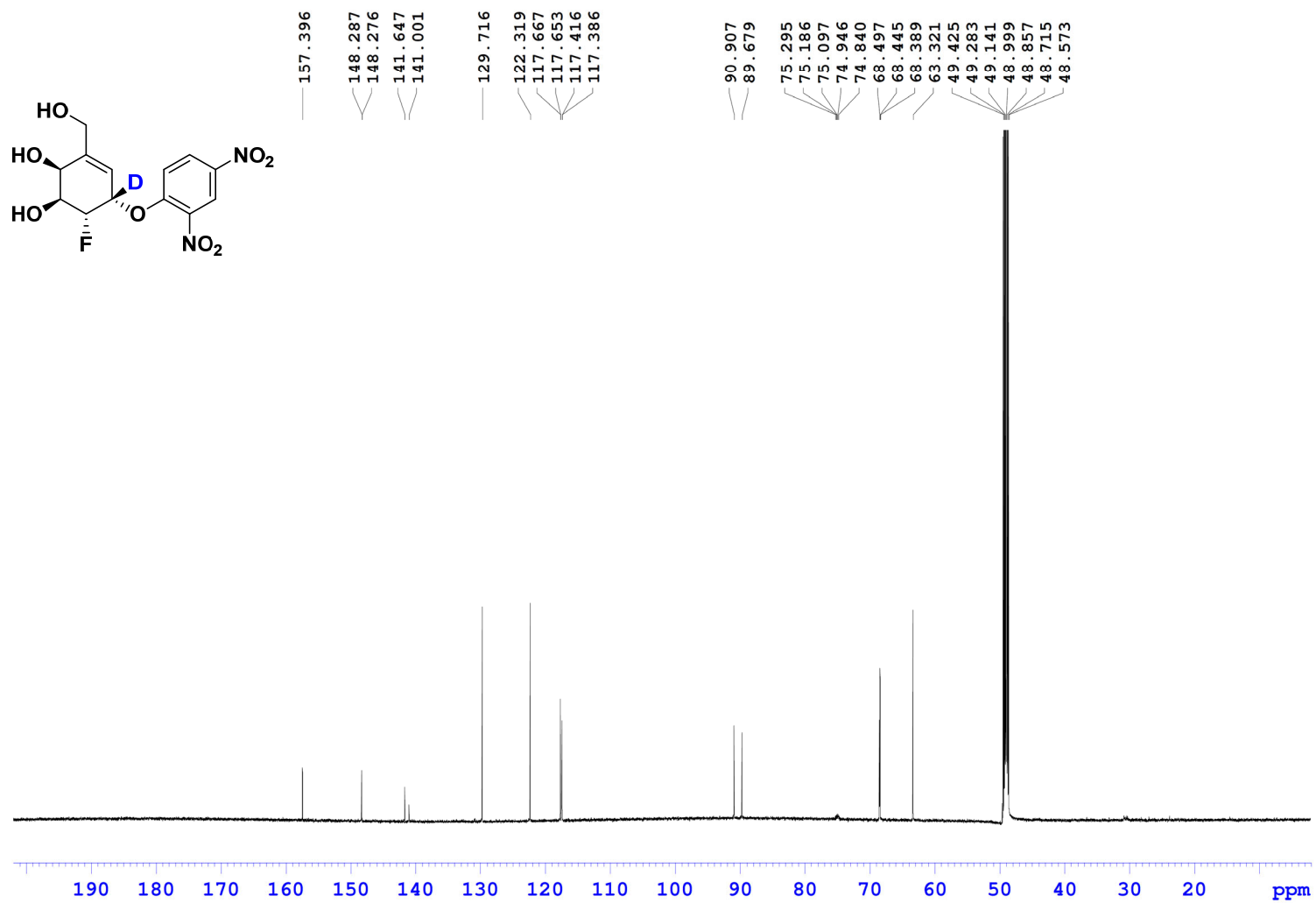


Figure S23. ^1H NMR spectrum for (1- ^{13}C)-4 in CDCl_3 .

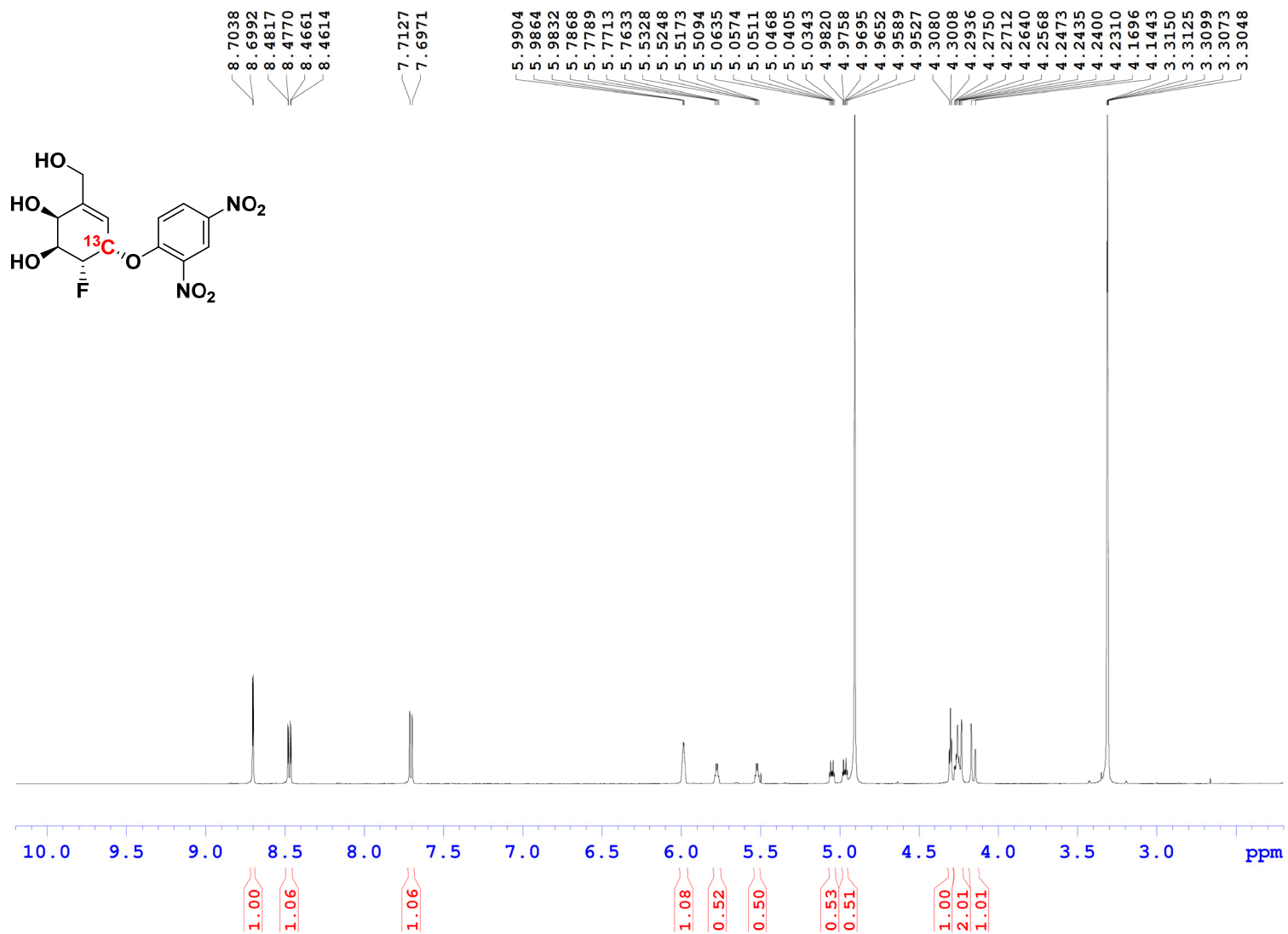


Figure S24. ^{13}C NMR spectrum for (1- ^{13}C)-4 in CDCl_3 .

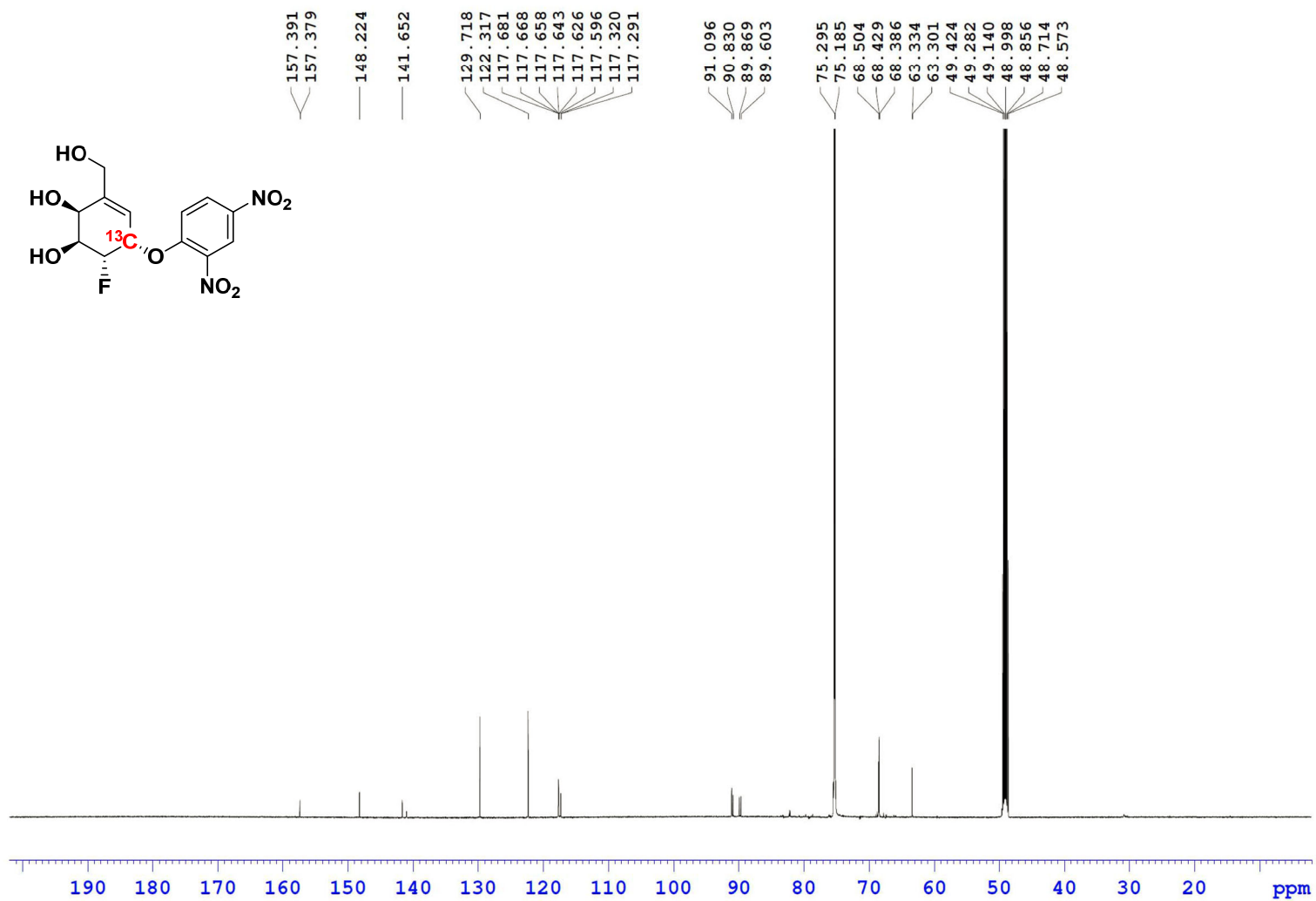


Figure S25. ^1H NMR spectrum for **16** in CDCl_3 .

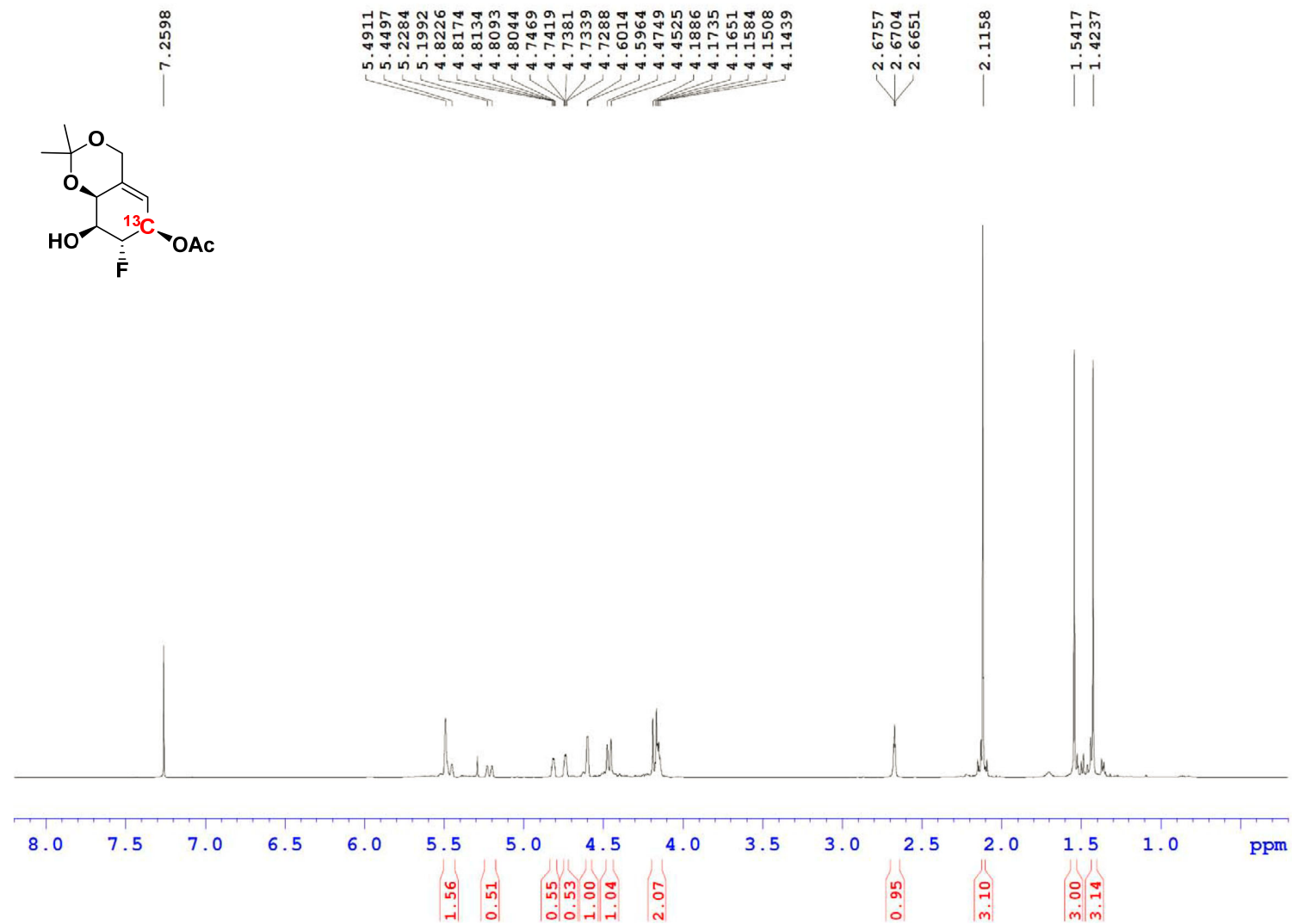


Figure S26. ^{13}C NMR spectrum for **16** in CDCl_3 .

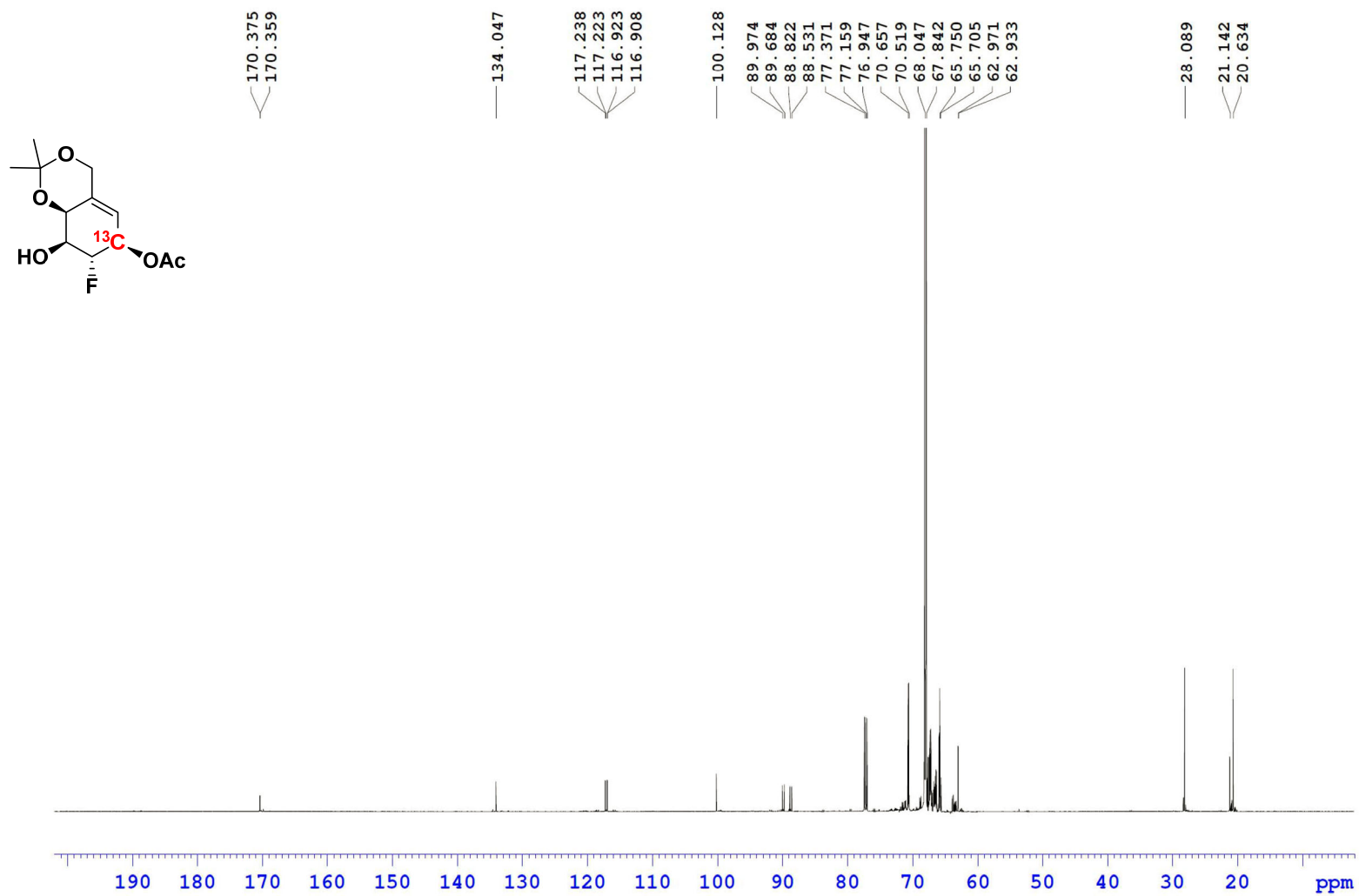


Figure S27. ^1H NMR spectrum for 60:40 mixture of ($1\text{-}^{13}\text{C}$)-4 and ($1\text{-}^{13}\text{C},1\text{-}^{18}\text{O}$)-4 in CDCl_3 .

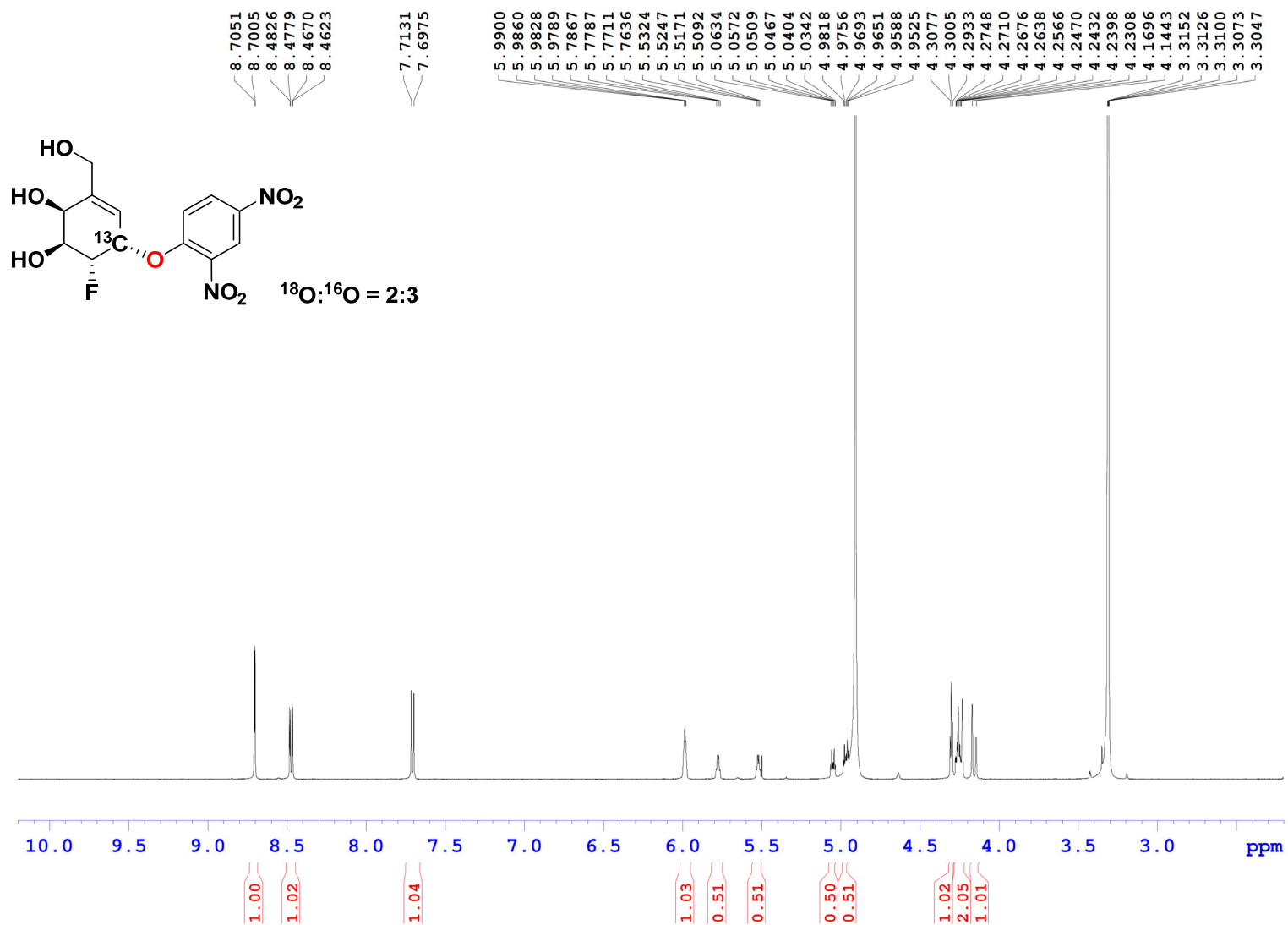


Figure S28. ^{13}C NMR spectrum for 60:40 mixture of (1- ^{13}C)-4 and (1- ^{13}C ,1- ^{18}O)-4 in CDCl_3 .

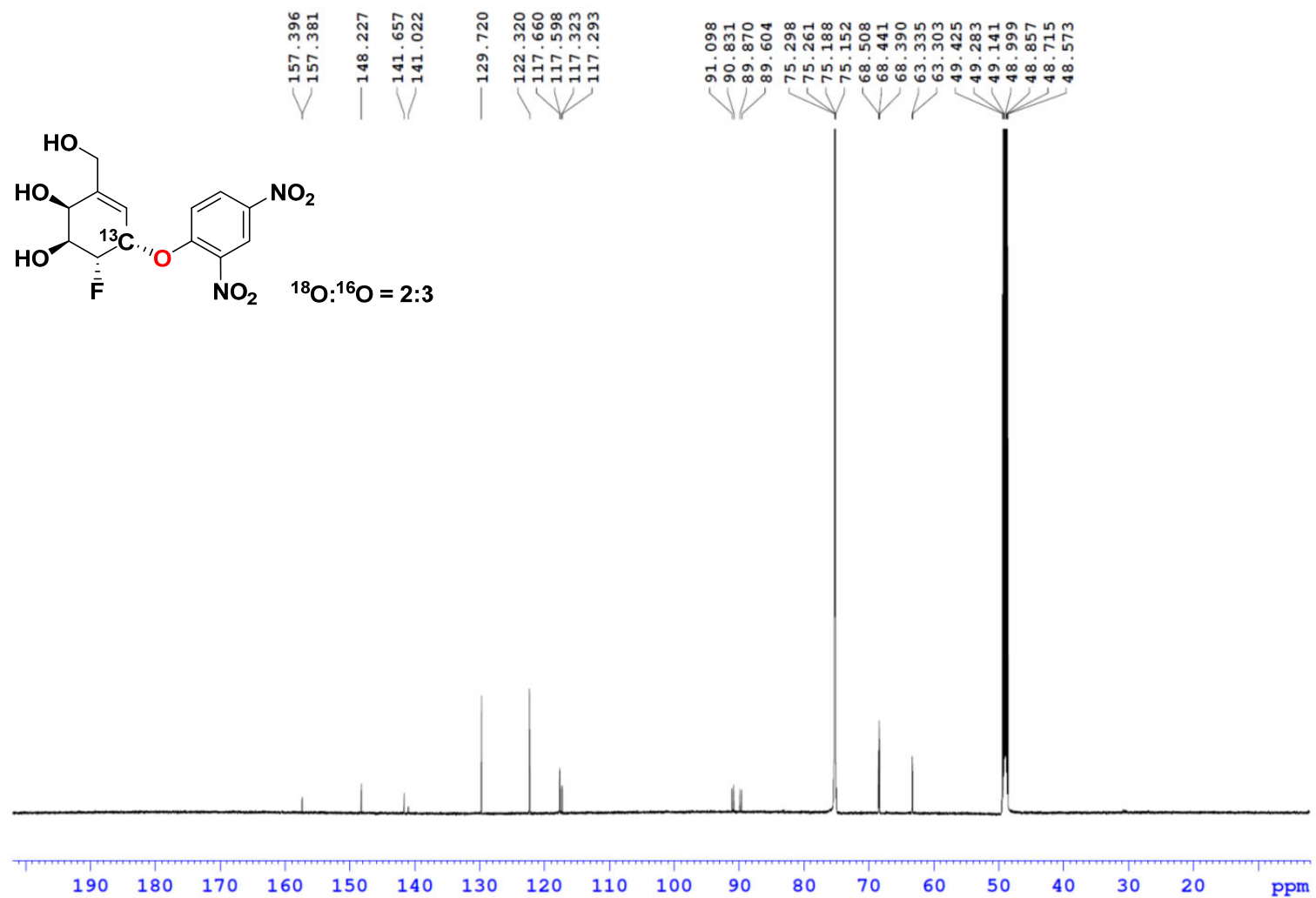


Figure S29. ¹H NMR spectrum for S-6 in CD₃OD.

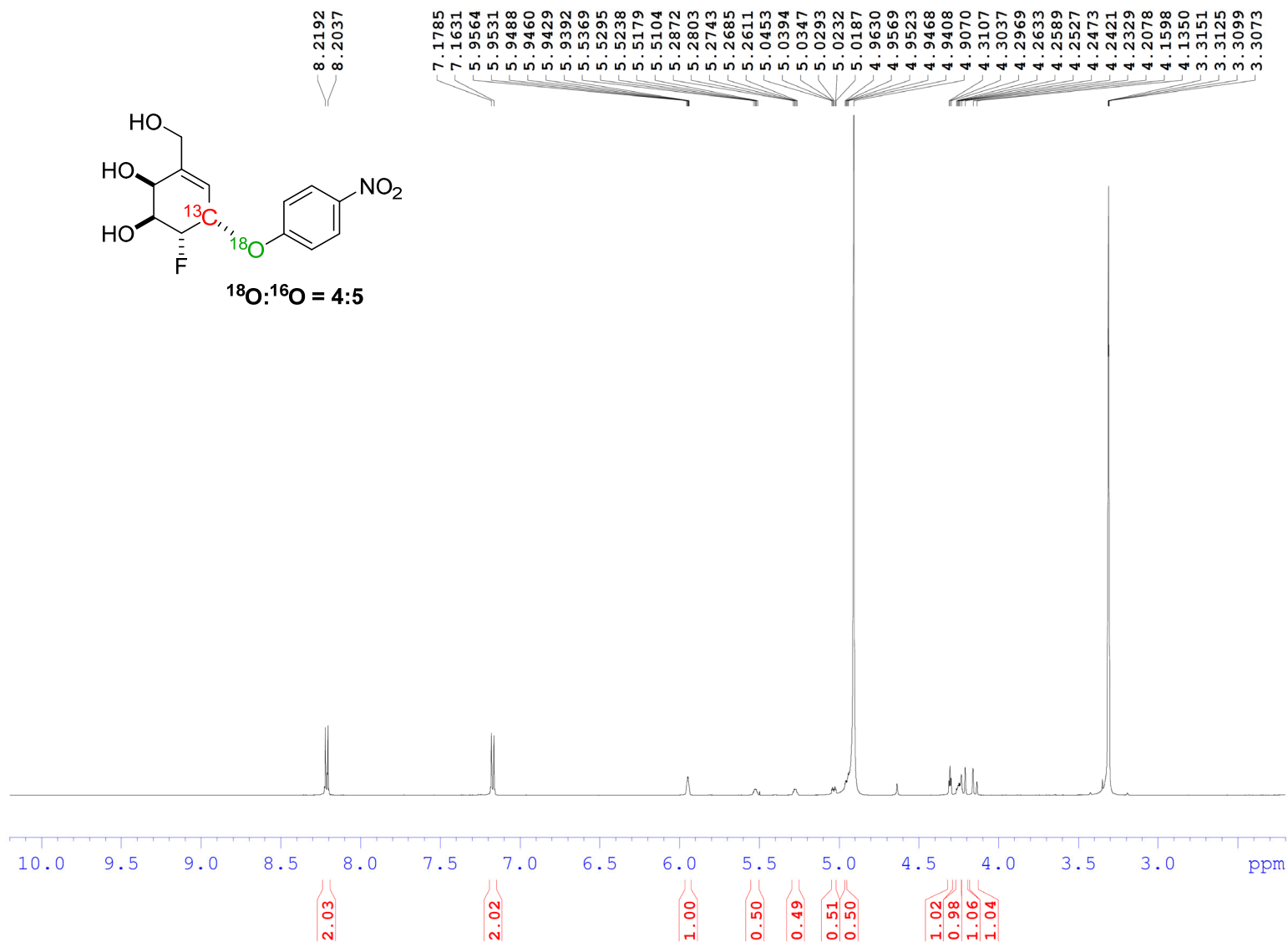


Figure S30. ^{13}C NMR spectrum for S-6 in CD_3OD .

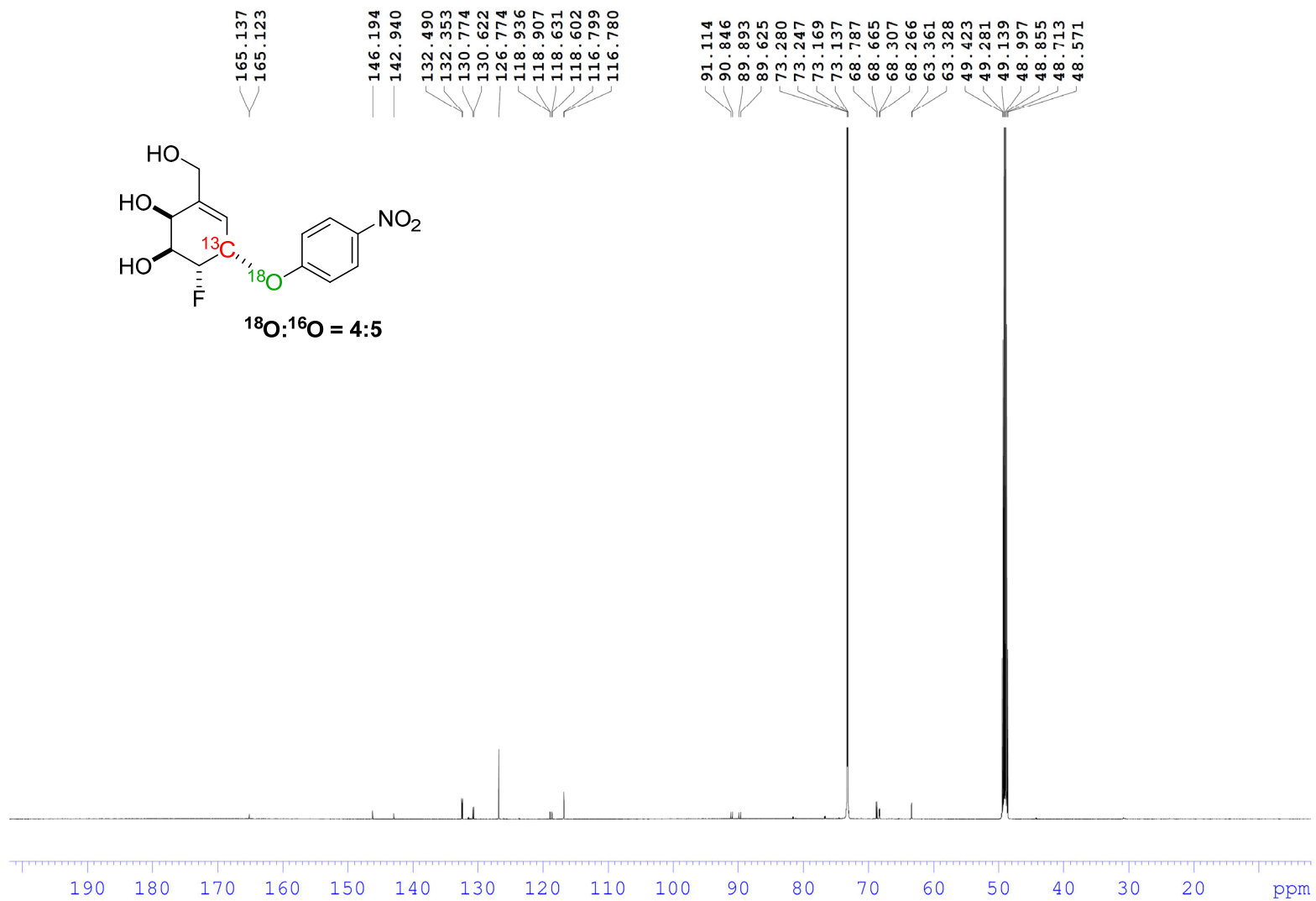
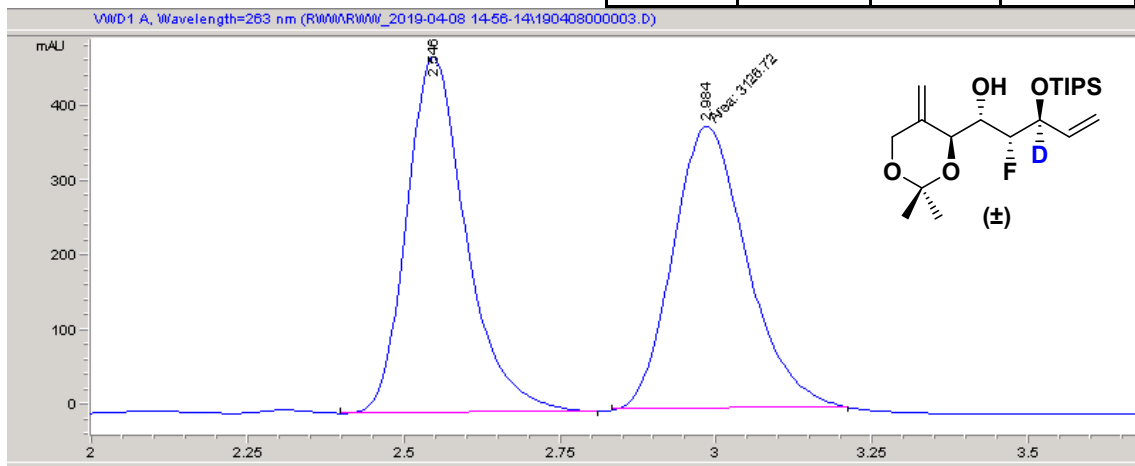


Figure S31. Enantiomeric excess determination for **10**.

Peak No	% Area	Area	Ret. Time
1	50.140	3144.3	2.546 min
2	49.860	3126.7	2.984 min



Peak No	% Area	Area	Ret. Time
1	95.944	724.3	2.515 min
2	4.056	30.6	2.931 min

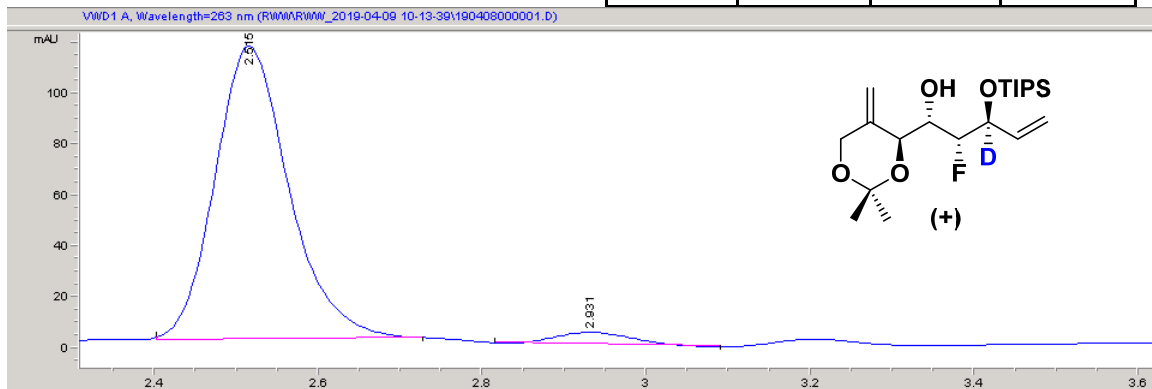
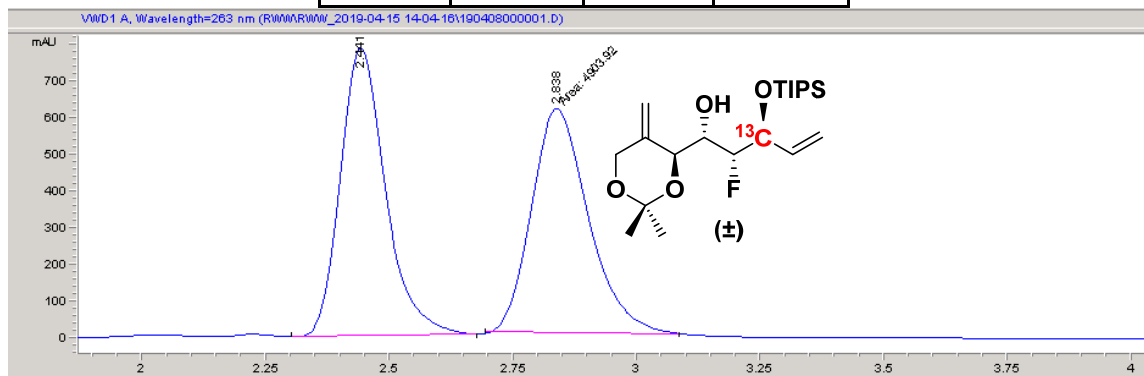


Figure S32. Enantiomeric excess determination for **12**.

Peak No	% Area	Area	Ret. Time
1	50.174	4938.3	2.441 min
2	49.826	4903.9	2.838 min



Peak No	% Area	Area	Ret. Time
1	96.183	1396.5	2.39 min
2	3.817	55.4	2.791 min

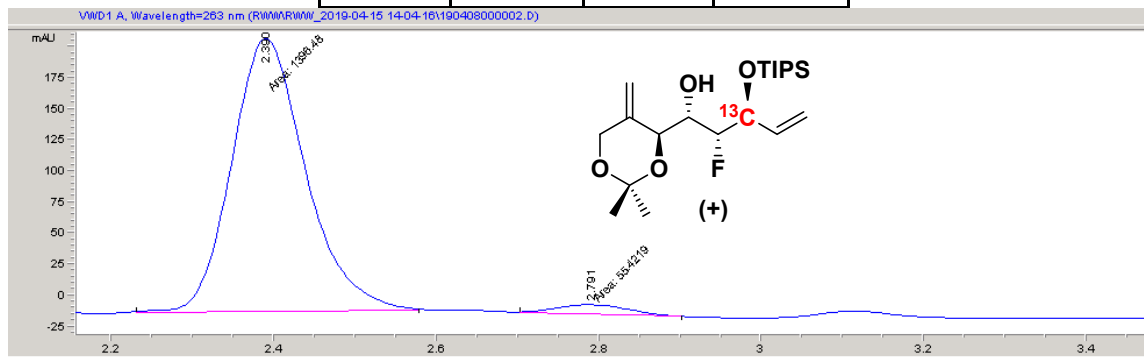
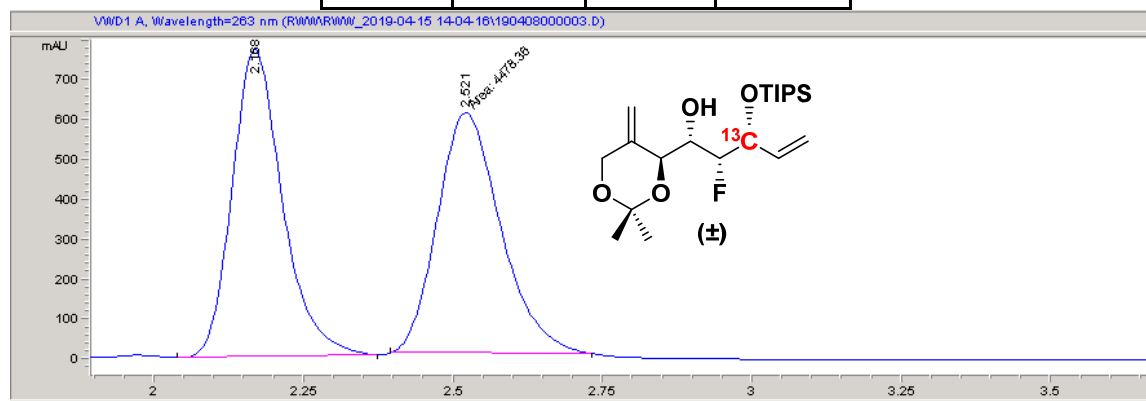
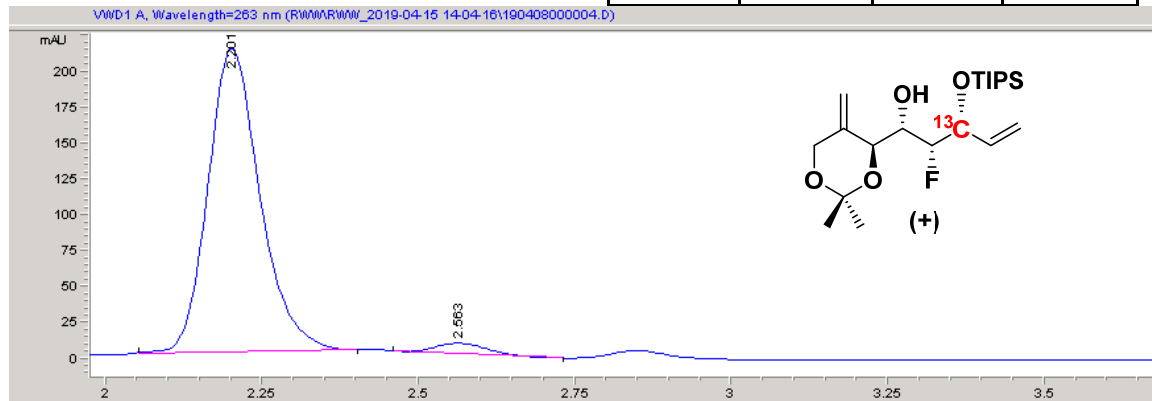


Figure S33. Enantiomeric excess determination for 13.

Peak No	% Area	Area	Ret. Time
1	50.163	4507.6	2.168 min
2	49.837	4478.4	2.521 min



Peak No	% Area	Area	Ret. Time
1	96.920	1228.9	2.201 min
2	3.080	39.1	2.563 min



References:

1. J. I. Brauman, *Anal. Chem.*, 1966, **38**, 607-610.
2. W. Ren, R. Pengelly, M. Farren-Dai, S. Shamsi Kazem Abadi, V. Oehler, O. Akintola, J. Draper, M. Meanwell, S. Chakladar, K. Świderek, V. Moliner, R. Britton, T. M. Gloster and A. J. Bennet, *Nat. Commun.*, 2018, **9**, 3243.
3. T. Taniguchi, D. Hirose and H. Ishibashi, *ACS Catal.*, 2011, **1**, 1469-1474.
4. G. Speciale, M. Farren-Dai, F. S. Shidmoosavee, S. J. Williams and A. J. Bennet, *J. Am. Chem. Soc.*, 2016, **138**, 14012-14019.
5. J. Chan, A. R. Lewis, M. Gilbert, M. F. Karwaski and A. J. Bennet, *Nat. Chem. Biol.*, 2010, **6**, 405-407.
6. T. D. W. Claridge, *High-resolution NMR techniques in organic chemistry*, Elsevier, Amsterdam ; Boston, 2nd edn., 2009.
7. G. F. Pauli, B. U. Jaki and D. C. Lankin, *J. Nat. Prod.*, 2005, **68**, 133-149.
8. L. Melander and W. H. Saunders, *Reaction Rates of Isotopic Molecules*, Wiley, New York, 1980.
9. C. Adamson, R. Pengelly, S. Shamsi Kazem Abadi, S. Chakladar, J. Draper, R. Britton, T. Gloster and A. J. Bennet, *Angew. Chem., Int. Ed.*, 2016, **55**, 14978-14982.
10. I. Accelrys Software, Discovery Studio Modeling Environment, Release 4.5, 2015.
11. J. M. Wang, W. Wang, P. A. Kollman and D. A. Case, *J. Mol. Graph.*, 2006, **25**, 247-260.
12. D. A. Case, T. A. Darden, T. E. Cheatham, C. L. Simmerling, J. Wang, R. E. Duke, R. Luo, R. C. Walker, W. Zhang, K. M. Merz, B. Roberts, S. Hayik, A. Roitberg, G. Seabra, J. Swails, A. W. Götz, I. Kolossváry, K. F. Wong, F. Paesani, J. Vanicek, R. M. Wolf, J. Liu, X. Wu, S. R. Brozell, T. Steinbrecher, H. Gohlke, Q. Cai, X. Ye, M. J. Hsieh, G. Cui, D. R. Roe, D. H. Mathews, M. G. Seetin, R. Salomon-Ferrer, C. Sagui, V. Babin, T. Luchko, S. Gusarov and A. Kovalenko, AMBER 12, 2012.
13. M. H. M. Olsson, C. R. Sondergaard, M. Rostkowski and J. H. Jensen, *J. Chem. Theory. Comput.*, 2011, **7**, 525-537.
14. T. J. Dolinsky, J. E. Nielsen, J. A. McCammon and N. A. Baker, *Nucleic Acids Res.*, 2004, **32**, W665-W667.
15. W. L. Jorgensen, J. Chandrasekhar, J. D. Madura, R. W. Impey and M. L. Klein, *J. Chem. Phys.*, 1983, **79**, 926-935.
16. J. C. Phillips, R. Braun, W. Wang, J. Gumbart, E. Tajkhorshid, E. Villa, C. Chipot, R. D. Skeel, L. Kale and K. Schulten, *J. Comput. Chem.*, 2005, **26**, 1781-1802.
17. L. Verlet, *Phys. Rev.*, 1967, **159**, 98-103.
18. M. J. Field, P. A. Bash and M. Karplus, *J. Comput. Chem.*, 1990, **11**, 700-733.
19. M. J. S. Dewar, E. G. Zoebisch, E. F. Healy and J. J. P. Stewart, *J. Am. Chem. Soc.*, 1985, **107**, 3902-3909.
20. Y. Zhao and D. G. Truhlar, *Theor. Chem. Acc.*, 2008, **120**, 215-241.
21. M. J. Frisch, G. W. S. Trucks, H. B., G. E. Scuseria, M. A. Robb, J. R. Cheeseman, G. Scalmani, V. Barone, B. Mennucci, G. A. Petersson, H. Nakatsuji, M. Caricato, X. Li, H. P. Hratchian, A. F. Izmaylov, J. Bloino, G. Zheng, J. L. Sonnenberg, M. Hada, M. Ehara, K. Toyota, R. Fukuda, J. Hasegawa, M. Ishida, T. Nakajima, Y. Honda, O. Kitao, H. Nakai, T. Vreven, J. A. J. Montgomery, J. E. Peralta, F. Ogliaro, M. Bearpark, J. J. Heyd, E. Brothers, K. N. Kudin, V. N. Staroverov, R. Kobayashi, J. Normand, K. Raghavachari,

- A. Rendell, J. C. Burant, S. S. Lyengar, J. Tomasi, M. Cossi, N. Rega, J. M. Millam, M. Klene, J. E. Knox, J. B. Cross, V. Bakken, C. Adamo, J. Jaramillo, R. Gomperts, R. E. Stratmann, O. Yazyev, A. J. Austin, R. Cammi, C. Pomelli, J. W. Ochterski, R. L. Martin, K. Morokuma, V. G. Zakrzewski, G. A. Voth, P. Salvador, J. J. Dannenberg, S. Dapprich, A. D. Daniels, Ö. Farkas, J. B. Foresman, J. V. Ortiz, J. Cioslowski and D. J. Fox, *Journal*, 2009.
22. M. J. Field, M. Albe, C. Bret, F. Proust-De Martin and A. Thomas, *J. Comput. Chem.*, 2000, **21**, 1088-1100.
 23. B. Roux, *Comput. Phys. Commun.*, 1995, **91**, 275-282.
 24. G. M. Torrie and J. P. Valleau, *J. Comput. Phys.*, 1977, **23**, 187-199.
 25. S. Kumar, D. Bouzida, R. H. Swendsen, P. A. Kollman and J. M. Rosenberg, *J. Comput. Chem.*, 1992, **13**, 1011-1021.
 26. Y. Y. Chuang, J. C. Corchado and D. G. Truhlar, *J. Chem. Phys. A*, 1999, **103**, 1140-1149.
 27. J. C. Corchado, E. L. Coitino, Y. Y. Chuang, P. L. Fast and D. G. Truhlar, *J. Chem. Phys. A*, 1998, **102**, 2424-2438.
 28. K. A. Nguyen, I. Rossi and D. G. Truhlar, *J. Chem. Phys.*, 1995, **103**, 5522-5530.
 29. R. J. Renka, *SIAM J. Stat. Comput.*, 1987, **8**, 393-415.
 30. R. J. Renka, *ACM Trans. Math. Software*, 1993, **19**, 81-94.
 31. J. J. Ruiz-Pernia, E. Silla, I. Tunon and S. Marti, *J. Phys. Chem. B*, 2006, **110**, 17663-17670.
 32. J. J. Ruiz-Pernia, E. Silla, I. Tunon, S. Marti and V. Moliner, *J. Phys. Chem. B*, 2004, **108**, 8427-8433.
 33. J. Baker, *J. Comput. Chem.*, 1986, **7**, 385-395.
 34. K. Fukui, *Acc. Chem. Res.*, 1981, **14**, 363-368.
 35. H. P. Hratchian, R. D. Dennington Ii, T. A. Keith, J. Millam, A. B. Nielsen, A. J. Holder and J. Hiscocks, GaussView 5, 2009.
 36. K. Świderek, I. Tuñón, I. H. Williams and V. Moliner, *J. Am. Chem. Soc.*, 2018, **140**, 4327-4334.
 37. S. Marti, V. Moliner, I. Tunon and I. H. Williams, *Org. Biomol. Chem.*, 2003, **1**, 483-487.
 38. S. Marti, V. Moliner, M. Tunon and I. H. Williams, *J. Phys. Chem. B*, 2005, **109**, 3707-3710.
 39. G. D. Ruggiero, S. J. Guy, S. Marti, V. Moliner and I. H. Williams, *J. Phys. Org. Chem.*, 2004, **17**, 592-601.
 40. J. R. Taylor, *An introduction to error analysis: The study of uncertainties in physical measurements*, University Science Books, Mill Valley, CA., 1982.